

Recommendations for Multimodality Assessment of Congenital Coronary Anomalies: A Guide from the American Society of Echocardiography

Developed in Collaboration with the Society for Cardiovascular Angiography and Interventions, Japanese Society of Echocardiography, and Society for Cardiovascular Magnetic Resonance

Peter Frommelt, MD, FASE, Leo Lopez, MD, FASE, V. Vivian Dimas, MD, FSCAI, Benjamin Eidem, MD, FASE, B. Kelly Han, MD, FASE, H. Helen Ko, BS, ACS, RDMS, RDCS, RCCS, FASE, Richard Lorber, MD, FASE, Masaki Nii, MD, PhD, Beth Printz, MD, PhD, FASE, Shubhika Srivastava, MBBS, FASE, Anne Marie Valente, MD, FASE, FSCMR, and Meryl S. Cohen, MD, FASE, *Milwaukee, Wisconsin; Palo Alto and San Diego, California; Dallas and San Antonio, Texas; Rochester and Minneapolis, Minnesota; New York, New York; Shizuoka, Shizuoka, Japan; Boston, Massachusetts; Philadelphia, Pennsylvania*

Keywords: Coronary artery, Congenital heart disease, Pediatric, Echocardiography

In addition to the collaborating societies listed in the title, this document is endorsed by the following American Society of Echocardiography International Alliance Partners: Argentine Federation of Cardiology, Argentine Society of Cardiology, Asian-Pacific Association of Echocardiography, Australasian Sonographers Association, British Society of Echocardiography, Canadian Society of Echocardiography, Cardiovascular Imaging Society of the Interamerican Society of Cardiology (SISIAC), Chinese Society of Echocardiography, Department of Cardiovascular Imaging of the Brazilian Society of Cardiology, Indian Academy of Echocardiography, Iranian Society of Echocardiography, Mexican Society of Echocardiography and Cardiovascular Imaging (SOME-ic), National Society of Echocardiography of Mexico (SONECOM), Philippine Society of Echocardiography, Saudi Arabian Society of Echocardiography, Thai Society of Echocardiography, Venezuelan Society of Cardiology.

TABLE OF CONTENTS

Summary	260		
I. Introduction	260		
II. Imaging Techniques for Assessment of Coronary Anomalies	261		
A. Echocardiography	261		
B. Cardiac Magnetic Resonance Imaging	262		
C. Cardiac Computed Tomography	263		
D. Nuclear Myocardial Perfusion Imaging	264		
E. Angiography	264		
III. Isolated Congenital Coronary Anomalies	265		
		A. Anomalous Aortic Origin of a Coronary Artery	265
		1. Background	265
		2. Goals of Echocardiographic Imaging	267
		3. Additional Imaging Techniques	267
		B. Anomalous Pulmonary Origin of a Coronary Artery	269
		1. Background	269
		2. Goals of Echocardiographic Imaging	270
		a. Pre-operative Assessment	270
		b. Post-operative Assessment	272

From the Children's Hospital of Wisconsin and the Medical College of Wisconsin, Milwaukee, Wisconsin (P.F.); Stanford University, Palo Alto, California (L.L.); University of Texas Southwestern, Dallas, Texas (V.V.D.); Mayo Clinic, Rochester, Minnesota (B.E.); Children's Minnesota and the Minneapolis Heart Institute, Minneapolis, Minnesota (B.K.H.); Kravis Children's Hospital, Mount Sinai Medical Center, New York, New York (H.H.K. and S.S.); Baylor College of Medicine, Children's Hospital of San Antonio, San Antonio, Texas (R.L.); Shizuoka Children's Hospital, Shizuoka, Shizuoka, Japan (M.N.); University of California San Diego and Rady Children's Hospital, San Diego, California (B.P.); Boston Children's Hospital, Brigham and Women's Hospital, Harvard Medical School, Boston, Massachusetts (A.M.V.), The Children's Hospital of Philadelphia, Philadelphia, Pennsylvania (M.S.C.).

The following authors reported no actual or potential conflicts of interest in relation to this document: Peter Frommelt, MD, FASE, Leo Lopez, MD, FASE, V. Vivian Dimas, MD, FSCAI, Benjamin Eidem, MD, FASE, B. Kelly Han, MD, FASE, H. Helen Ko, BS, ACS, RDMS, FASE, Richard Lorber, MD, FASE, Masaki Nii, MD, PhD,

Beth Printz, MD, FASE, Shubhika Srivastava, MD, FASE, Anne Marie Valente, MD, FASE, FSCMR, Meryl S. Cohen, MD, FASE.

Reprint requests: American Society of Echocardiography, Meridian Corporate Center, 2530 Meridian Parkway, Suite 450, Durham, NC 27713 (E-mail: ase@asecho.org).

Attention ASE Members:

Visit www.aseuniversity.org to earn free continuing medical education credit through an online activity related to this article. Certificates are available for immediate access upon successful completion of the activity. Nonmembers will need to join the ASE to access this great member benefit!

0894-7317/\$36.00

Copyright 2019 by the American Society of Echocardiography.

<https://doi.org/10.1016/j.echo.2019.10.011>

Abbreviations

2D = two-dimensional
AAOCA = anomalous aortic origin of a coronary artery
AAOLCA = anomalous aortic origin of the left coronary artery
AAORCA = anomalous aortic origin of the right coronary artery
ALCAPA = anomalous left coronary artery from the pulmonary artery
ARCAPA = anomalous right coronary artery from the pulmonary artery
CA = coronary artery
CAF = coronary artery fistula
CHD = congenital heart disease
CMR = cardiac magnetic resonance
CCT = cardiac computed tomography
ECG = electrocardiography
HLHS = hypoplastic left heart syndrome
LAD = left anterior descending
LCx = left circumflex
LCA = left coronary artery
LV = left ventricle
MR = mitral regurgitation
PET = positron emission tomography
PA = pulmonary artery
RCA = right coronary artery
RV = right ventricle
SPECT = single-photon emission computed tomography
SVAS = supraaortic stenosis
TOF = tetralogy of Fallot
TEE = transesophageal echocardiography
TGA = transposition of the great arteries
TTE = transthoracic echocardiography
VSD = ventricular septal defect

3. Additional Imaging Techniques	272
C. Isolated Congenital Coronary Artery Fistulas	274
1. Background	274
2. Goals of Echocardiographic Imaging	276
a. Pre-intervention Assessment	276
b. Post-interventional Assessment	276
3. Additional Imaging Techniques	276
IV. Congenital Coronary Anomalies Associated with Other Congenital Heart Diseases	278
A. Supraaortic Stenosis	278
1. Background	278
2. Goals of Echocardiographic Imaging	279
3. Additional Imaging Techniques	280
B. Transposition of the Great Arteries	280
1. Background	280
2. Goals of Echocardiographic Imaging	281
a. Preoperative Assessment	281

b. Postoperative Assessment	283
3. Additional Imaging Techniques	283
C. Tetralogy of Fallot	284
1. Background	284
2. Goals of Echocardiographic Imaging	285
a. Preoperative Assessment	285
b. Postoperative Assessment	285
3. Additional Imaging Techniques	285
D. Truncus Arteriosus	286
1. Background	286
2. Goals of Echocardiographic Imaging	287
3. Additional Imaging Techniques	287
E. Coronary Anomalies Associated with Single Ventricle Lesions	288
1. Pulmonary Atresia With Intact Ventricular Septum	288
a. Background	288
b. Goals of Echocardiographic Imaging	288
c. Additional Imaging Techniques	288
2. Hypoplastic Left Heart Syndrome	289
a. Background	289
b. Goals of Echocardiographic Imaging	289
c. Additional Imaging Techniques	289

SUMMARY

Congenital coronary artery anomalies, both in isolation and associated with other forms of congenital heart disease, have been recognized as important lesions with significant potential morbidity and mortality, including sudden cardiac death in children and adolescents. Multimodality imaging techniques have demonstrated increasing utility in the characterization of most congenital coronary anomalies, both in children and adults, and may reduce the need for diagnostic catheterization in many cases. This document provides multimodality guidelines for optimization of imaging for congenital coronary anomalies, with a review of the benefits and limitations of the different imaging techniques (echocardiography, cardiac computed tomography, cardiac magnetic resonance imaging, nuclear myocardial perfusion imaging and angiography). Strategies for imaging congenital coronary anomalies when the coronary anomaly is in isolation (anomalous aortic origin of a coronary artery, anomalous left coronary from the pulmonary artery, and coronary artery fistulas) as well as coronary anomalies associated with other congenital heart disease (supraaortic stenosis, transposition of the great arteries, tetralogy of Fallot, truncus arteriosus, pulmonary atresia with intact septum, and hypoplastic left heart syndrome) are described.

I. INTRODUCTION

Congenital coronary artery (CA) anomalies, both in isolation and associated with other forms of congenital heart disease (CHD), have been recognized as important lesions with significant potential morbidity and mortality. Echocardiographic findings in patients with congenital CA anomalies have been well characterized, and the feasibility and utility of complementary noninvasive CA imaging with cardiac computed tomography (CCT) and cardiac magnetic resonance (CMR) have also been described. Prospective identification of congenital CA anomalies using transthoracic echocardiography (TTE) as a screening tool has become routine and has helped dispel the notion that CA anatomy cannot be identified noninvasively. In fact, multimodality imaging techniques have replaced cardiac catheterization as the primary tool for characterization of most congenital CA anomalies in children. This has become particularly relevant to those performing cardiac imaging,

with recognition that the prevalence of congenital CA anomalies associated with sudden cardiac death, specifically anomalous aortic origin of a CA (AAOCA) from the opposite sinus of Valsalva, is estimated at 0.7% [95% CI: 0.48-0.95%].¹ These potentially lethal anomalies are thus relatively common in the general population, and so evaluation of coronary artery takeoff and course should be included as part of a complete noninvasive imaging exam. With this background, it is apparent that a summary document providing multimodality guidelines for optimization of imaging for congenital CA anomalies is needed. A review of the benefits and limitations of the different imaging techniques (Table 1) will preface descriptions of known congenital CA conditions that warrant careful imaging assessment.

II. IMAGING TECHNIQUES FOR ASSESSMENT OF CORONARY ANOMALIES

A. Echocardiography

Knowledge of the normal origin and course of the CAs is important in order to recognize congenital CA anomalies. Each CA usually originates from its respective sinus above the aortic valve leaflets, with the right CA (RCA) arising from the right sinus of Valsalva and the left main CA (LCA) arising from the left sinus of Valsalva (Figure 1).

Echocardiographic techniques for imaging of CA origin and course are well described.²⁻⁴ TTE is the ideal modality because it is risk-free, noninvasive, portable, and widely available. Echocardiography, with its high temporal and spatial resolution, permits rapid visualization of soft tissue and cardiac chambers, and can be readily performed in all clinical settings. In young children, echocardiography usually does not require deep sedation or general anesthesia as does cardiac catheterization or CMR imaging, nor does it involve radiation exposure, unlike CCT or cardiac catheterization. The CAs are small and superficial structures; thus, optimal imaging is best performed with the highest frequency transducer that allows for adequate penetration to maximize spatial resolution. Depending on the ultrasound frequency that is used for scanning, the axial resolution can range from 0.13 mm to 0.39 mm, corresponding to 12 MHz and 4 MHz frequency transducers, respectively. In terms of imaging the coronary arteries, one should follow basic ultrasound principles to optimize two-dimensional (2D) images by aligning the emitted B-mode pulses perpendicular to anatomic structures, and optimize color flow mapping by orienting the color Doppler sector parallel to flow.

2D and color Doppler TTE imaging of CA origins should be part of a complete examination in every child.⁵ This is best accomplished from a parasternal short-axis view, where both CA origins can be visualized by scanning the aortic sinuses above the aortic valve (Figure 2). If one considers the aortic root as a clock face when visualized in this view, the left main CA origin is normally at approximately 4 o'clock and the RCA origin is at approximately 11 o'clock. Additional color flow mapping of the interarterial space can also help identify an anomalous proximal course. Clockwise rotation of the transducer in the parasternal short-axis view (Figure 2B) frequently allows for imaging of the left main CA as it bifurcates into the left anterior descending branch (LAD), which courses along the anterior interventricular groove, and the left circumflex branch (LCx), which courses in the left anterior atrioventricular groove. In contrast, counterclockwise transducer rotation can facilitate imaging of the RCA. Color flow mapping is also important since documentation of direction and timing of flow is helpful in diagnosing anomalies (Figure 2C). It is paramount that the color flow map be positioned to profile flow from the sinus to the coronary ostium and then into its proximal

Table 1 Comparison of techniques for imaging coronary arteries

Characteristic	TTE	IVUS	CMR	CCT	Cath
Spatial resolution	++	++++	+++	++++	++++
Temporal resolution	+++	++++	++	varies	+++
Evaluation of origin/ostia	++	+++	+++	++++	+++
Evaluation of proximal course	++	+++	+++	++++	+++
Evaluation of distal course and branches/dominance	+	-	++	+++	++++
Intracoronary structure	+	++++	++	+++	+++
Intracardiac morphology	++++	-	++++	+++	++
Evaluation of extracardiac structures	++	-	++++	++++	+
Myocardial ischemia	++	-	+++	-	+++
Radiation exposure	-	-	-	+	+++
Iodinated contrast medium	-	-	-	++++	++++
Imaging duration	++	+++	+++	+	++++
Sedation requirements in children	++	++++	++++	++	++++

Cath, Cardiac catheterization; *CCT*, cardiac computed tomography; *CMR*, cardiac magnetic resonance; *IVUS*, intravascular ultrasound; *TTE*, transthoracic echocardiography.

course. The CAs usually have low-velocity flow; therefore, the Nyquist limit should be decreased to about 20-40 cm/second, which is frequently available as a CA evaluation preset on many ultrasound machines.

CA origin and course can also be assessed from other TTE views. In infants and small children with good subcostal windows, the LCA origin can be seen from a coronal plane, allowing for distinction between a coronary origin from the sinus, sinotubular junction, or ascending aorta. The RCA origin is frequently best seen from a parasternal long-axis view with slight rightward tilt of the transducer, again allowing identification of the coronary origin from the sinus, sinotubular junction, or ascending aorta. The LAD course along the anterior interventricular groove can also be well seen in a parasternal long-axis view with leftward anterior tilt as the imaging plane sweeps from the aortic root to the pulmonary trunk.

A limitation of TTE in imaging the CAs is that they are superficial cardiac structures, with potential acoustic interference by the ribs, lungs, and pleura. In addition, the rapid heart rates in neonates can make the evaluation of CAs even more challenging, while larger body habitus in older children and adults may limit acoustic windows. Spatial resolution can sometimes be limited, making it difficult to distinguish whether a CA is arising from a particular cusp or an area adjacent to that cusp. When there is anomalous origin of a CA, false dropout can create the appearance of normal CA origin from the appropriate sinus, especially in the setting of a prominent transverse sinus. Therefore, still frames of CA origins should never be used in isolation. Lastly, the distinction between an interarterial (between the aorta and the pulmonary artery [PA]) and an intramural course (traveling within the wall of the aorta) is difficult by echocardiography. This is discussed in more detail below.

Transesophageal echocardiographic (TEE) imaging of CA origins and their proximal course can also be a complementary technique, particularly when there are poor TTE windows as seen in obese patients or those with lung disease. This is best accomplished with a multiplane probe from the mid-esophageal window just above the aortic valve. The LCA and its branches are best seen with the imaging plane at approximately 20-50°, whereas the RCA is best seen at 90-120°. Color flow mapping of both CAs is also important to evaluate the direction and timing of flow.

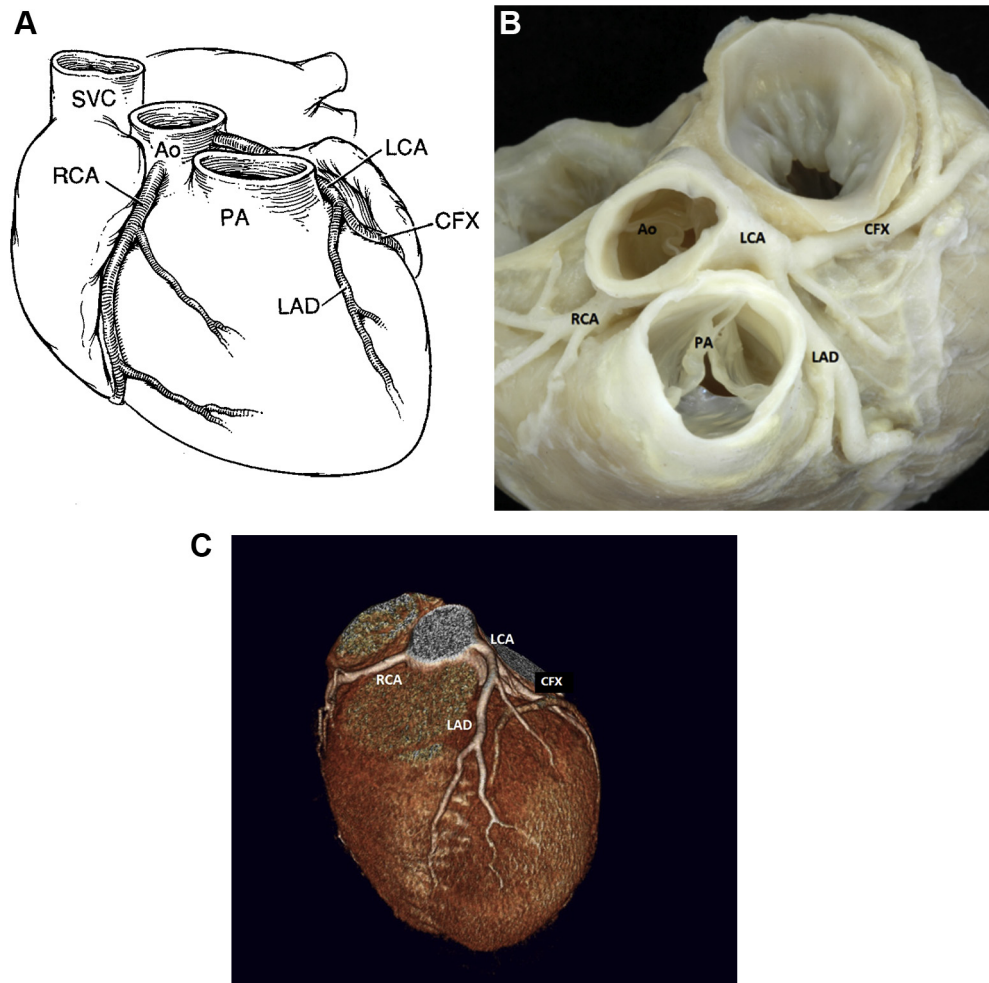


Figure 1 Illustration (A), pathology specimen (B), and cardiac CT (C) of normal coronary origins from the aorta (Ao), demonstrating the epicardial position of the major coronary branches, including the right coronary artery (RCA), left coronary artery (LCA), left anterior descending (LAD), and circumflex (CFX) coronary arteries. PA, Pulmonary artery; SVC, superior vena cava.

B. Cardiac Magnetic Resonance Imaging

CMR is frequently used as a complementary imaging modality to echocardiography for evaluation of suspected or confirmed congenital CA anomalies. CMR has some advantages over other imaging modalities because it requires no radiation exposure and is not dependent on acoustic windows. Several techniques are typically utilized as part of a comprehensive CMR exam to assess patients with known or suspected congenital CA anomalies.⁶ Three-dimensional (3D) image datasets acquired by CMR can be reformatted into any imaging plane to aid in identification of anomalies of CA origin and proximal course, to assess the relation of the CAs to adjacent structures, and to evaluate for the presence of associated anatomic abnormalities. CMR representation of CA anatomy can be displayed in standard axial, sagittal, and coronal projections, or the images can be reformatted into 'echo-equivalent' views that facilitate multimodality comparison of CA anatomy. Specialized post-processing techniques and display formatting include virtual angiography, where images are presented as if the viewer is sitting within the CA lumen itself,⁷⁻⁹ allowing for the assessment of the shape and caliber of the ostium. CMR perfusion imaging can be added to help identify perfusion defects in patients with CA anomalies before and/or after surgical intervention, either at rest or with pharmacologic stress.

Most commonly when screening for CA anomalies, an isotropic (i.e., of equal value from all orientations) set of images is acquired from above the level of the aortic root to the ventricular apex utilizing electrocardiographic (ECG) triggering, fat saturation (nulling the CMR signal from fat), T2-preparation (to increase the ability to differentiate CA flow from the adjacent myocardium), and a respiratory navigator to track diaphragm motion and correct for cranial-caudal motion of the heart during image acquisition.¹⁰ An alternative to acquisition of this so-called 'whole heart' method is volume-targeted imaging, where separate smaller 3D volumetric slabs targeted to the particular CA segment(s) of interest are acquired; this technique may be more suited to confirmation of a known CA anomaly rather than comprehensive evaluation of the entire CA system.^{11,12} ECG triggering to confine image acquisition to a specified time in the cardiac cycle with the least CA motion has been used to visualize CAs in younger children and others with higher heart rates.¹³⁻¹⁵

CA anomalies are associated with increased risk of myocardial ischemia, especially with exertion, which can be assessed by CMR pharmacologic stress imaging. Agents used include those that cause increased myocardial oxygen demand (such as dobutamine) or increased CA blood flow (such as Persantine®, adenosine, or regadenoson).¹⁶⁻¹⁸ Intravenous gadolinium-based contrast agents are typically given to enhance intravascular signal intensity, optimize CA

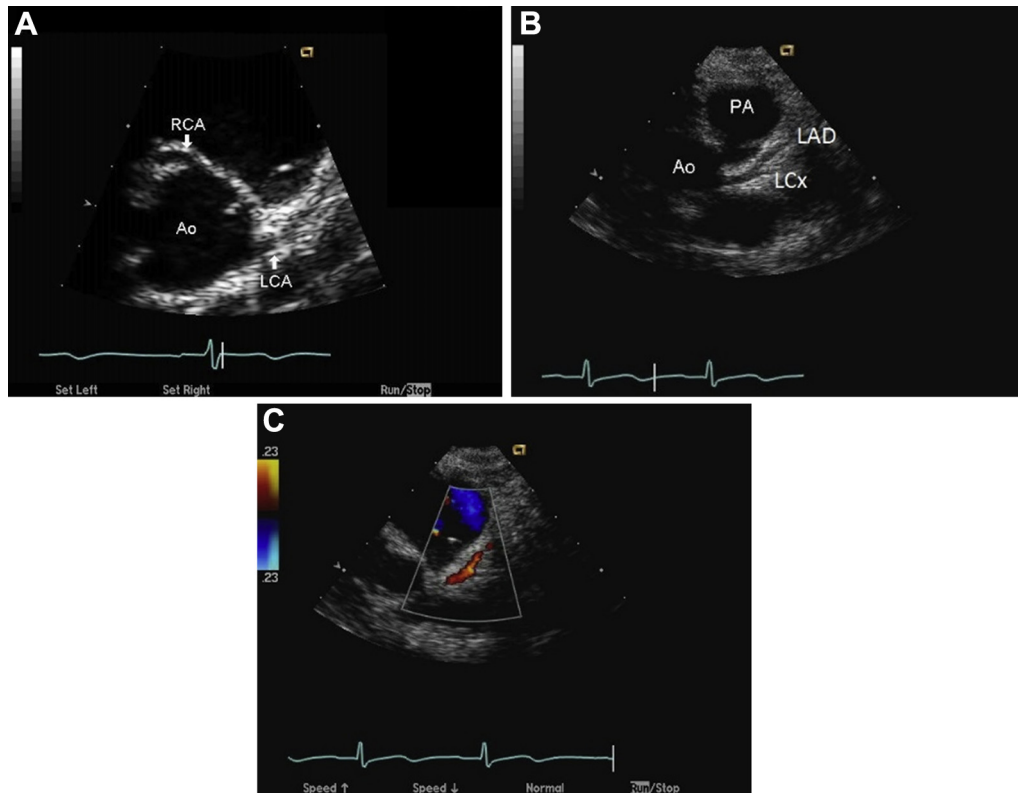


Figure 2 Parasternal short-axis images of the normal CA origins from the aortic root (Ao). In **A**, the normal origins of the left main coronary artery (LCA) from the left sinus of Valsalva and right coronary artery (RCA) from the right sinus of Valsalva are well visualized. With clockwise rotation of the probe from this position (**B**), a longer length of the left main coronary and its bifurcation into the left anterior descending (LAD) and circumflex (LCx) branches are visualized. Finally, color Doppler assessment of flow direction in the coronaries can be obtained (**C**) by lowering the color Nyquist limit (in this case to 23 cm/s) to visualize the low-velocity diastolic anterograde flow in the left coronary, seen as a red color flow signal coursing appropriately toward the transducer and away from the aortic root during diastole.

image resolution, and visualize late myocardial enhancement as a marker of fibrosis/infarction. A matched defect on both contrast-enhanced rest and stress imaging, with evidence of post-contrast myocardial late gadolinium enhancement, identifies an irreversible perfusion defect, while a perfusion defect during stress but not at rest is classified as reversible. Recently, adenosine stress and rest imaging using T1 mapping has been shown to differentiate normal from ischemic or infarcted myocardium without the need for gadolinium contrast.¹⁹

CMR limitations for CA imaging include: 1) the need for cooperative patients in order to obtain high quality imaging, thereby requiring deep sedation or general anesthesia for infants and young children; 2) lower spatial and temporal resolution of CMR compared with TTE, which can be exacerbated in infants and small children because of small patient size, high heart rates, and respiratory motion artifact,²⁰ so that assessment of coronary origins, angle of origin, and/or length and course of anomalous segments may be inadequately demonstrated; 3) suboptimal imaging in the setting of arrhythmias or irregular heart rate; 4) image degradation by artifact from ferromagnetic materials following catheter-based or surgical interventions; 5) implanted pacemakers or cardioverter defibrillators (which are relative contraindications); 6) inability to use gadolinium-based contrast agents in advanced renal disease; and 7) poor correlation of CA measurements obtained by CMR with 2D echo-derived CA measurements, precluding the use of echocardiographic reference values for CMR-derived CA size measurements.¹⁵

C. Cardiac Computed Tomography

Modern cardiovascular multidetector CT is also an excellent complementary technique for evaluation of congenital CA anomalies. Temporal resolution is as low as 66 msec, allowing definitive CA imaging even at fast heart rates, which is an advantage over CMR. Modern multislice scanners with appropriate spatial resolution and the use of ECG gating are required to adequately image the CAs in pediatric patients. Excellent visualization of CA origins can be achieved using CCT in infants with tetralogy of Fallot,²¹ and lower radiation exposure at an estimated dose of approximately 1 millisievert has been reported with successful imaging of the CAs in pediatric patients with CHD.^{22,23}

CCT imaging can provide high resolution images of the distal vessels with 3D display of the CAs and their relationship to extracardiac structures and the sternum, as well as detection of calcified and stenotic CA segments. As with CMR imaging, ventricular function and associated cardiovascular anomalies can be evaluated from the same dataset used for CA imaging. CCT images of CAs should also be projected in echo-equivalent views for consistent interpretation and reporting. Optimizing CCT techniques for imaging specific CA lesions should include: a) consideration of heart rate-lowering medications or CA vasodilators²⁴ since lower radiation doses are achieved for slow and steady heart rates^{25,26}; b) consideration of suspended respiration for high resolution imaging in patients unable to cooperate, particularly if distal CA vessel visualization is required; c) use of low tube potential and automated tube current modulation^{27,28}; d) use of ECG pulse modulation with a narrow acquisition window

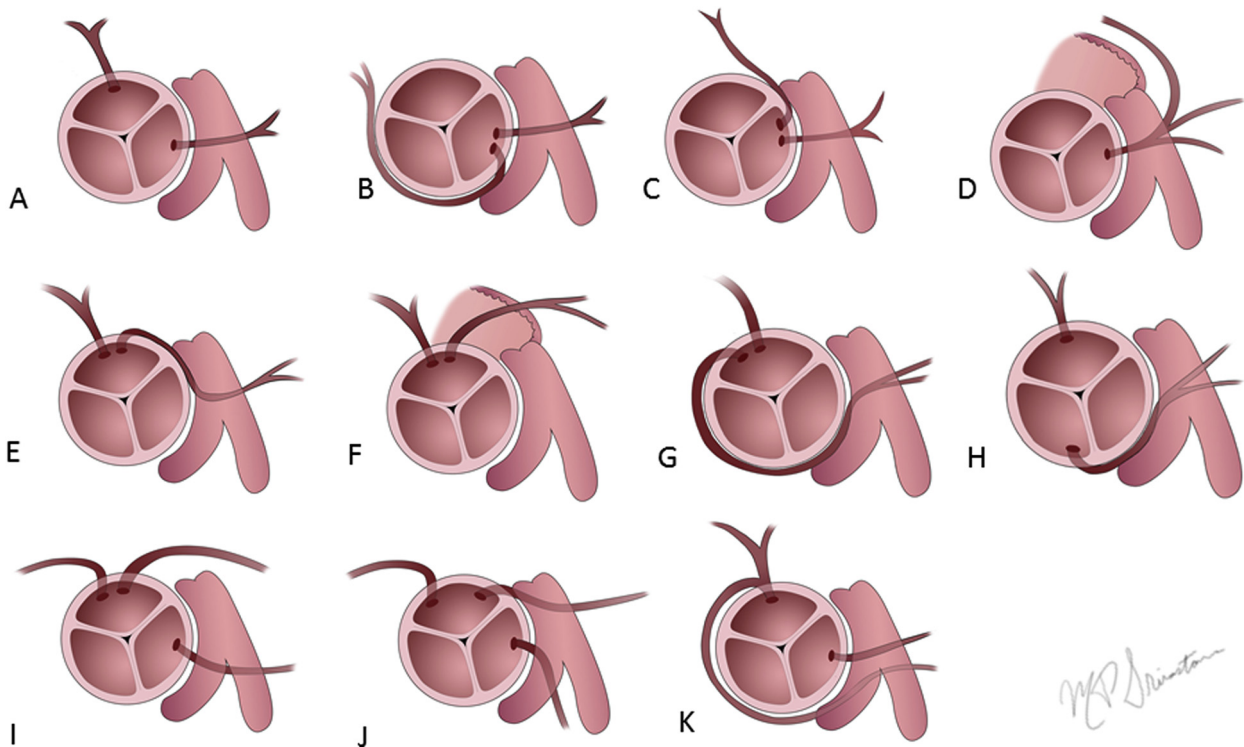


Figure 3 Variation in coronary course with anomalous aortic origin. Select illustrations of the possible variety of coronary artery anomalies. Panel **A**: Normal coronary anatomy; **B**: Anomalous aortic origin of the right coronary artery (AAORCA) with right coronary artery (RCA) originating from the left coronary sinus with a retro-aortic course; **C**: Interarterial AAORCA with the RCA originating from the left sinus with an intramural course in the anterior aortic wall; **D**: “Single left” coronary artery with all coronaries arising from the left sinus and RCA then coursing anterior to the PA. **E**: Interarterial anomalous aortic origin of the left coronary artery (AAOLCA) with the left coronary originating from the right coronary sinus with an intramural course; **F**: Intraconal AAOLCA with the left coronary originating from the right sinus and coursing within the myocardial sulcus below the right ventricular outflow tract; **G**: AAOLCA with the left coronary originating from the right sinus with a retro-aortic course; **H**: AAOLCA with the left coronary originating from the non-coronary sinus with a retro-aortic course; **I-K**: Anomalous aortic origin of the left anterior descending coronary artery from the right sinus, with an anterior course in front of the pulmonary artery (**I**), an interarterial course (**J**), and a retro-aortic course after originating from the right coronary artery (**K**). Illustration created by Maansi Dayal Srivastava.

adjusted to heart rate; e) use of prospective ECG triggering sequence whenever possible, reserving retrospective ECG gating for highly irregular heart rates such as atrial fibrillation²⁹; f) use of iterative reconstruction techniques; g) patient-specific tailoring of image quality requirements and radiation dose optimization, since the image quality required for high resolution CA imaging is often not needed to determine CA location and course in patients with CHD and should be reserved for patients with symptoms or those at risk for CA lesions (such as those with supra-avalvular aortic stenosis); and h) patient-specific tailoring of the contrast administration when indicated so that all information for a patient with CHD can be obtained in a single scan whenever possible (e.g., a patient with tetralogy of Fallot should have a contrast injection protocol that will allow visualization of both right- and left-sided structures, including CAs, in the same scan acquisition).

D. Nuclear Myocardial Perfusion Imaging

Nuclear myocardial perfusion imaging is not a sensitive or accurate technique for detecting anomalous coronary artery origin, but is frequently used to assess myocardial perfusion when a coronary anomaly places a patient at risk for ischemia. Single-photon emission computed tomography myocardial perfusion imaging (SPECT) is extensively utilized in adults to evaluate cardiac perfusion and func-

tion at rest and during dynamic exercise or pharmacologic stress for the diagnosis and management of patients with chest pain and possible CA ischemia. 99m-technetium (Tc99m)-labeled perfusion agents (99m-Tc-sestamibi and 99m-Tc-tetrofosmin) are the most commonly used radioisotopes. The sensitivity of stress myocardial perfusion imaging in children is reported to be 70-90%, while the specificity is about 60%.³⁰ The relatively high false-positive rate results from motion artifact during image acquisition, frequently related to respiration, and slow liver isotope clearance. New ultrafast SPECT cameras with cadmium-zinc-telluride-based detectors are faster and produce higher quality images with lower isotope dose, resulting in significantly reduced ionizing radiation exposure and decreased imaging times as compared to conventional SPECT cameras.³¹ A stress-only imaging protocol can decrease the length of the test from 3-4 hours to less than 90 minutes and decrease the radiation dose by 30–60%. Limited data are available on the utility of positron emission tomography (PET) in the evaluation of perfusion defects in children, and it is more expensive and not as readily available.

E. Angiography

Even as noninvasive imaging continues to improve, cardiac catheterization remains an important imaging modality in pediatric patients with CA anomalies. Advantages lie in the ability to evaluate the entire CA course and distribution in small infants and children with higher

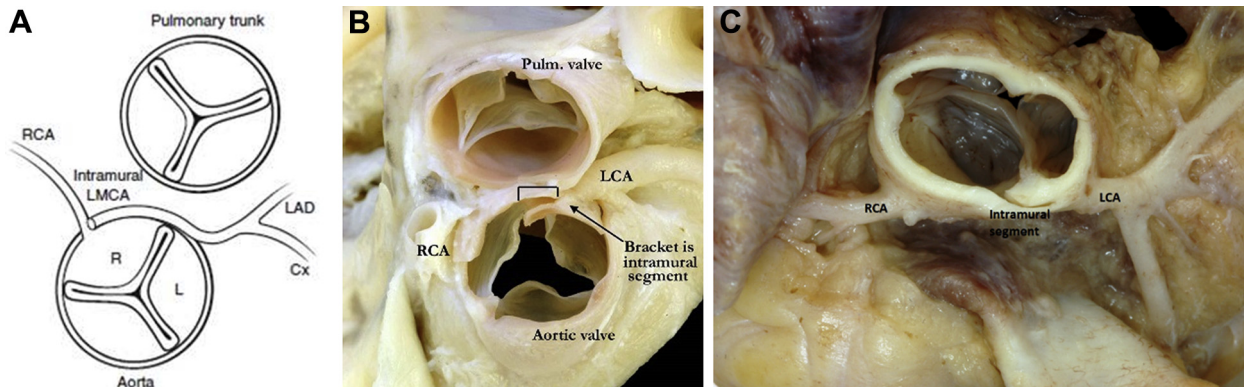


Figure 4 Illustration (A) and pathology specimens (B and C) of intramural anomalous left coronary artery originating from the right sinus of Valsalva. The cartoon shows the typical long intramural course of the left main coronary artery (LMCA) as it arises from the right sinus and courses within the anterior aortic wall before exiting the aortic root from the left sinus of Valsalva to provide the normally distributed left anterior descending (LAD) and circumflex (LCx) coronaries. Similar to A, Figure 4B demonstrates the anatomy from the echocardiographer's view, with the pulmonary valve (Pulm. valve) anterior, and the intramural segment of the left coronary artery (LCA) has been opened (bracket) as it courses through the anterior aortic wall. In C, with the orientation inverted, the slit-like length of the intramural segment within the aortic wall is clearly seen with the right coronary artery (RCA) also arising from the right sinus of Valsalva in its normal position. The illustration is from Frommelt MA, Frommelt PC. Vascular abnormalities. In: Eidem BW, O'Leary PW, Cetta F, eds. *Echocardiography in pediatric and adult congenital heart disease*. 2nd ed. Philadelphia, PA: Wolters Kluwer Health; 2015:470-485. The pathology images are from the Web Portal of the Archiving Working Group of The International Society for Nomenclature of Paediatric and Congenital Heart Disease (ISNPCHD) (<http://ipccc-awg.net>) and courtesy of Diane E. Spicer BS, PA (ASCP), University of Florida, Department of Pediatric Cardiology.

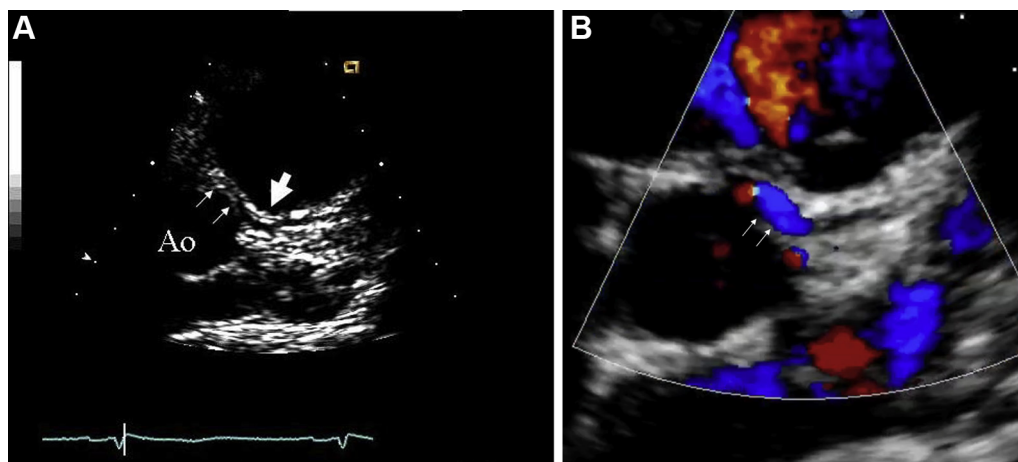


Figure 5 Short-axis image in a patient with interarterial AAOLCA with an intramural course of the anomalous coronary. In the 2-dimensional image (A), the left coronary appears to be exiting the aorta (Ao) appropriately from the left sinus of Valsalva (large arrow); however, on closer inspection, a long anomalous intramural segment can be appreciated coursing within the anterior aortic wall (small arrows). Color Doppler imaging (B) shows the linear diastolic flow of the anomalous coronary within the anterior aortic wall (arrows); the blue color signal confirms anomalous coronary flow away from the transducer, consistent with the coronary originating from the right sinus and coursing toward the more posteriorly positioned left sinus. A low Nyquist limit is needed to visualize the low-velocity coronary flow signal.

heart rates, whereas ECG gating and spatial resolution can be challenging with other noninvasive imaging modalities.²⁰ Selective angiography is also particularly useful in situations where small discrete CA occlusion or interruption exists with vessel reconstitution by collaterals. Distal distribution of flow and patency is also best assessed by direct imaging with catheterization as there remain limitations by other noninvasive means of imaging.^{32,33} Finally, intravascular ultrasound, to directly image CA wall architecture, and fractional flow reserve, to quantify flow changes across CA stenosis, are additional invasive adjunct techniques to assess anomalous CA pathology. Angiography may also be preferentially used at institutions where expertise and technical support to perform pediatric CCT/CMR is

lacking. As with other modalities requiring radiation such as CCT, the radiation dosing with newer equipment is significantly reduced without reduction in image quality.³⁴

III. ISOLATED CONGENITAL CORONARY ANOMALIES

A. Anomalous Aortic Origin of a Coronary Artery

1. Background. Anomalous aortic origin of a coronary artery (AAOCA) is a congenital anomaly whereby a CA arises from the

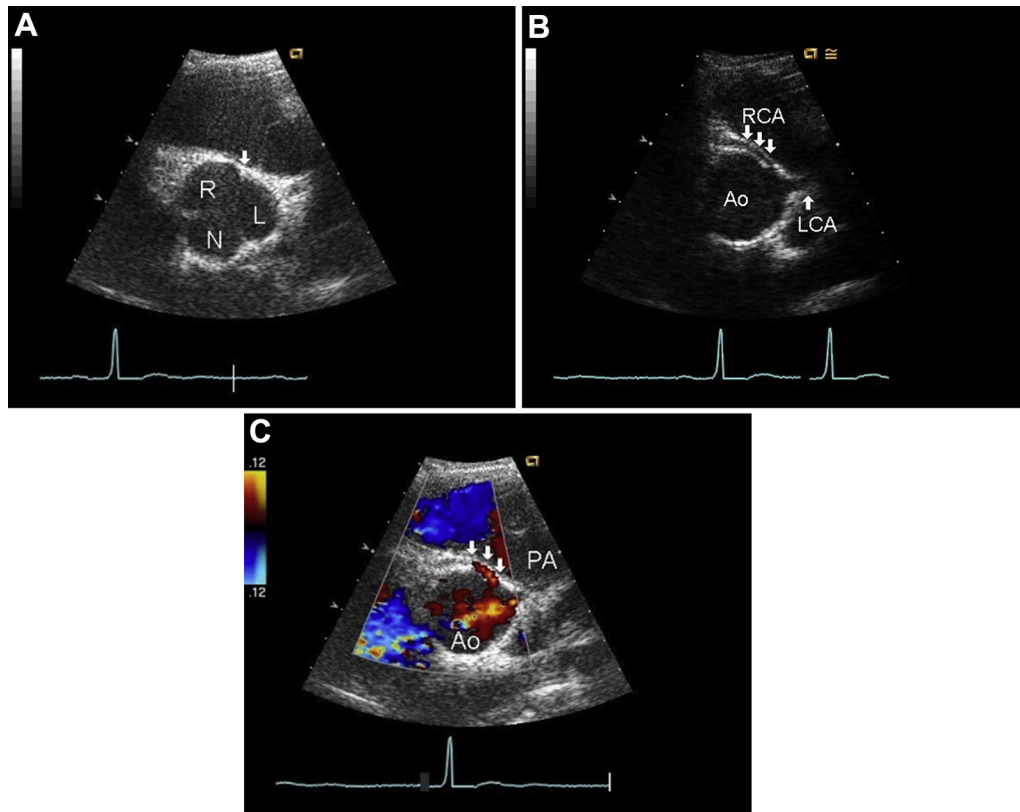


Figure 6 Short-axis imaging in a patient with interarterial AAORCA and an intramural course of the anomalous coronary. In **A**, the position of the aortic sinuses at the level of the aortic valve are visualized; the commissure between the right (R) and left (L) cusps is identified by an arrow. The non-coronary sinus (N) is seen posteriorly. Tilting the transducer more superiorly above the valve leaflets (**B**), the anomalous right coronary artery (RCA) can be seen arising at an acute angle from the left sinus of Valsalva near the origin of the left main coronary artery (LCA) and coursing intramurally within the anterior aortic (Ao) wall (arrows) between the aorta and the right ventricular outflow tract toward the right sinus of Valsalva. Comparing **A** and **B**, it can be appreciated that the anomalous coronary originates close to the commissure but clearly from the left sinus. Color Doppler imaging (**C**) shows the linear diastolic flow of the anomalous CA within the anterior aortic wall (arrows) between the aorta and pulmonary artery (PA); the red color signal confirms anomalous coronary flow toward the transducer, consistent with the coronary originating from the left sinus and coursing toward the more anteriorly positioned right sinus. Note the low Nyquist limit (12 cm/s) needed to visualize the low-velocity coronary flow signal. From Frommelt MA, Frommelt PC. Vascular abnormalities. In: Eidem BW, O’Leary PW, Cetta F, eds. *Echocardiography in pediatric and adult congenital heart disease*. 2nd ed. Philadelphia, PA: Wolters Kluwer Health; 2015:470-485.

opposite or contralateral sinus of Valsalva; in rare instances a CA can arise from the non-coronary sinus. This anomaly has been associated with myocardial ischemia and sudden death in children and adolescents, particularly when the anomalous CA courses between the great arteries.³⁵⁻³⁹ In fact, it is the second leading cause of sudden cardiac death in young athletes.³⁸ Noninvasive imaging is frequently the first modality utilized to make the diagnosis. The incidence of AAOCA is estimated at 0.7%, and anomalous aortic origin of the RCA from the left sinus of Valsalva (AAORCA) is six times more prevalent than anomalous origin of the LCA from the right sinus of Valsalva (AAOLCA).¹ The anomalous CA can arise from the opposite sinus and course anterior to the pulmonary artery (PA), posterior to the aorta (retro-aortic), or between them (interarterial) (Figure 3). AAOCA with an interarterial course is associated with increased risk for cardiac complications.

An interarterial CA can course within the myocardium between the great arteries (septal, intramyocardial, or intraconal course) or within the anterior wall of the aorta between the great arteries (intramural). AAOLCA with an interarterial and intramural course is associated with the greatest risk for sudden cardiac death (Figure 4),

although AAORCA with an intramural course has also been associated with sudden death. The etiology of sudden death in individuals with an interarterial AAOCA is likely myocardial ischemia, especially in younger patients (age <40 years) during or following strenuous activity, resulting from proximal vessel narrowing, ostial stenosis, an acute angle of origin of the anomalous CA, and/or compression/distortion of the interarterial segment with increased cardiac output during vigorous activity.^{40,41} Anomalous origin of the LCA from the non-coronary sinus with an intramural course and sudden cardiac death has also been reported.⁴⁰

The need for and timing of surgical intervention for AAOCA is quite controversial, with documented symptoms/signs of myocardial ischemia as the most common indication. Multiple surgical techniques have been used, including CA bypass graft placement, patch enlargement of the anomalous CA origin, reimplantation of the anomalous CA to the appropriate sinus, translocation of the pulmonary trunk, and unroofing of the intramural segment of the anomalous CA. The unroofing procedure is commonly used, particularly when there is an intramural CA, where the shared wall of the intramural segment is removed with creation of a neo-ostium in the

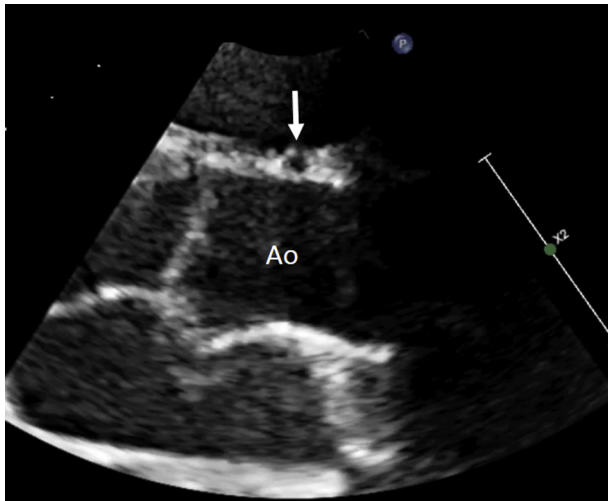


Figure 7 Parasternal long-axis imaging of an interarterial and intramural anomalous coronary coursing between the great arteries within the anterior aortic wall; the coronary can be seen as a discrete circle (arrow) immediately anterior to the aortic (Ao) root near the sinotubular junction.

appropriate sinus.⁴² Imaging of AAOCA anatomic features should involve delineation of the origin and course that provides the necessary information for optimal management, including the need and type of surgical intervention. Unfortunately, despite multiple imaging techniques that allow identification of AAOCA, effective risk stratification remains elusive with variable recommendations for best practices.^{9,43}

2. Goals of Echocardiographic Imaging. TTE can prospectively identify AAORCA and AAOLCA, particularly when there is an interarterial course.⁴⁴ Moreover, TTE is often the screening tool used to identify this lesion because many children are asymptomatic, and the diagnosis is often made when TTE has been ordered for other reasons. The CA origins can frequently be imaged by TTE when good transthoracic parasternal windows are available. The intramural course of AAOCA can be difficult to detect by echocardiography, particularly because the CA exit from the aortic wall is frequently at the usual or appropriate sinus of Valsalva (Figure 5A) with an unusually high origin from the sinus. In addition, the location of the ostium relative to the commissure/sinuses can sometimes be difficult to judge, especially when the anomalous coronary arises close to the commissure and/or has a high take-off.

The intramural segment in AAOLCA is longer and usually traverses at least half of the right sinus before exiting the aortic wall from the left sinus (Figure 5A). In contrast, the intramural course of AAORCA is usually characterized by a shorter (2 to 3 mm) intramural segment from the left sinus with the anomalous CA ostium arising adjacent to the commissure between the right and left coronary cusps (Figure 6A and B). An acute angle of ostial takeoff and linear diastolic flow adjacent to the aortic wall (visualized by color Doppler) are hallmark features of an intramural course by TTE.^{40,45,46} Color Doppler with a low Nyquist limit (20-30 cm/sec) is particularly useful because it helps to differentiate whether the anomalous CA arises from the right or left sinus. With AAOLCA, a blue Doppler signal is seen in the intramural segment as flow moves away from the right sinus toward the more posteriorly positioned left sinus (Figure 5C). In

AAORCA from the left sinus, a red Doppler signal will be seen in the intramural segment as flow moves toward the right sinus from its origin in the left sinus (Figure 6C).

Other transthoracic windows can also provide imaging evidence for AAOCA. From the parasternal long-axis view, the anomalous CA between the great arteries can be seen as a discrete circle immediately anterior to the aortic root as an initial clue (Figure 7). The parasternal long-axis view may also help identify a higher origin of the RCA from the sinotubular junction or ascending aorta. Subcostal scanning from the aortic root more anteriorly to the pulmonary trunk can identify an anomalous CA between the great arteries, suggesting an intramural course.⁴⁰ It is important to remember, however, that no imaging modality defines the histologic diagnosis of a shared tunica media. Ostial stenosis with AAOCA is frequently a concern, but despite reports that this can be identified by Doppler echocardiography,⁴⁷ this is very challenging to diagnose using echocardiography because of the need to use lower Nyquist limits for CA flow assessment, and so other imaging modalities are generally utilized to make that assessment. An intraconal CA course can be identified by visualization of the CA within the muscular conal septum inferior to the pulmonary valve annulus in subcostal and parasternal views (Figure 8A-C); these intraconal and interarterial AAOCA usually arise from a single coronary orifice (usually a single right CA).

Using transverse/axial esophageal imaging planes as previously described for CA visualization, TEE can provide complementary imaging in the assessment of CA origins, especially when the CA is interarterial and intramural (Figure 9).

3. Additional Imaging Techniques. Intravascular ultrasound (IVUS), although invasive, has been utilized to assess CA ostial stenosis, CA hypoplasia and localized systolic lateral compression of the intramural segments of an anomalous CA that courses within the aortic wall.⁴⁸ Not surprisingly, this degree of compression can be variable, likely causing unpredictable responses to exercise in this patient group. The CA narrowing can be exacerbated by a pharmacologic challenge that mimics exercise conditions with changes in aortic wall tension and resultant intramural coronary distortion.

The sagittal stack with CCT can provide sequential images of the CA lumen adjacent to the aortic wall in the interarterial space, allowing for recognition of the acute angle takeoff, the CA course “hugging” the aortic wall, and abrupt change in caliber as it separates from the aortic wall more distally from the opposite sinus, all highly suggestive of an intramural course (Figure 10). The distance of the intramural or interarterial segment can be measured. The change in both caliber and sphericity at the levels of the ostium, the interarterial segment, and the distal vessel should be evaluated to assess for change from circular to oval shape.^{49,50} 3D reconstructions can help determine ostial and proximal coronary artery anatomy as well as the relationship of the anomalous CA to the great arteries (Figure 11). An intraseptal or intraconal CA course, as described above, can be imaged by following the CA from the aortic sinus inferiorly to the interventricular septum where the “hammock sign” is seen when the LCA courses into the conal septum from the right and then exits the conus to its final distal epicardial location, thus mimicking the appearance of a hammock (Figure 8D). Both CCT and CMR can help differentiate the intraconal and intramural forms of AAOCA.⁸

CMR also can provide high-quality imaging for AAOCA (Figure 12) and has potential added value in documentation of ostial abnormalities⁷ and myocardial fibrosis (suggestive of infarction), as

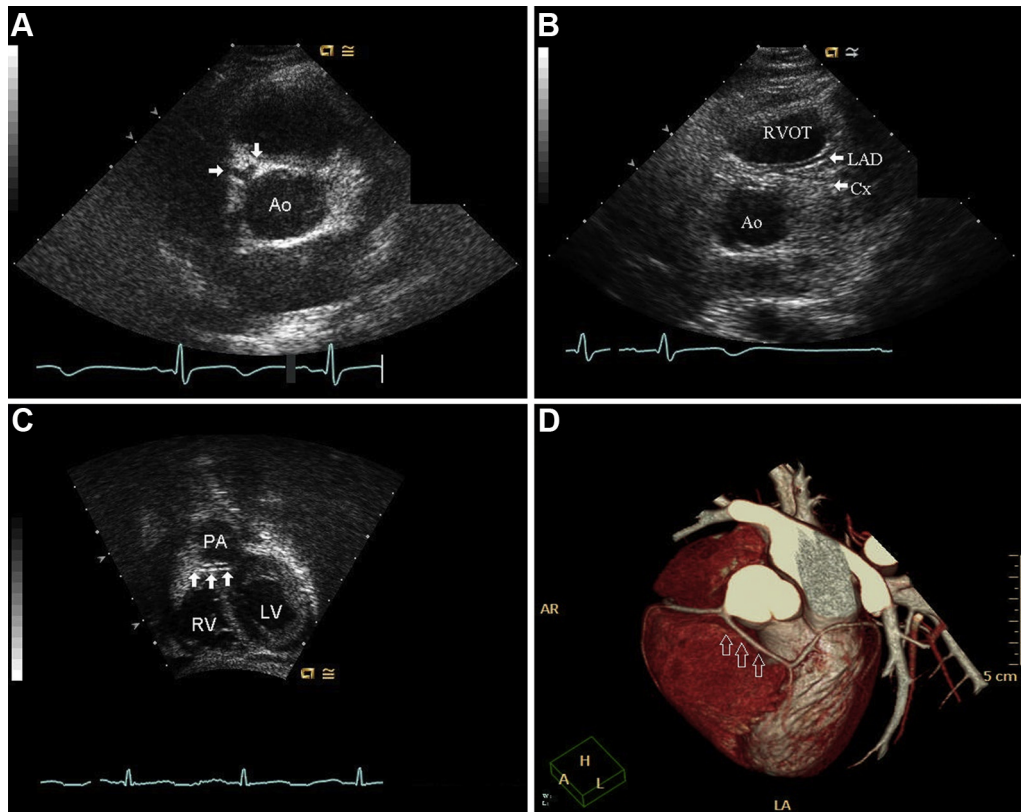


Figure 8 Echocardiographic and CT imaging in a patient with AAOLCA and an intraconal course of the anomalous coronary. In **A**, a single coronary originates from the aorta (Ao), arising from the right sinus of Valsalva and immediately bifurcating into the right and left main coronaries (arrows). No coronary is seen arising from the left aortic sinus. In **B**, the anomalous left coronary can be seen coursing between the aorta and right ventricular outflow tract (RVOT) within the myocardial sulcus before bifurcating into the left anterior descending (LAD) and circumflex (Cx) branches. Again, no coronary is seen arising from the left aortic sinus, and the anomalous coronary is clearly separate from the anterior aortic wall (helping to differentiate it from an intramural interarterial course). In **C** and **D**, the “hammock sign” appearance of the anomalous coronary is demonstrated as it courses through the myocardial sulcus of the right ventricular outflow tract (arrows) below the pulmonary artery (PA). The echocardiographic image (**C**) is a subcostal view of the coronary course, and **D** shows the anomalous coronary and hammock sign by CT reconstruction. Echocardiographic images are from Frommelt MA, Frommelt PC. Vascular abnormalities. In: Eidem BW, O’Leary PW, Cetta F, eds. *Echocardiography in pediatric and adult congenital heart disease*. 2nd ed. Philadelphia, PA: Wolters Kluwer Health; 2015:470-485.

well as assessment of myocardial perfusion at rest and with stress imaging.^{9,16,17} Thus far, none of the techniques for provocative myocardial perfusion testing has yielded additional risk stratification for AAOCA, particularly when found in an asymptomatic child or young adult serendipitously.

Key Points for Anomalous Aortic Origin of a Coronary Artery

- AAOCA is relatively common and usually benign, but certain forms, particularly when a CA courses between the great arteries, are associated with sudden death.
- Echocardiography identifies AAOCA with an interarterial course, and important markers include:
 - Oblique origin of the anomalous CA from the opposite sinus
 - When intramural, an anomalous course within the anterior aortic wall with an acute angled origin that can be demonstrated by color Doppler mapping

- When intraconal, an anomalous course within the muscular conal septum inferior to the pulmonary valve annulus
- Complementary imaging techniques, particularly CCT and CMR, can help define AAOCA anatomy, specifically the ostia, caliber, and distal branching, but accurate risk stratification for sudden death remains elusive.
- The utility of myocardial stress imaging and IVUS in asymptomatic patients in decision-making about intervention is also unclear.

Recommended Imaging Strategy for Anomalous Aortic Origin of a Coronary Artery

- TTE should be the initial screening tool for suspected AAOCA, particularly in forms that are associated with myocardial ischemia (those with an interarterial course).
- When an interarterial AAOCA is identified, delineation of anomalous ostial origin/size and course should be confirmed with CCT and/or CMR.

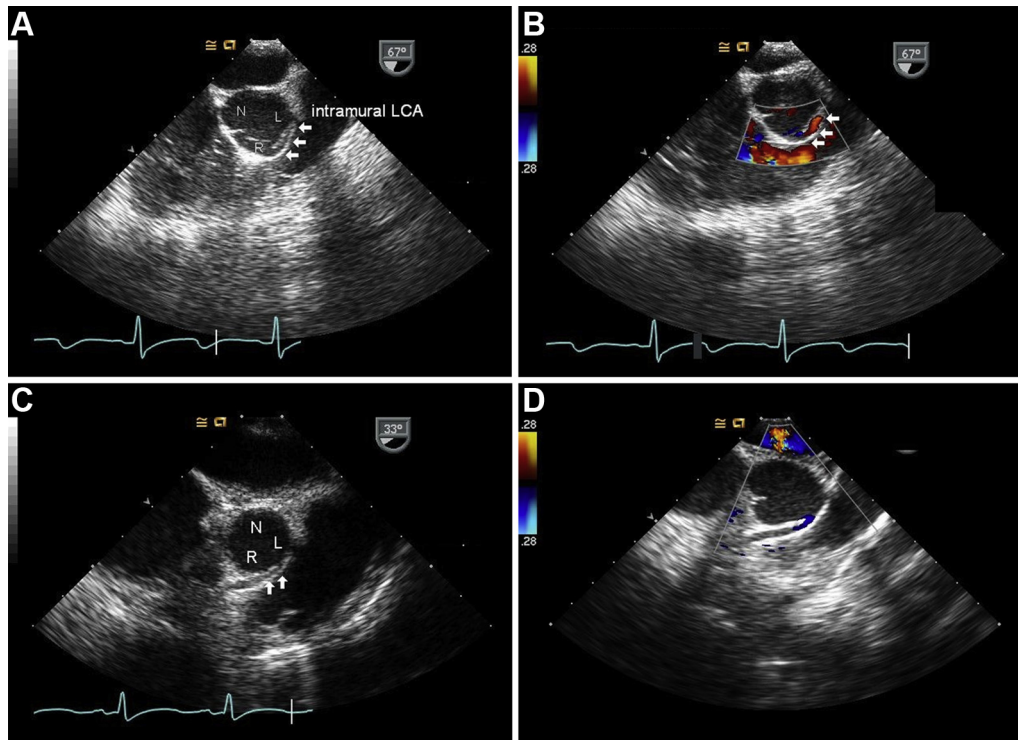


Figure 9 Transesophageal images from a mid-esophageal short-axis view through the aortic root in a patient with AAOLCA (**A** and **B**) and AAORCA (**C** and **D**), both with an intramural course of the anomalous coronary. In **A**, the anomalous left coronary artery (LCA) can be seen arising from the right sinus of Valsalva (R) and coursing intramurally within the anterior aortic wall (*arrows*) between the aorta and right ventricular outflow tract toward the left sinus of Valsalva (L). Color Doppler (**B**) shows the direction of flow toward the transducer (*red color signal*) as the anomalous coronary courses from the more anteriorly positioned right sinus to the more posteriorly positioned left sinus. In **C**, the anomalous RCA can be seen arising from the left sinus of Valsalva and coursing intramurally within the anterior aortic wall (*arrows*) between the aorta and right ventricular outflow tract toward the right sinus of Valsalva. Color Doppler (**D**) again shows the direction of flow away from the transducer (*blue color signal*) as the anomalous coronary courses from the more posteriorly positioned left sinus to the more anterior right sinus. In both examples, the non-coronary cusp (N) is seen posteriorly. From Frommelt PC. Congenital coronary anomalies. In: Wong, Miller-Hance, Silverman, eds. *Transesophageal Echocardiography for Congenital Heart Disease*. New York, NY: Springer; 2014.

- Resting and stress myocardial perfusion assessment may be used to help identify ischemia and/or correlate symptoms in AAOCA.

B. Anomalous Pulmonary Origin of a Coronary Artery

1. Background. Anomalous origin of the LCA from the PA (ALCAPA) is a rare but well recognized CA anomaly, occurring in 1 in 300,000 children.⁵¹ The majority of these CA anomalies present in infancy and constitute one of the most significant causes of myocardial ischemia and heart failure in the pediatric age group. Anomalous origin of the RCA from the PA (ARCAPA), as well as anomalous origin of LCA branches (such as the LCx) from the PA are much rarer than ALCAPA and have a variable presentation. ARCAPA incidence has been reported as 0.002%,⁵² or 0.12% of all CHD cases.⁵³ ARCAPA is often associated with other congenital cardiac abnormalities, most commonly aorto-pulmonary window or tetralogy of Fallot.^{52,54} In rare instances, ALCAPA and origin of the circumflex CA from the PA has also been noted with other forms of congenital heart lesions and should be considered as a possible etiology for worsening ventricular function and mitral regurgitation after repair. This

discussion will focus on the clinical and imaging findings in isolated ALCAPA.

The typical time and mode of clinical presentation in patients with ALCAPA are related to the transitional fall in PA pressures and vascular resistance in the first weeks of life and the subsequent development of collateral CA flow from the RCA to supply the LV myocardium. Infants with inadequate collateralization develop signs of myocardial ischemia, which may present clinically as feeding intolerance, tachypnea, pallor, and failure to thrive. Myocardial ischemia results in LV dilation and dysfunction, papillary muscle fibrosis/scarring and mitral regurgitation (MR), with eventual development of dilated cardiomyopathy, worsening MR, and heart failure. If left unrecognized, there is an overall mortality of 90% in those infants who do not undergo surgical repair in the first year of life.⁵⁵

Children with ALCAPA who have well-developed collateral CA flow will often have preserved LV systolic function and a delayed clinical presentation into adolescence or adulthood.⁵⁵⁻⁵⁷ This cohort does not characteristically present with heart failure but rather comes to clinical suspicion by the presence of a cardiac murmur or exercise intolerance; rarely, this cohort may also present with sudden cardiac death as adults.⁵⁸ Patients with isolated ARCAPA may present during infancy with heart failure and/or ischemia symptoms, but

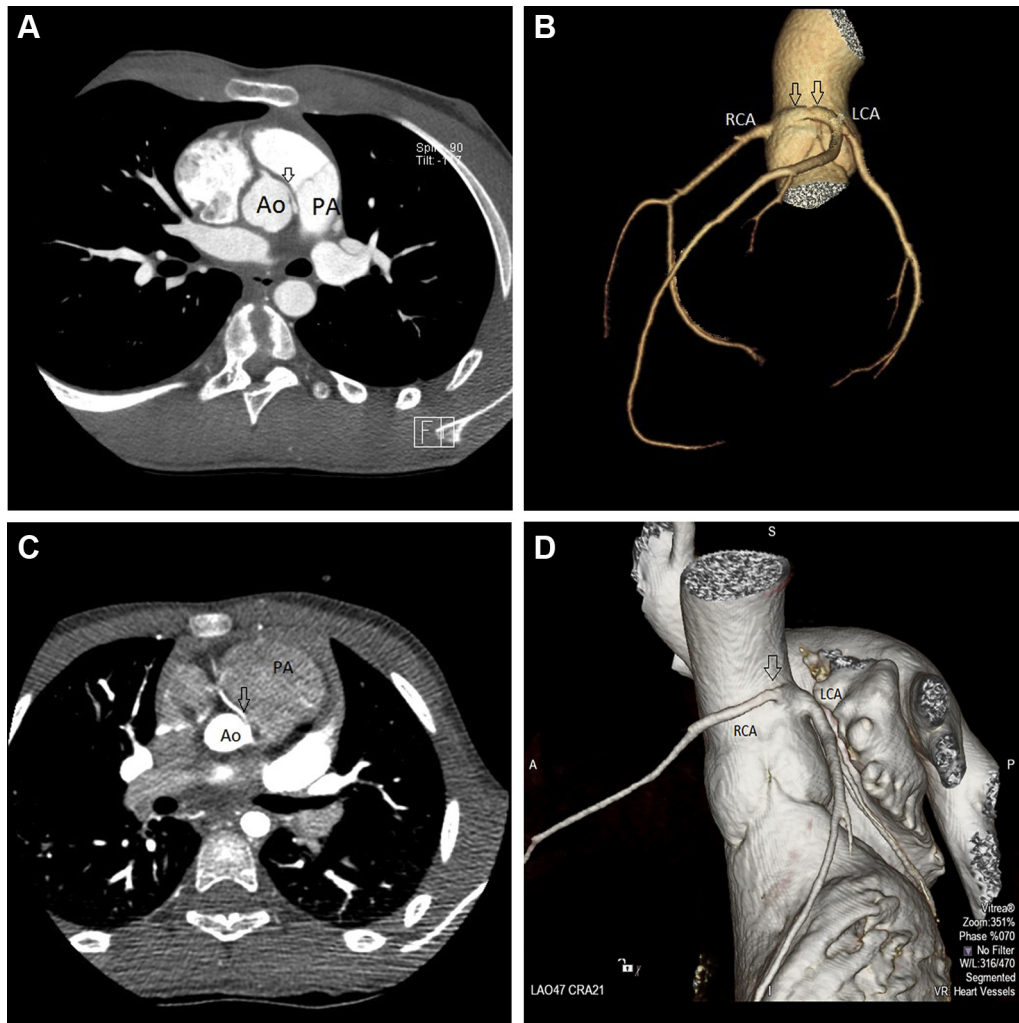


Figure 10 2D and 3D CT imaging of a patient with AAOLCA with an interarterial intramural course (**A** and **B**) and a patient with AAORCA with an interarterial intramural course (**C** and **D**). In both cases, the intramural course (*arrows*) can be seen from short-axis 2D imaging (**A** and **C**) and from 3D reconstructions (**B** and **D**) of the coronaries as the anomalous coronary arises obliquely from the opposite sinus with a proximal course within the anterior aortic wall between the aorta (Ao) and pulmonary artery (PA). The longer intramural course of the anomalous left coronary artery (LCA) compared to the anomalous right coronary artery (RCA) can be appreciated, and the more superior origin of the anomalous RCA from above the sinotubular junction is also apparent.

more commonly are diagnosed serendipitously when an echocardiogram is performed in an asymptomatic older child or adult for other indications (such as a heart murmur or cardiomegaly), or when assessed for associated CHD.

Surgical correction in patients with ALCAPA is performed to re-establish anterograde flow from the aorta to the LCA.⁵⁹ Surgical intervention is indicated in all patients whenever the lesion is identified, regardless of age. Direct reimplantation of the anomalous CA into the aorta is the surgery of choice⁵⁹ and often results in rapid recovery of myocardial function with excellent overall survival.⁶⁰⁻⁶³ Alternative surgical approaches, such as the Takeuchi procedure,⁶⁴ rely on the creation of a tunnel from the PA to the aorta in patients with an unfavorable anatomy for direct reimplantation (LCA origin far from the aorta), but this procedure is associated with a higher incidence of postoperative complications, including supravalvular pulmonary stenosis and baffle leaks.^{65,66} Long-term remodeling after surgical repair most commonly results in improved LV geometry, increased LV ejection fraction, and decreased MR. Diastolic dysfunction

from the previous myocardial ischemia and infarction frequently persists.

2. Goals of Echocardiographic Imaging. a. Pre-operative Assessment.—TTE is the diagnostic imaging modality of choice in the identification of ALCAPA in infants, whereas alternative imaging modalities such as cardiac CCT, CMR, and/or cardiac catheterization may be needed to confirm the diagnosis in some infants and in older children and adults when the diagnosis is unclear/acoustic windows are limited. This is particularly true when there is associated CHD. Goals of the pre-operative TTE examination with 2D and color Doppler imaging include demonstration of the anomalous origin of the LCA from the PA as well as the direction of flow within the LCA.⁶⁷ In addition, characterizing the normal origin of the RCA from the right sinus of Valsalva as well as any dilation of the RCA system by both color Doppler and 2D imaging is also important.^{68,69} Finally, quantitative assessment of biventricular size and function, mitral valve function, and

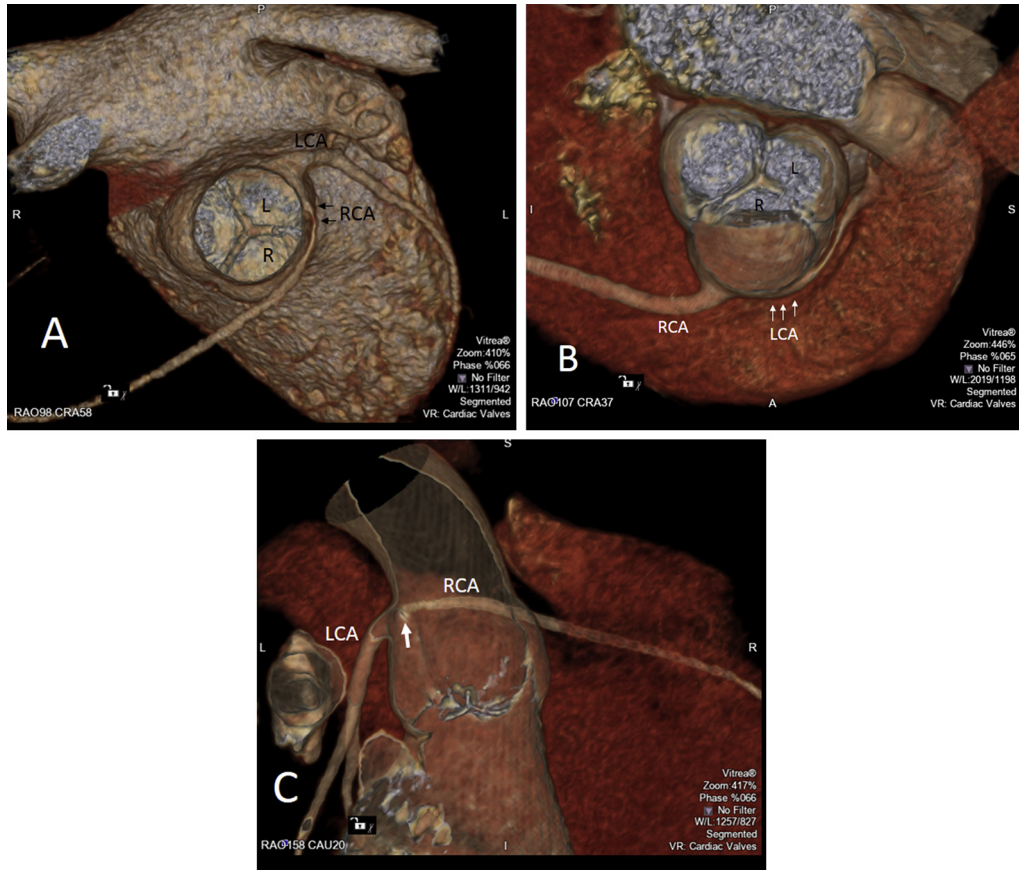


Figure 11 3D CT reconstructions of interarterial AAORCA and AAOLCA. In **A**, the anomalous right coronary artery (RCA) can be seen arising from the left (L) sinus of Valsalva in a short-axis equivalent view. The acute angle of origin from the left sinus (in contrast to the perpendicular angle of origin of the normally arising left coronary artery (LCA)) and narrowed ostium of the RCA (arrows) and its relationship to the aortic valve leaflets and right sinus (R) are clearly demonstrated. Similarly, in **B**, the anomalous LCA is seen arising at an acute angle from the right sinus and coursing posteriorly towards the left sinus. Figure **C** shows an endoluminal posterior view that demonstrates severe ostial stenosis and anomalous origin of the RCA from the superior aspect of the left aortic sinus.

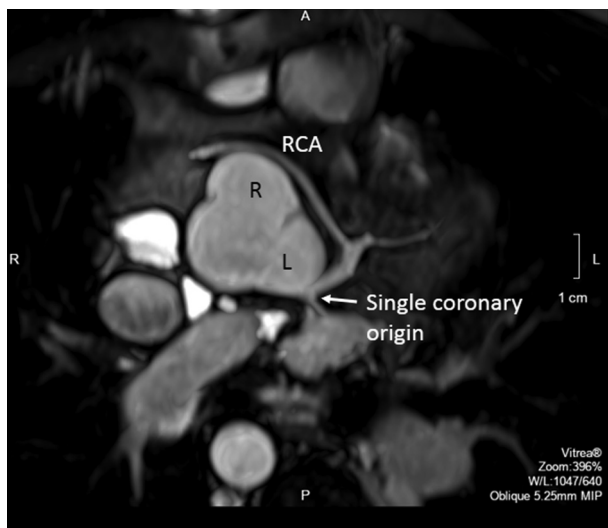


Figure 12 MRI coronary imaging from a short-axis equivalent view of a single left coronary artery arising from the left sinus of Valsalva with the right coronary branch coursing anterior to the aortic root to its usual distribution.

exclusion of additional associated cardiac lesions are also important, both clinically and surgically.

Direct TTE visualization of the anomalous CA origin from the PA is best accomplished from the parasternal short-axis and long-axis scan planes (Figure 13A). The anomalous LCA typically inserts into the posterior and leftward aspect of the main PA, coursing close to its normal origin in the left sinus of Valsalva. This is the least commonly identified finding, however, because dropout of the tissue separating the CA from the aorta can give the false impression of a normal LCA origin.⁷⁰ Identification of retrograde filling of the LCA using color Doppler is an essential echocardiographic component of the diagnosis of ALCAPA (Figure 13B). Color flow in the normally originating LCA progresses away from the aortic root (red Doppler signal in parasternal short-axis view). In ALCAPA, color Doppler identifies retrograde LCA filling (flow reversal in the LCA from myocardium to PA), and this retrograde flow can often be seen emptying into the main PA.⁶⁷ Very rarely, persistent pulmonary hypertension can maintain anterograde flow in the anomalous left coronary, so that retrograde flow is not appreciated.⁷¹ In older patients with delayed clinical presentation, extensive collateralization that provides the LV myocardium with its necessary CA supply results in RCA vessels that become significantly dilated (Figure 14A) and tortuous with prominent color flow Doppler signals within the ventricular septum

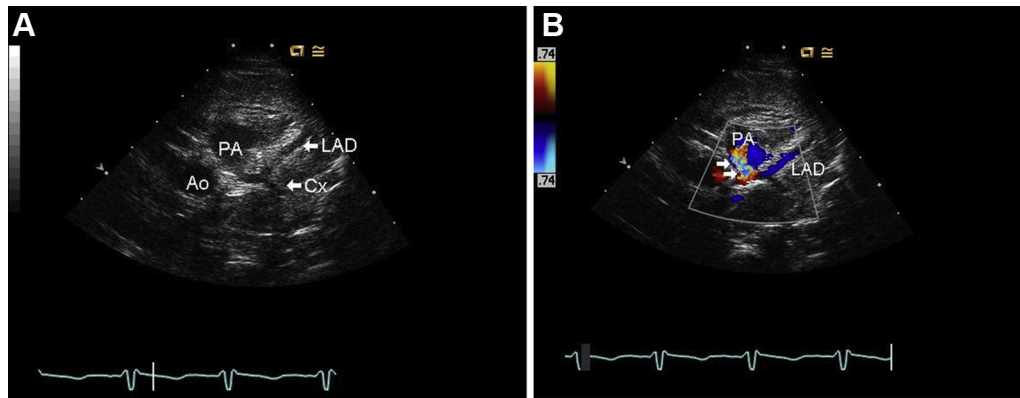


Figure 13 Parasternal short-axis images of anomalous origin of the left coronary artery from the posterior aspect of the proximal main pulmonary artery (PA) in an infant with ALCAPA. In **A**, the left anterior descending (LAD) and circumflex (Cx) coronary arteries are both seen arising from the left main coronary segment, clearly a long distance from the normal entrance into the aortic root (Ao). Color Doppler interrogation of the left coronary (**B**) identifies retrograde flow in the LAD. Flow in the LAD is blue as it moves away from the transducer toward the PA, which is abnormal since blood flow should be away from the aortic root (and thus displaying a red color Doppler signal) rather than toward it. A turbulent flow signal (arrows) is also seen in the PA as the anomalous left coronary empties into the low-pressure PA. From Frommelt MA, Frommelt PC. Vascular abnormalities. In: Eidem BW, O’Leary PW, Cetta F, eds. *Echocardiography in pediatric and adult congenital heart disease*. 2nd ed. Philadelphia, PA: Wolters Kluwer Health; 2015:470-485.

and LV myocardium (Figure 14B).⁶⁹ This prominent flow can be mistaken for multiple muscular ventricular septal defects. The timing of flow in the ventricular septum is helpful to make the distinction.

Finally, in patients with inadequate RCA collateralization, LV dilation with both systolic and diastolic LV dysfunction is often demonstrated. Bright endocardial scarring, almost always inclusive of the mitral papillary muscles, is often evident on 2D imaging and is consistent with endocardial fibroelastosis. This myocardial and/or papillary muscle scarring can result in significant MR, chamber dilation, and worsening heart failure (Figure 15).⁷¹ Echocardiographic findings of ALCAPA are variably identified and are summarized in Table 2⁷⁰; of note, no finding is 100% identified by echocardiography, so other modalities may be required to make the diagnosis if there is high suspicion based on the clinical presentation and/or echocardiographic demonstration of LV dilation and endocardial fibroelastosis in an infant.

b. Post-operative Assessment.—Serial TTE evaluation after ALCAPA repair is essential to characterize the presence and extent of LV remodeling, improvement in ventricular performance, and the decrease in degree of MR.^{59,71} In most patients, there is significant improvement in all of these parameters. However, LV dysfunction and MR may persist and occasionally require additional intervention, including mitral valve repair/replacement and, in rare cases, heart transplantation. Ongoing assessment of LCA patency and adequacy of CA supply to the LV myocardium is also essential, with stress echocardiography and deformation imaging providing insights into the long-term viability and functional reserve of the myocardium.^{72,73} Post-operative imaging assessment should also include evaluation of the main PA in patients who undergo Takeuchi-type repair, as main PA stenosis or baffle leak in the region of the baffled CA artery may occur (Figure 16).⁷⁴

3. Additional Imaging Techniques. As previously stated, additional imaging modalities may be required when there is high suspicion for ALCAPA but TTE is inconclusive, particularly in those with associated CHD. They are used to better delineate residual and/or recurrent cardiac abnormalities following ALCAPA surgical repair.

Although angiography has been the gold standard for confirmation of ALCAPA, CCT is now commonly used to confirm the origin and course of suspected cases of ALCAPA (Figure 17) or ARCAPA in infants and children, and to better characterize collaterals as well as to delineate CA anatomy after surgical intervention. ALCAPA is best evaluated with a double oblique centerline obtained through the PA and evaluated cranially until the anomalous CA origin is visualized. Once this origin is visualized, the centerline should be placed in the CA, displaying the length of the CA and the relationship to both the aorta and the PA.⁷⁵ The CA arising normally from the aorta is often enlarged if it has supplied a significant amount of the anomalous CA territory. Both angiography and CCT are excellent techniques for post-op assessment of ALCAPA after surgical intervention, particularly if there are concerns about CA patency, either with direct reimplantation and with baffling procedures.

CMR can also be quite useful in the assessment of older children and adults with ALCAPA or ARCAPA, both prior to and following surgical repair.^{72,76} In particular, CMR has been used to assess for residual CA stenosis and/or thrombosis, degree of MR, and for the presence of regional myocardial dysfunction or myocardial fibrosis, both at rest and with CMR adenosine stress perfusion imaging.⁷⁷

Key Points for Anomalous Left Coronary Artery from the Pulmonary Artery

- ALCAPA is a rare but treatable cause of dilated cardiomyopathy in infants and children and should be ruled out at presentation.
- Echocardiography is the diagnostic imaging modality of choice in ALCAPA, but other imaging techniques may be necessary if the diagnosis is uncertain.
- Characteristic echocardiographic hallmarks in the diagnosis of ALCAPA include:
 - Direct visualization of the origin of the LCA from the PA by 2D imaging
 - Retrograde color flow Doppler from the LCA into the PA
 - Extensive RCA dilation and tortuosity by 2D imaging

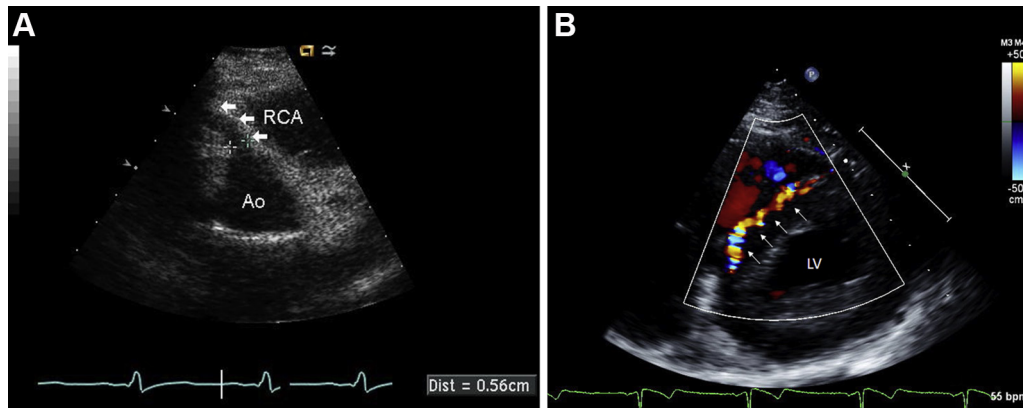


Figure 14 Parasternal short-axis imaging of a 10-year-old child with ALCAPA. In **A**, the right coronary artery (RCA) arises appropriately from the anterior aspect of the aorta (Ao) and is markedly dilated (*arrows*) because of the chronically increased flow into that coronary, which measured 5.6 mm in diameter proximally. Color Doppler interrogation of the ventricular septum (**B**) shows coronary collateral flow. A turbulent linear diastolic flow signal is seen in the ventricular septum (*arrows*) anterior to the left ventricle (LV). The color Doppler and spectral Doppler timing of flow in diastole helps differentiate this septal collateral from a VSD, which is generally characterized by a high-velocity systolic flow signal.

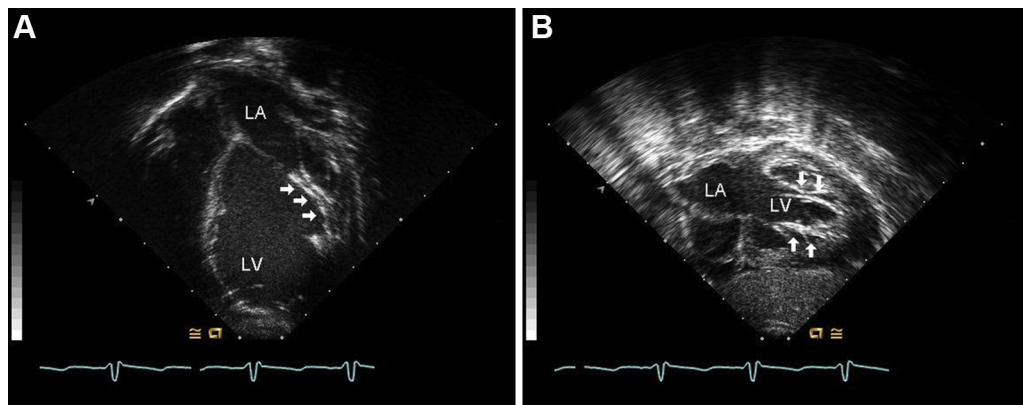


Figure 15 Apical 4-chamber (**A**) and subcostal 4-chamber (**B**) images of an infant with dilated cardiomyopathy and ALCAPA showing marked left atrial (LA) and left ventricular (LV) chamber dilation with echo-dense fibrotic changes of the mitral valve papillary muscles (*arrows*), consistent with chronic endocardial ischemia/fibroelastosis. From Frommelt MA, Frommelt PC. Vascular abnormalities. In: Eidem BW, O’Leary PW, Cetta F, eds. *Echocardiography in pediatric and adult congenital heart disease*. 2nd ed. Philadelphia, PA: Wolters Kluwer Health; 2015:470-485.

Table 2 Incidence of echocardiographic markers of ALCAPA from preoperative echocardiograms

Marker	Total studies reviewed	Positive finding	Sensitivity (%)
Visualization of anomalous CA origin	35	19	54
Flow reversal in LCA	33	30	91
Collateral CA flow	33	28	85
RCA dilation	31	25	81
Abnormal Doppler signal in PA	34	27	79
Mitral valve insufficiency	35	26	74
LV systolic dysfunction (LVEF < 45%)	35	23	66
LV EFE	35	20	57

ALCAPA, Anomalous left coronary artery from the pulmonary artery; CA, coronary artery; EFE, endocardial fibroelastosis; LCA, left coronary artery; LV, left ventricular; LVEF, left ventricular ejection fraction; PA, pulmonary artery.

Adapted from Patel SG, Frommelt MA, Frommelt PC, Kutty S, Cramer JW. Echocardiographic Diagnosis, Surgical Treatment, and Outcomes of Anomalous Left Coronary Artery from the Pulmonary Artery. *J Am Soc Echocardiogr*. 2017; 30(9):896-903.

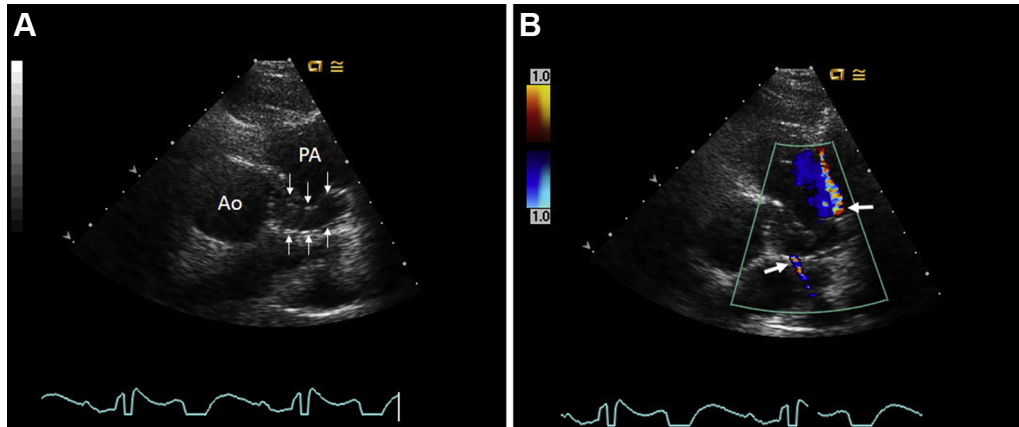


Figure 16 Parasternal short-axis imaging in a young adult with ALCAPA s/p Takeuchi-type repair. In **A**, the widely patent baffling (arrows) of the anomalous left coronary to the aorta (Ao) through the main pulmonary artery (PA) is seen. In **B**, color Doppler interrogation shows 2 discrete jets (arrows) of baffle leaks from the coronary tunnel into the main PA.

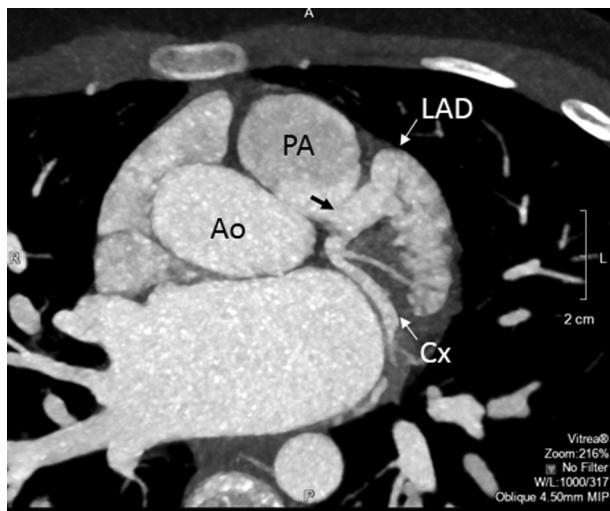


Figure 17 Contrast CT image from a short-axis plane shows ALCAPA with the anomalous left coronary (arrow) arising from the posterior aspect of the pulmonary artery (PA). The separation between the left coronary and aorta (Ao) is clearly evident. The left anterior descending (LAD) and circumflex (Cx) branches can be seen arising from the anomalous left main coronary.

Table 3 Location of coronary origin and termination site for coronary fistula

Origin	Coronary artery fistula termination site					
	PA	RV	RA	LV	LA	Other
LCA	16%	41%	26%	5%	7%	5%
LMT	50%	19%	19%	9%	3%	-
LAD	28%	57%	4%	11%	-	-
LCX	-	35%	31%	10%	6%	18%
RCA	13%	49%	26%	8%	1%	3%

LCA, Left coronary artery; LMT, left main trunk; LAD, left anterior descending; LCX, left circumflex; RCA, right coronary artery; PA, pulmonary artery; RV, right ventricle; RA, right atrium; LV, left ventricle; LA, left atrium.

Revised from Holzer R. *et al.* *Cardiol Young* 2004 14; 380-385.

- After repair, CCT and/or CMR may be used when there are concerns about coronary anatomy and/or persistent myocardial perfusion abnormalities.

- Prominent intramyocardial color Doppler signals within ventricular septum and LV myocardium due to dilated RCA collaterals
- Significant LV chamber dilation and dysfunction
- Mitral valve papillary muscle fibrosis with significant MR

Recommended Imaging Strategy for Anomalous Left Coronary Artery from the Pulmonary Artery

- TTE should be the primary screening tool and is usually diagnostic in suspected ALCAPA in infants and children.
- Confirmation of the diagnosis using CCT or CMR should be reserved for cases where the anatomy is unclear; cardiac catheterization is rarely needed for diagnosis.

C. Isolated Congenital Coronary Artery Fistulas

1. Background. A congenital CA fistula (CAF) is a direct communication between a CA and any cardiac chambers, the coronary sinus, the systemic or pulmonary veins, or the pulmonary arteries, bypassing the myocardial capillary bed.^{78,79} Although rare, a CAF may cause myocardial ischemia, volume overload of the cardiac chambers, or pulmonary hypertension when it increases pulmonary blood flow. The majority of isolated CAFs involves only a single fistula, and the involved coronary bed is more commonly the LCA (39-63%); less often the RCA (29-55%), and least often both (7-19%).⁸⁰⁻⁸⁵ The site of drainage for CAFs is usually a right heart structure; the LV or left atrium are the least common termination sites. CAF termination sites according to CA origin are summarized in Table 3. In individuals with CHD, pulmonary atresia with intact septum and hypoplastic left heart syndrome are most commonly associated with CAF, and these entities are discussed later in this article. CAFs are otherwise rare in CHD, although acquired fistulas

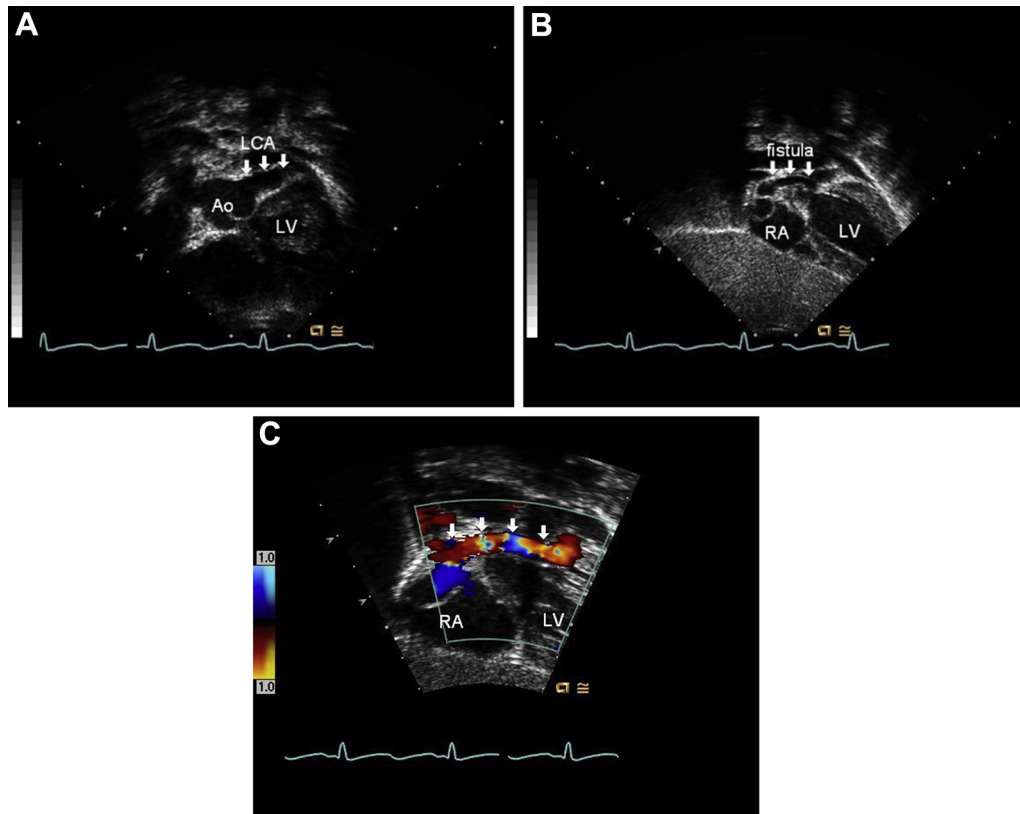


Figure 18 Subcostal images of a coronary artery fistula entering the right atrium in a child with a left coronary artery to right atrial fistula. The markedly dilated left coronary artery (LCA) arising from the aorta (Ao) above the left ventricle (LV) is seen in **A**. The transducer is tilted more posteriorly in **B** as the fistula courses posterior to the aorta (arrows) with the terminal segment of the fistula emptying into the right atrium (RA). With color Doppler (**C**), the turbulent flow throughout the length of the fistula as it courses toward the right atrium is well visualized (arrows). From Frommelt MA, Frommelt PC. Vascular abnormalities. In: Eidem BW, O’Leary PW, Cetta F, eds. *Echocardiography in pediatric and adult congenital heart disease*. 2nd ed. Philadelphia, PA: Wolters Kluwer Health; 2015:470-485.

are seen after surgical RV muscle bundle resection, most commonly as part of tetralogy of Fallot repair.

Size of the CAF is important, as the physiologic impact is related to the amount of flow through that abnormal channel. A small CAF, with low-volume fistulous flow, is usually benign, clinically silent, and may close spontaneously. A large CAF, however, rarely closes spontaneously and frequently enlarges with time because of the high-volume flow; there is a progressive increase in CA size proximal to the fistulous site, which sometimes leads to aneurysmal dilation. A large CAF can cause significant complications, including congestive heart failure due to the large shunt through the fistulous connection, myocardial ischemia related to steal of CA blood flow from the CAF, thrombus formation in the dilated proximal CA segment, ventricular arrhythmias, infectious endocarditis, pulmonary hypertension, syncope, stroke, and even sudden death.⁸⁶ American College of Cardiology/American Heart Association guidelines recommend closure of all large CAFs regardless of symptomatology; smaller than moderate sized CAFs with symptoms; or CAFs associated with documented myocardial ischemia, arrhythmia, otherwise unexplained ventricular systolic/diastolic dysfunction, ventricular enlargement, or endarteritis.⁸⁷ Either transcatheter device closure or surgical ligation to obliterate the shunt without compromising the normal CA branches is utilized when intervention is needed.

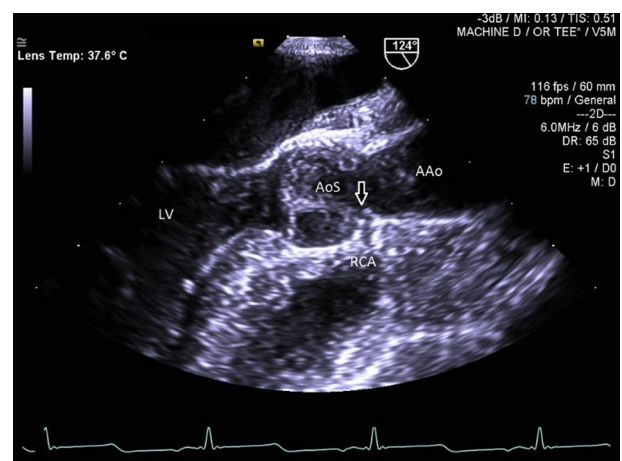


Figure 19 Longitudinal TEE image of the left ventricular outflow tract and aorta in a child undergoing surgery for supravulvar aortic stenosis. The right coronary artery (RCA) arises immediately below the supravulvar ridge (arrow) from a more superior position in the aortic sinus (AoS) near the sinotubular junction, with the potential for alternating coronary flow. AAo, Ascending aorta.



Figure 20 CT 3D reconstruction of the aortic root and ascending aorta (AAo) in a child with supravalvular aortic stenosis. The origins of both the right (RCA) and left (LCA) coronary arteries are immediately below the supravalvular narrowing (arrow) with both coronaries arising from a more superior position in the aortic sinus. The left coronary origin is also covered by the left coronary cusp, as the sinus appears walled off from the rest of the aortic root.

2. Goals of Echocardiographic Imaging. *a. Pre-intervention Assessment.*—TTE can be useful in identifying a CAF, with enlargement of the proximal CA that supplies the fistula as a constant observation when the shunt flow is significant.⁸⁸ The proximal CAs can become quite dilated and tortuous (Figure 18A), and the recipient chambers can also become dilated.^{79,89} The parasternal short-axis view is useful to identify this dilation. If the fistulous site is located distally, the dilation and tortuous deformation tends to involve the entire CA (Figure 18B). If the fistula is located more proximally, the proximal CA tends to develop aneurysmal dilation, and the CA distal to the fistulous site is usually normal in shape.⁷⁸ Significant CA dilation may progress to aortic sinus deformation, which in turn may lead to aortic valve regurgitation.⁹⁰

The origin, pathway, and exit of the CAF are usually visualized using color Doppler mapping (Figure 18C). When the CAF origin is unclear based on 2D imaging, high-velocity flow signals in the CA can identify the artery from which the fistula originates.⁸⁹ A continuous high-velocity signal is observed when the CAF drains into a low-pressure chamber, such as the right atrium or coronary sinus; however, when it empties into a high-pressure chamber (the LV or a hypertensive RV), the shunt flow only occurs during diastole.⁸⁹ Scanning the cardiac chambers from all available views with color Doppler mapping, particularly from the subcostal window, can be useful in evaluating the CAF, since continuous or diastolic high-velocity signals can be imaged along the length of the CAF to the termination site.⁹¹ Although it is rare to observe dilation of cardiac chambers or diastolic retrograde flow in the descending aorta with a CAF, it may present when the shunt volume is significant. Although invasive, TEE can improve sensitivity in detecting the CAF course, and it is certainly a

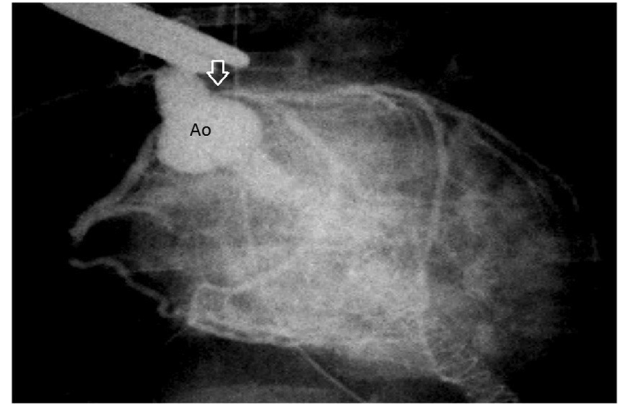


Figure 21 Aortography in a patient with Williams syndrome. Note the proximal luminal stenosis of the left coronary artery (arrow) as it arises from the aorta (Ao) near the sinotubular junction.

complementary tool to help guide device deployment during catheter intervention.^{79,91,92}

b. Post-interventional Assessment.—The primary goal of post-interventional imaging is to document success in fistula closure; the success rate is quite good for both transcatheter closure and surgical ligation.⁹³⁻⁹⁸ If a residual fistula is detected, careful follow-up is required as it tends to increase in size over time.⁸² The same strategies utilized for pre-intervention imaging should be used in the post-intervention assessment. Adverse CA events may occur in patients with a significantly dilated distal CAF due to thrombus formation, because of stagnant blood flow in a residually dilated CA after fistula closure and resultant occlusion of normal CA branches.^{99,100} Ectasia of the CA can persist and is more significant when the fistula terminates in the atrium, and so long-term monitoring for development of thrombosis/late ischemia after closure is important.¹⁰¹ Discrete intimal stenosis may also occur in a surgically modified large CAF after closure, which can also be a cause of postoperative myocardial ischemia.^{99,100,102-104} Wall motion abnormalities should be assessed, and stress echocardiography may be useful for detecting ischemia if there is suspicion of CA insufficiency.¹⁰⁵

3. Additional Imaging Techniques. Cardiac catheterization has been the gold standard for complete anatomic and hemodynamic characterization of a CAF. Although its spatial resolution of the CAF course is superb, angiography is sometimes limited in outlining the anatomical relationships with surrounding cardiac structures and visualizing the drainage sites because of significant dilution of the contrast when it drains into a low-pressure chamber.¹⁰⁶ Cardiac catheterization is indicated in patients with a suspected pathophysiologic burden identified or suspected on noninvasive imaging, and in those undergoing planned transcatheter intervention. An ECG-gated CCT provides excellent delineation of the precise location and anatomy of the fistula. A volume-rendered 3D image of CCT also provides an excellent overview of the spatial relationship of cardiac/vascular chambers to the fistula origin, course and termination site when surgical intervention is needed.¹⁰⁷ CMR is also useful in evaluating CAF anatomy; it can also quantify the volume of cardiac chambers and CAF flow by estimating Qp:Qs shunt fraction, assess for ischemia in myocardial areas distal to the fistula take-off, and define the degree of myocardial fibrosis related to fistula steal using late gadolinium enhancement.⁸³

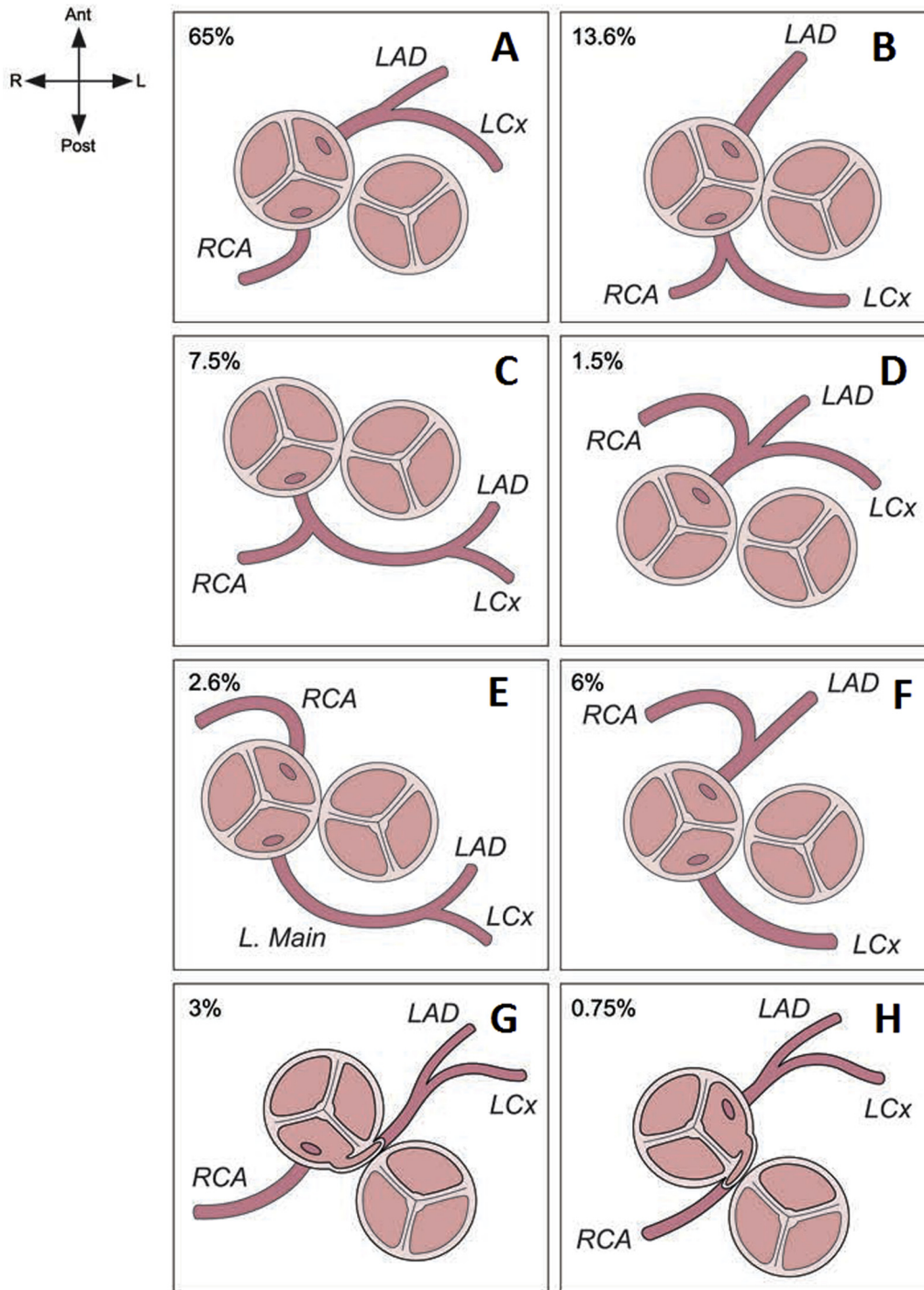


Figure 22 Anatomic coronary artery variations in transposition of the great arteries. The most common coronary artery patterns seen in TGA are displayed in descending order of frequency. **A:** Usual pattern with the left coronary artery (LCA) arising from the left-facing sinus and the right coronary artery (RCA) arising from the posterior- and rightward-facing sinus. **B:** Origin of the circumflex coronary artery (LCx) from the RCA, coursing posterior to the pulmonary trunk. **C:** Single RCA from the posterior-facing sinus with the left coronary system coursing posterior to the pulmonary trunk. **D:** Single LCA from the left-facing sinus with the right coronary coursing anterior to the aortic root. **E:** Inverted artery origins with the left coronary arising from the right-facing sinus and the right coronary arising from the left-facing sinus. **F:** Inverted RCA and LCx. **G:** Intramural LCA. **H:** Intramural RCA. The intramural coronary artery in TGA usually arises from the opposite-facing sinus and passes within the wall of the aorta before exiting the adventitia. From Mertens LL, Vogt MO, Marek J, Cohen MS. Transposition of the great arteries. In: Lai WW, Mertens LL, Cohen MS, Geva T, eds. *Echocardiography in Pediatric and Congenital Heart Disease*. Hoboken, NJ: Wiley-Blackwell; 2009.

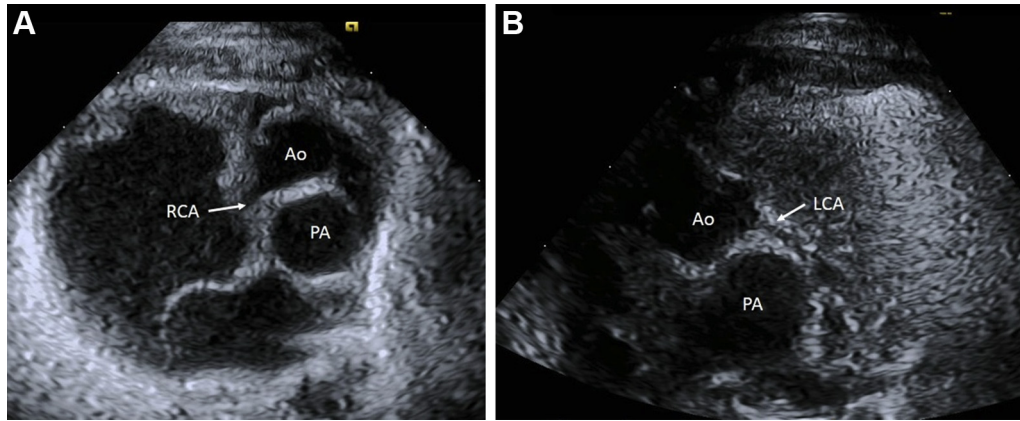


Figure 23 Parasternal short-axis imaging in an infant with TGA and the typical coronary artery pattern. The high right parasternal window **(A)** demonstrates the right coronary artery (RCA) arising from the right-facing sinus of the aorta (Ao), while the high left parasternal window **(B)** provides excellent visualization of the left coronary artery (LCA) arising from the left-facing sinus. PA, Pulmonary artery.

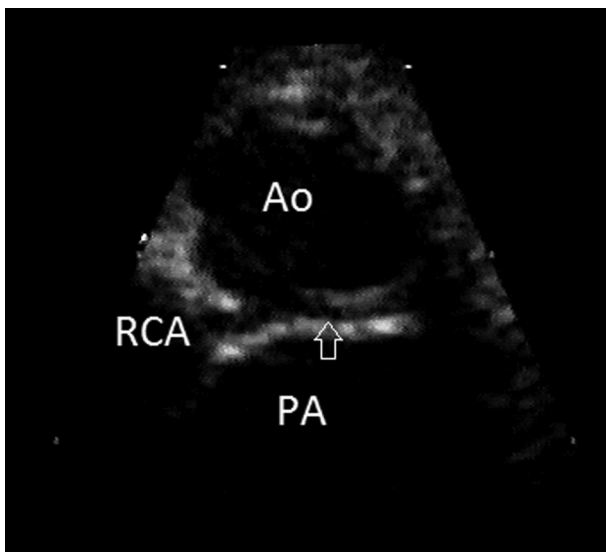


Figure 24 Parasternal short-axis imaging in an infant with TGA and an intramural left coronary artery. The right coronary artery (RCA) can be seen arising from its usual origin from the right-facing sinus of the aorta (Ao). The left coronary origin is also from the right-facing sinus, immediately adjacent to the RCA, with an intramural course within the posterior aortic wall (*arrow*). PA, Pulmonary artery.

- Alternative imaging techniques (CCT, CMR, angiography) can clearly identify the CAF anatomy/hemodynamics and should be employed when intervention is considered.

Recommended Imaging Strategy for Isolated Coronary Artery Fistulas

- TTE should be the initial screening tool for suspected CAF and is effective in serial monitoring of size/physiologic effects.
- When intervention for a significant CAF is planned, delineation of origin, course and exit should be confirmed with cardiac catheterization, CCT or CMR.
- Supplementary hemodynamic information may be obtained by cardiac catheterization or CMR when the need for closure is unclear.
- Coronary ectasia following CAF closure can persist and should be monitored for development of thrombus/ischemia.

Key Points for Isolated Coronary Artery Fistulas

- CAFs are rare and frequently benign, but fistulas can enlarge over time and lead to myocardial ischemia and/or heart failure.
- Echocardiography may identify CAFs, with common markers including:
 - Dilatation of the involved CA with increased flow by color Doppler
 - Turbulent continuous flow throughout the length of the involved CA when draining into a low-pressure chamber (usually the right heart)
 - Turbulent flow into the chamber at the exit point of the CAF by color Doppler

IV. CONGENITAL CORONARY ANOMALIES ASSOCIATED WITH OTHER CONGENITAL HEART DISEASES

A. Supravalvular Aortic Stenosis

1. Background. Supravalvular aortic stenosis (SVAS) is a congenital localized or diffuse luminal narrowing of the ascending aorta at the sinotubular junction.¹⁰⁸⁻¹¹⁰ SVAS is strongly associated with Williams syndrome and familial forms of the disease, now recognized as genetic mutations that affect elastin production. In some cases, all the major arteries, including the pulmonary, carotid, and CAs, may be affected.^{109,111} SVAS may be associated with CA pathologies, which are mainly stenoses. However, a spectrum of mechanisms listed below can occur alone or in combination:

- CA ostial stenosis occurs in 9% of patients presenting in the first year of life^{112,113} secondary to obstruction by a thickened aortic or sinus wall and by a thickened proximal CA wall, especially when the CA orifice is superiorly

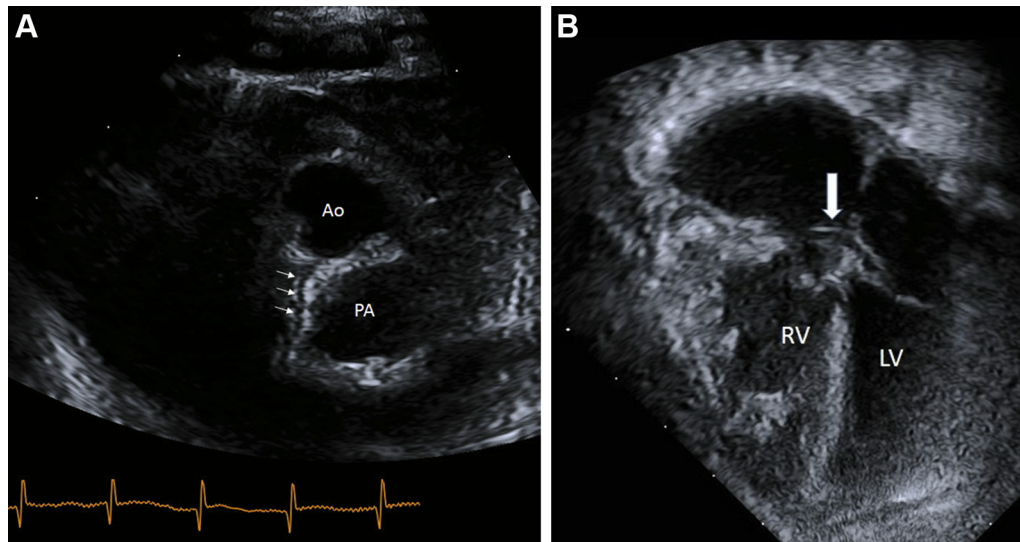


Figure 25 Parasternal short-axis (**A**) and apical (**B**) imaging in an infant with TGA and the circumflex coronary arising from the right sinus. In **A**, the left circumflex coronary artery (*arrows*) is arising from the posterior right-facing sinus of the aorta (Ao), as it courses posterior to the pulmonary artery (PA). The apical view shows a length of the circumflex coronary (*arrow*) as it courses just anterior to the mitral valve.



Figure 26 Contrast CT imaging of the coronary origins from a short-axis plane in a child with TGA after arterial switch surgery. The left coronary is severely narrowed (*arrows*) at it arises from the anterior aspect of the neo-aortic (Ao) root behind the pulmonary artery (PA).

displaced near the sinotubular ridge.^{108,110,114,115} Ostial stenosis affects the LCA more frequently than the RCA, and it may be progressive in some cases even after the effective surgical release of SVAS.¹¹⁶

- Fusion of the free edge of the aortic valve with the sinotubular ridge, or shelf formation by a thickened aortic leaflet and protruded sinotubular ridge can cover the CA orifice and compromise CA flow (CA hooding).^{110,117,118} This is most frequently found in the left coronary sinus of Valsalva.^{108,114,119} Total isolation of the LCA or RCA from the sinus as a result of complete fusion of the entire leaflet edge to the prominent sinotubular ridge has also been reported.¹²⁰
- Diffuse CA narrowing with intimal and medial hyperplasia and fibrosis is more frequently observed in patients with the diffuse form of SVAS than in those with discrete SVAS.^{110,119} The luminal narrowing is usually greater in the proximal segment of the affected CA than in the distal segment.^{110,121}

- Diffuse CA dilation, aneurysm formation, and tortuosity can occur when the CA orifices are below the sinotubular junction and exposed to high pre-stenotic systolic and pulse pressures.^{110,122,123}

The myocardial perfusion reserve is already limited in patients with significant SVAS because of hypertrophied myocardium with increased oxygen demand and intramyocardial pressure. A critical perfusion mismatch can occur when coronary blood flow is compromised by stenosis.^{114,124} Chronic myocardial ischemia associated with SVAS can result in LV dysfunction, acute myocardial infarction, or sudden death.^{124,125} The estimated risk of sudden cardiac death is 25-100 times higher in patients with Williams syndrome compared to an age-matched normal population.¹²⁶ Up to 58% of deaths are related to general anesthesia or sedation, and 50-79% are associated with evidence of CA stenosis and myocardial ischemia.^{121,126-128}

2. Goals of Echocardiographic Imaging. Deep sedation or general anesthesia involves substantial risk of sudden death in patients with SVAS, especially in younger patients or those with biventricular outflow tract obstruction, and so the choice of imaging modality must be considered in light of sedative needs. TTE can assess the severity of SVAS, ventricular wall thickness and motion, and additional anatomical abnormalities. However, its capability for assessing CA ostial luminal stenosis or CA hooding is limited, and sedation may be needed in uncooperative infants and young children. TTE can identify the CA origins, providing insights into the risk for potential CA complications and myocardial ischemia. If either CA ostium is located superiorly near the sinotubular ridge, then the risk of ostial luminal stenosis is significantly increased.^{108,110,114,115} Flow turbulence by color Doppler at the CA ostium may indicate stenosis, particularly when assessed at higher Nyquist limits. Parasternal long-axis views are helpful in visualizing the position of the RCA ostium relative to the sinotubular ridge. Both the apical five-chamber and subcostal left anterior oblique views are useful in identifying the LCA ostium and its position relative to the sinotubular ridge.

Aneurysmal dilation or long-segment narrowing of the CAs can be assessed using parasternal and subcostal windows. Dilation of the CAs tends to be associated with discrete hourglass SVAS, and dilation is most commonly seen when the CA ostia are normally positioned in

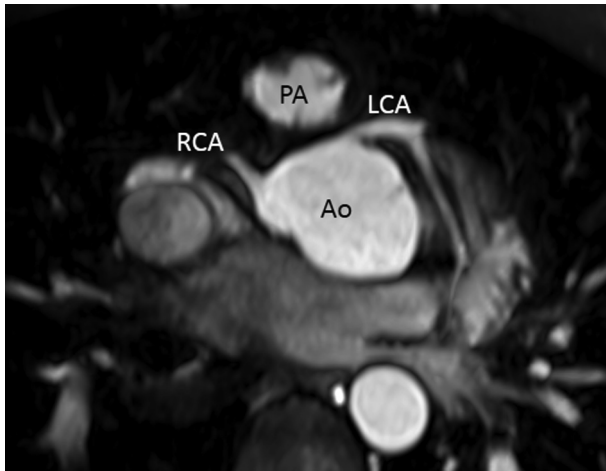


Figure 27 MRI of the coronary origins from a short-axis equivalent window in a child with TGA after arterial switch. Both the left coronary artery (LCA) and right coronary artery (RCA) are widely patent as they arise from the anterior aspect of the neo-aortic (Ao) root. The pulmonary artery (PA) is seen directly anterior to the aorta.

the sinus of Valsalva, remote from the sinotubular ridge.^{108,119} Epicardial echocardiography or TEE during invasive evaluations or surgery may also be helpful in visualizing the precise CA ostial location (Figure 19). Similarly, stress echocardiography can assess myocardial perfusion mismatch but should be used with caution, particularly preoperatively when there is associated significant outflow obstruction.

3. Additional Imaging Techniques. ECG-gated CCT provides excellent delineation of the precise location and anatomy of the CAs (Figure 20),^{118,129} thereby balancing the procedural risks in this patient population. The spatial resolution of CMR can be challenging for precise assessment of CA ostial anatomy, and the data acquisition time is longer than that of CCT. Moreover, CMR usually requires general anesthesia or deep sedation in young children.^{130,131} Cardiac catheterization has been the gold standard, especially in small children (Figure 21). However, the risk of cardiac arrest or sudden death is significant in SVAS patients, especially with severe biventricular outflow tract obstruction or age less than 3 years.¹³² Myocardial perfusion imaging can assess CA perfusion without deep sedation. Although relatively low specificity in children is a major limitation, its usefulness in patients with SVAS has been reported in children as young as 2.5 years.^{30,123}

Key Points for Congenital Coronary Anomalies Associated with Supravalvular Aortic Stenosis

- SVAS can be associated with potentially life-threatening CA stenosis.
- Echocardiography is limited in diagnosing CA stenosis in SVAS, but identification of an ostial location near the sinotubular ridge increases risk of stenosis.
- Alternative imaging techniques (CCT, CMR, angiography) can help identify CA stenosis, but use of deep sedation during these procedures can trigger an ischemic event.

Recommended Imaging Strategy for Congenital Coronary Anomalies Associated with Supravalvular Aortic Stenosis

- TTE may be an effective screening tool for CA anomalies with SVAS, particularly in identification of anatomic subtypes associated with ischemia.
- CCT is the preferred imaging modality to document/confirm coronary ostial abnormalities, since it can be performed without deep sedation/anesthesia in this high-risk population.

B. Transposition of the Great Arteries

1. Background. Transposition of the great arteries (TGA) is a conotruncal malformation defined as concordance of the atrioventricular connections and discordance of the ventriculo-arterial connections. The aorta arises from the RV and the PA arises from the LV, resulting in parallel systemic and pulmonary circulations and severe cyanosis at birth.¹³³ Approximately 40% of cases have a ventricular septal defect (VSD), which may affect the type of surgery performed. The primary surgery for TGA (with intact ventricular septum or with simple types of VSD) is the arterial switch operation (ASO), which entails transfer of the aorta to the pulmonary valve, transfer of the PA to the aortic valve, and translocation of the CAs to the “neo” aorta.¹³⁴ In typical TGA, the aorta is positioned rightward and anterior to the PA. Thus, the CAs do not arise from the normal location.

There is significant variability in CA anatomy in TGA, and it is important to identify the anatomical pattern prior to the ASO (Figure 22). CA imaging recommendations have been previously reviewed in the American Society of Echocardiography imaging guidelines document on TGA published in 2016.¹³³ Particular variations of CA anatomy have been associated with worse outcomes after the procedure.¹³⁵ The most common CA pattern occurs in approximately 65% of TGA cases: the left main CA arises from the left-facing aortic sinus and divides into the LAD and the LCx, and the RCA arises from the right-facing aortic sinus. The second most common pattern (14% of cases) is when the LCx arises from the RCA at the right-facing sinus and the LAD arises separately from the left-facing sinus. In this case, the LCx courses behind the PA as it makes its way toward the left atrioventricular groove. The other 20% of TGA cases have more unusual patterns that include single right and left CAs, and variations of inverted CAs whereby the left main or one of its tributaries arises from the right-facing sinus and the RCA arises from the left-facing sinus. Patients who have TGA and a VSD are more likely to have an unusual CA pattern compared to patients with TGA and an intact ventricular septum.¹³⁶

It is important to make a preoperative diagnosis of an intramural CA pattern (Figure 22G and H), which occurs when one of the CAs is inverted but courses between the aorta and the PA rather than anterior or posterior to these vessels. The interarterial course makes it likely that the CA is also intramural. Translocation of an intramural CA is technically more challenging for the surgeon and more likely to result in kinking or occlusion of the vessel with associated worse outcome.^{135,137}

The Rastelli operation may be performed for TGA with a large VSD and LV outflow tract obstruction.¹³⁸ In these cases, the ASO is not a feasible strategy because the neo-aortic outflow would be obstructed. The Rastelli procedure entails a baffle from the LV to the aorta through the VSD and the creation of an unobstructed pathway

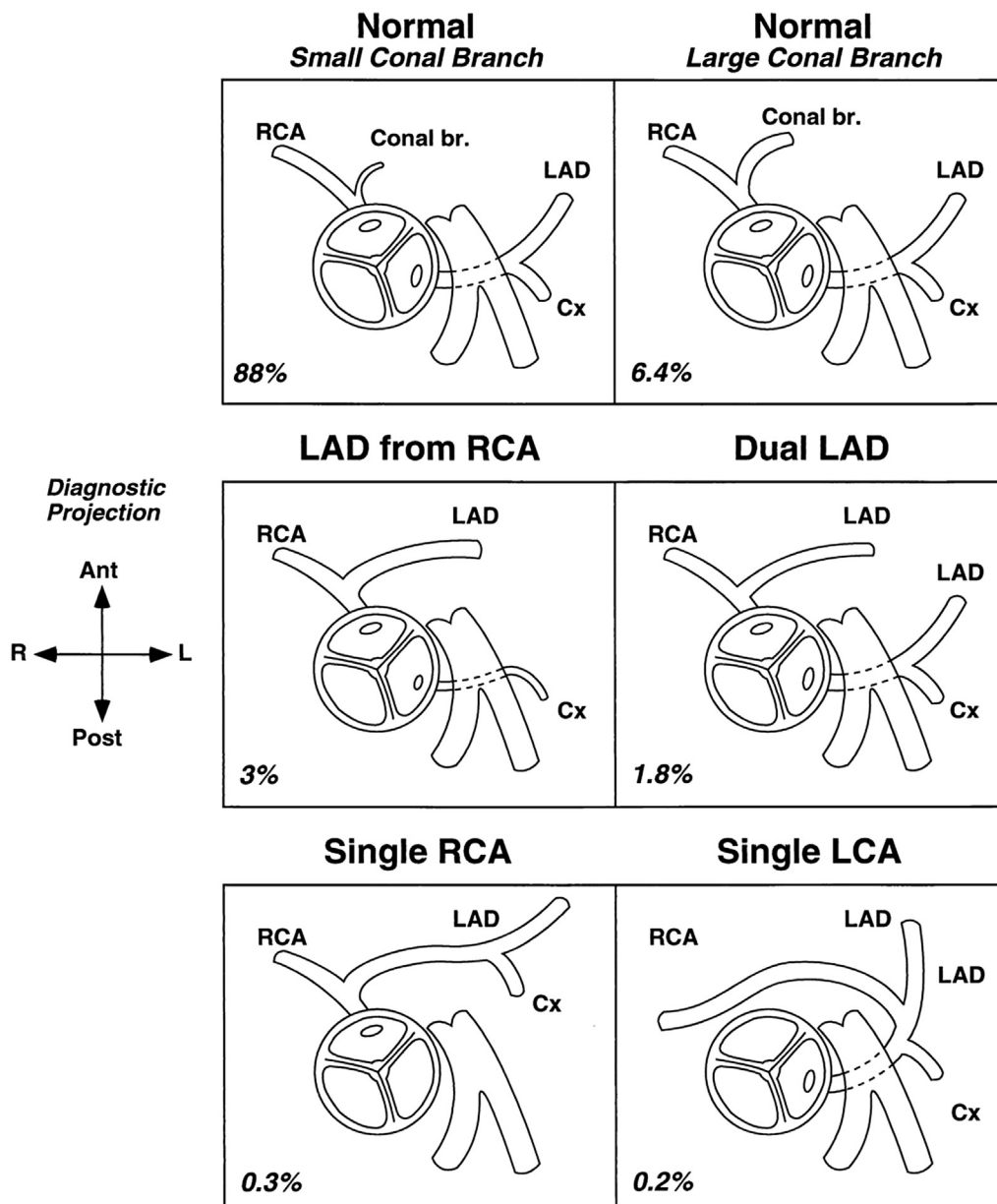


Figure 28 Coronary artery variations in tetralogy of Fallot. The most common coronary artery patterns seen in TOF are displayed in descending order of frequency, with the frequency of each variation listed in the lower left corner of the illustration. *Ant*, Anterior; *Conal br*, conal branch; *Cx*, left circumflex coronary artery; *L*, left; *LAD*, left anterior descending coronary artery; *LCA*, left coronary artery; *Post*, posterior; *R*, right; *RCA*, right coronary artery. From Need LR, Powell AJ, del Nido P and Geva T. Coronary echocardiography in tetralogy of Fallot: diagnostic accuracy, resource utilization and surgical implications over 13 years. *J Am Coll Cardiol*. 2000; 36:1371-7.

from the RV to the PA, usually with a valved conduit. The CAs do not have to be mobilized for this procedure. Thus, preoperative assessment of CA anatomy may not have a significant impact on outcome.

The Nikaidoh operation is performed for TGA with LV outflow tract obstruction when there is concern that the baffled pathway from the LV to the aorta may become obstructed over time.¹³⁹ During this procedure, the small posterior pulmonary annulus is transected, and the aortic root is mobilized and translocated to the region where the pulmonary valve had been. This allows the aorta to sit closer to the LV, which may prevent future LV outflow tract obstruction. The VSD is then closed and a pathway from the RV to the PA is

created. The CAs require translocation in some but not all cases. Some have reported that the Nikaidoh procedure cannot be performed if there are major CA anomalies such as single CA or abnormal course of the LAD.¹⁴⁰ Thus, identifying these variants may help with surgical planning.

2. Goals of Echocardiographic Imaging. *a. Preoperative Assessment.*—The goal of CA imaging in the preoperative patient with TGA is to identify the origin and course of both CAs. This is typically achieved by TTE. Identification of the type of TGA is the first step in localizing the CA. The great artery relationship and the position of

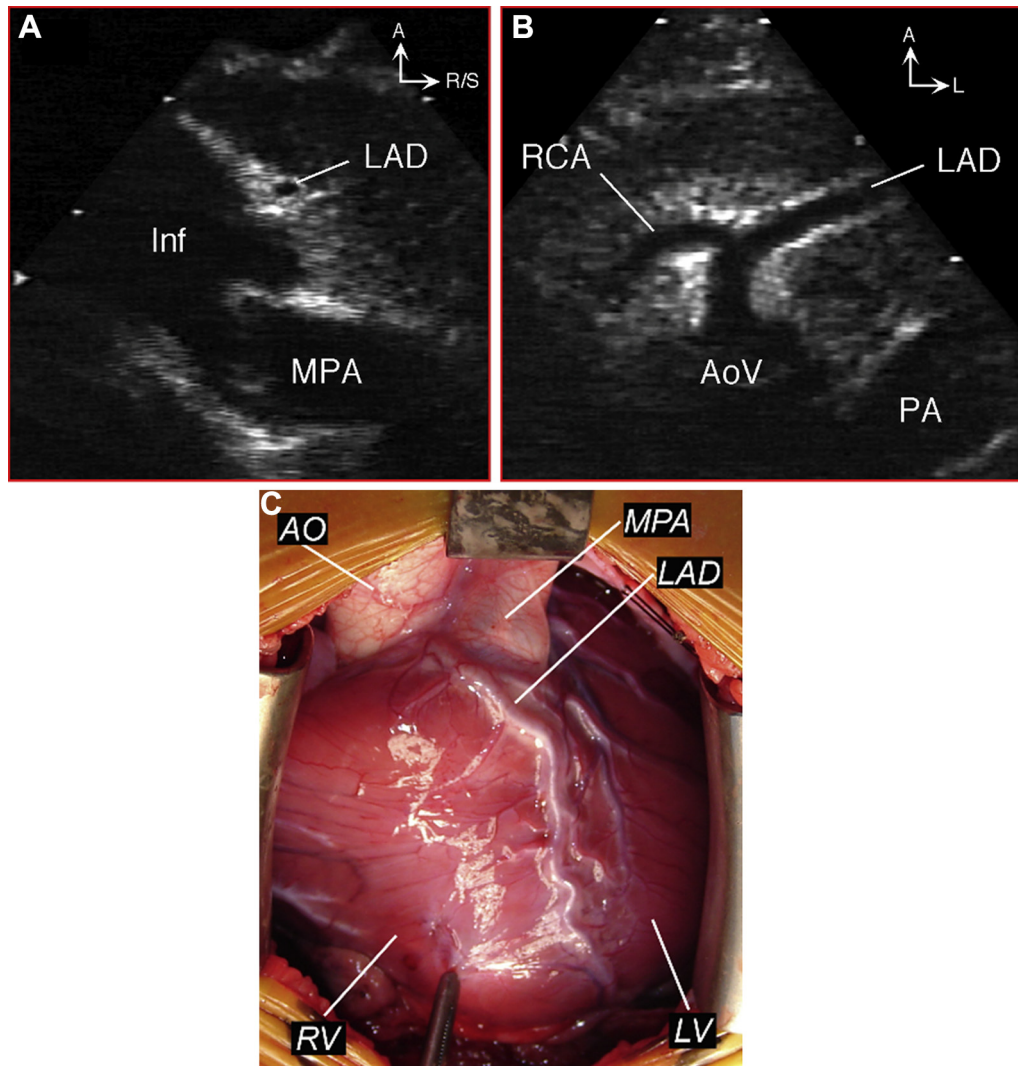


Figure 29 Parasternal imaging and intraoperative photography from an infant with TOF and the left anterior descending coronary artery (LAD) arising from the right coronary artery (RCA) and crossing the right ventricular outflow tract. From the parasternal long-axis view (**A**), the LCA can be seen in cross section anterior to the right ventricular infundibulum (Inf), raising concern for an anomalous coronary course. From the parasternal short-axis view (**B**), the LAD is clearly seen arising from the RCA and crossing anterior to the pulmonary artery (PA). The intraoperative photo of the epicardial surface of the heart (**C**) confirms the anatomy, again showing the LAD coursing across the right ventricular outflow tract below the main pulmonary artery (MPA). AoV, Aortic valve; AO, aorta.

the heart in the chest should be noted. Once the spatial orientation has been ascertained, there are five other points to keep in mind while scanning for the coronaries: a) the semilunar valve cusp alignment, b) the location of the CAs relative to the commissures, c) the vertical location within the sinuses, d) the distance to the translocation site on the PA, and e) the course of each CA.

Varying echocardiographic windows can aid in the localization of the CAs. The parasternal short-axis view, employing either the right or left parasternal window to get perpendicular to a particular CA, is usually quite helpful because the semilunar valves appear *en face*. The high right parasternal window may permit visualization of the CA arising from the right-facing sinus (Figure 23A), whereas the high left parasternal window may yield a better view of the CA arising from the left-facing sinus (Figure 23B). The parasternal short-axis view is also important in identifying the cusp alignment and to help determine the distance the CA must be moved during translocation.

The parasternal short-axis view is also the best imaging plane to detect an intramural course between the two great arteries (Figure 24). Color Doppler can confirm the flow between the two great arteries in patients suspected of having an intramural CA course, as described in the section on AAOCA. This view can also be used to show the LCA division into the LAD and LCx in patients with usual CA anatomy. When the LCx arises from the right-facing sinus, it can often be seen coursing behind the PA (Figure 25A). When the RCA arises from the left-facing sinus, it can often be seen crossing anterior to the aorta. Intraoperative TEE can provide analogous views that may complement TTE imaging in identifying each CA origin and course.

Other echocardiographic planes can be used to detect unusual CA patterns and courses. In the apical and subcostal views, the LCx from the right-facing sinus can often be seen coursing posterior to the PA and anterior to the mitral valve in the frontal or left anterior oblique sweep (Figure 25B). In patients with an inverted RCA (arising from

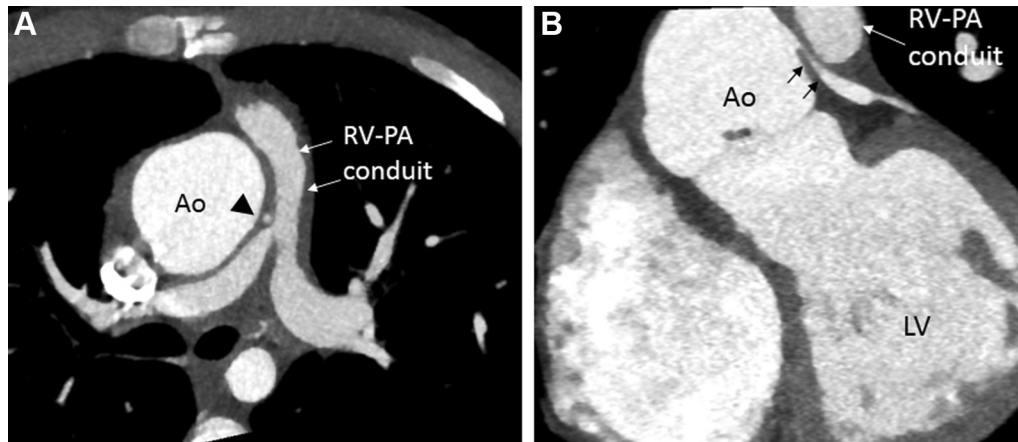


Figure 30 Contrast CT imaging of the left coronary in a patient with TOF repair s/p right-ventricular-to-pulmonary artery (RV-PA) conduit placement. From a short-axis plane (**A**), the left coronary (*triangle*) is seen in cross section coursing between the aorta (Ao) and the narrowed conduit, with the potential for compression during interventional dilatation of the conduit as part of percutaneous replacement. This relationship is well illustrated from a long-axis plane (**B**), where the potential for compression of the left coronary (*arrows*) between the aorta and the conduit can again be appreciated. LV, Left ventricle.

the left-facing sinus), further anterior sweeping in the subcostal view will demonstrate the RCA coursing in front of the aorta.

b. Postoperative Assessment.—It is essential during the ASO (or the Nikaidoh operation if the CAs are translocated) that the CAs are reimplanted into the neo-aorta without narrowing of the orifices or kinking of the vessels. Often, intraoperative TEE is performed to assess ventricular performance and assure that there are no regional wall motion abnormalities suggestive of myocardial ischemia.¹³³ Velocity and direction of flow in the CA, as assessed by TEE, may be predictive of outcome.^{141,142} A velocity-time integral greater than 0.14 and CA peak systolic velocity of greater than 0.6–0.8 cm/sec are measures that have been associated with need for revision of the CA anastomosis during the ASO,¹⁴¹ and systolic reversal of flow in the LCA has also been associated with adverse outcomes.¹⁴² Following surgical CA reimplantation, there should be suspicion of myocardial ischemia if ventricular dysfunction and/or ventricular arrhythmias are present, as CA events may still occur.¹⁴³ Serial TTE can screen for regional wall motion abnormalities, but CA narrowing or atresia can be challenging to detect. Myocardial deformation imaging may add information about regional ventricular function that could prompt further CA investigation.

3. Additional Imaging Techniques. There are some circumstances where clarification of the anatomy may be helpful during the preoperative evaluation. In patients where there is suspicion of an intramural CA, CCT or CMR imaging may confirm this finding. Although cardiac catheterization is primarily used for the performance of a balloon atrial septostomy to improve mixing prior to surgery, an angiogram of the aortic root can frequently identify the origin and course of each CA.

After the ASO, CCT, CMR, or angiography can be used to visualize the origin and course of the translocated CAs to determine if CA revision is required. CCT angiography is excellent for evaluation of CA patency after the arterial switch operation¹⁴⁴ and for definition of the mechanism of obstruction (Figure 26).^{145,146} CMR can define the origin and course of the CAs (Figure 27), and it can also determine

myocardial viability. Using late gadolinium enhancement, CMR can identify areas of fibrosis, which may have resulted from ischemia.¹⁴⁷ Some practitioners routinely assess CA perfusion after ASO. This can be performed using stress echocardiography to detect regional wall motion abnormalities or by perfusion imaging such as SPECT or PET.

Key Points for Congenital Coronary Anomalies Associated with Transposition of the Great Arteries

- Variations in CA origin and course are common in TGA and can impact surgical planning and risk of postoperative CA complications.
- Echocardiography may identify concerning CA patterns in TGA preoperatively, particularly an intramural course between the great arteries and CAs coursing anterior to the aorta or posterior to the pulmonary artery.
- Ventricular dysfunction and regional wall motion abnormalities after the arterial switch operation should prompt alternative imaging techniques (CCT, CMR, angiography) to assess CA patency.

Recommended Imaging Strategy for Congenital Coronary Anomalies Associated with Transposition of the Great Arteries

- TTE should be the primary imaging tool for delineation of coronary artery anatomy in the preoperative assessment of TGA.
- When an intramural coronary is suspected, clear delineation of this higher-risk variant using CCT may be warranted prior to arterial switch surgery.
- Postoperative CCT, CMR, and/or cardiac catheterization should be performed when there is suspicion of coronary compromise.

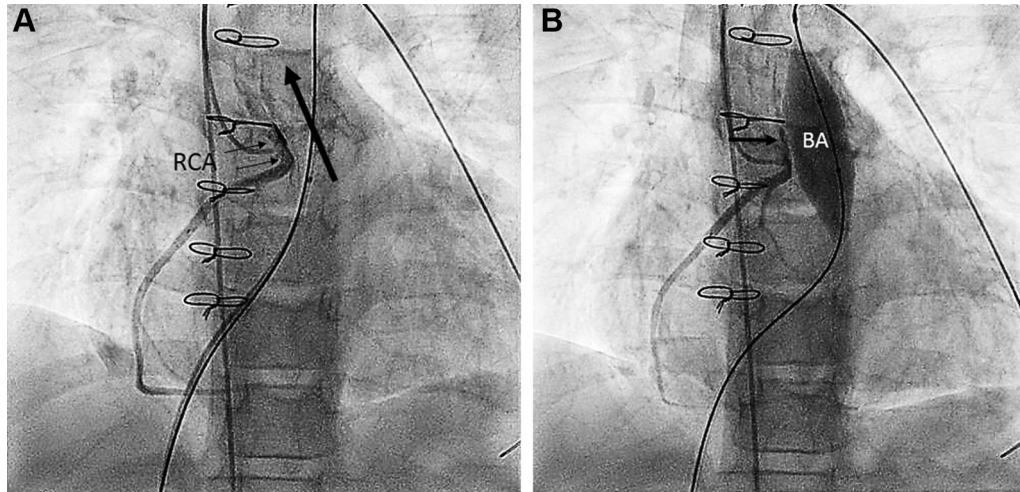


Figure 31 Right coronary angiography during planned transcatheter pulmonary valve replacement in a patient with recurrent right ventricular outflow tract obstruction after TOF repair. Prior to test-balloon inflation (**A**) in the calcified right ventricular-to-pulmonary-artery conduit (*large arrow*), the right coronary (*small arrows*) can be seen arising without obstruction immediately adjacent to the conduit. With balloon inflation (BA) that expands the conduit (**B**), the right coronary artery is significantly narrowed (*arrow*), demonstrating the risk of coronary compression in placing a new pulmonary valve using interventional techniques.

C. Tetralogy of Fallot

1. Background. Tetralogy of Fallot (TOF) is the most common form of cyanotic CHD, with an estimated incidence of 32.6 per 100,000 live births. Approximately 5-14% of patients with TOF will have CA anomalies.¹⁴⁸⁻¹⁵⁰ The most common CA anomalies in TOF (Figure 28) include the LAD originating from the RCA or right sinus, dual LADs (with one crossing the RVOT), single CA, and the LCx originating from the RCA. A large right conal CA branch is relatively common, and a dominant LCA is present in ~25% of TOF patients.¹⁴⁸ Additionally, the orifice of the LCA is commonly located more posteriorly and the RCA is located more anteriorly and leftward than in the normal heart, related to the clockwise rotation of the aortic root in TOF.¹⁴⁸ Rare CA anomalies in TOF include CAF, CA atresia, and origination of the LCA from the PA or from an aortopulmonary collateral.^{151,152}

Surgical intervention is always required for this lesion to close the VSD and relieve RV outflow/pulmonary stenosis. Techniques to relieve the outflow obstruction can vary, based on anatomic findings, but frequently involve pulmonary valvotomy, patch enlargement of the RV outflow tract and pulmonary valve, or placement of a conduit from the RV to the pulmonary artery. CA variants in which a major branch crosses the RV outflow tract are important to recognize prior to surgical intervention. In a retrospective single center study of 607 patients with TOF, 13% had a CA anomaly identified, and of those, 62% had a CA that crossed the RV outflow tract.¹⁵³ It is critical to define both CA origin and course prior to surgical intervention, since an anomaly can determine the approach to relieving RV outflow tract obstruction, particularly if a transannular patch is considered. A CA coursing anterior to the RV outflow tract may require a palliative procedure prior to definitive repair or an alternate surgical approach to relieve RV outflow tract obstruction such as a modified patch or RV-to-PA conduit.¹⁵⁴

Pulmonary valve replacement (either surgical or catheter-deployed) is commonly performed in adolescents and adults after TOF repair because of residual pulmonary stenosis or regurgitation. The 2018 ACC/AHA Guidelines for Management of Adults with

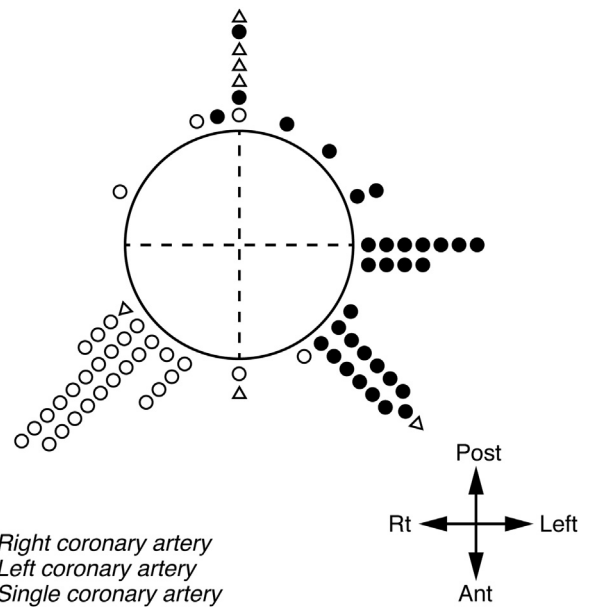


Figure 32 Diagram of the variability in coronary artery origins in truncus arteriosus. The center circle represents the circumference of the truncal wall, divided into 4 quadrants, with the number and type of coronary arising from each quadrant. Post, Posterior; Rt, right; Ant, anterior. From de la Cruz MV, Cayre R, Angelini P, Noriega-Ramos N and Sadowinski S. Coronary arteries in truncus arteriosus. *Am J Cardiol.* 1990; 66:1482-6.

Congenital Heart Disease recommend that CA anatomy should be delineated in any patient with repaired TOF prior to intervention on the RV outflow tract.¹⁵⁵ CAs that are directly substernal or directly anterior to the RV outflow tract require careful planning for sternal entry to avoid CA injury with re-intervention. Advanced imaging prior to transcatheter pulmonary valve placement should place specific emphasis on definition of the CA anatomy and predict those at high risk for CA compromise with

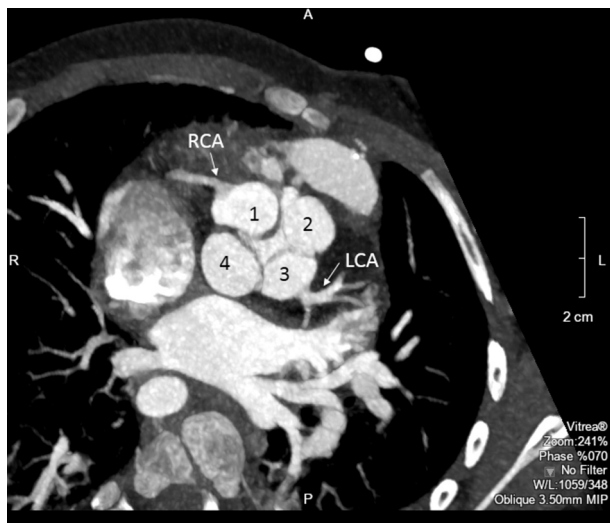


Figure 33 Contrast CT imaging from a short-axis plane in an infant with truncus arteriosus. The aortic valve is quadricuspid, with each of the leaflets numbered. The right coronary artery (RCA) can be seen arising from the anterior and rightward cusp, while the left coronary artery arises from the posterior and leftward cusp.

transcatheter valve placement and pre-stenting, which is commonly used.

2. Goals of Echocardiographic Imaging. *a. Preoperative Assessment.*—In a retrospective review of 598 children with TOF, echocardiography for CA delineation exhibited a sensitivity of 82% and a specificity of 99% with an accuracy of 98.5%.¹⁴⁹ In this series, 5.4% of patients were found to have a major CA crossing the RV outflow tract at the time of surgery (Figure 29C), a majority of which did not necessitate the placement of an RV-to-PA conduit in patients with TOF and pulmonary stenosis. CA imaging using TTE involves primarily the parasternal short- and long-axis views (Figure 29A and B). In the parasternal short-axis view, the left main CA is visualized as it originates from the left sinus of Valsalva. Rotating the transducer with a slight apical tilt will profile the LAD coursing in the anterior interventricular groove and often identify the origin of the LCx. In order to image the RCA, it is often found slightly higher than the LCA in the parasternal short-axis view. A sweep in the parasternal long-axis view, tilting toward the left shoulder, is particularly helpful to identify an anomalous origin of the LAD from the RCA (Figure 29A). In the parasternal long-axis view, the LCA and its branches are visualized between the aortic root and the main PA. It is important to examine the infundibular free wall to identify any vessels coursing on the epicardial surface. Occasionally, the apical and subcostal windows can provide additional information.

Other than very rare anomalies, the CAs arise from the aorta in a majority of TOF cases. Color Doppler settings that accentuate low-velocity CA flow can provide visualization of antero-grade color flow into the CA ostia. Rarely, if a CA arises from the PA or an aortopulmonary collateral, flow may be biphasic or retrograde into the CA ostia depending on pulmonary pressures. A CA arising from a collateral or the PA will perfuse with systemic pressure in the presence of a large and unrestrictive

VSD and may be difficult to diagnose until after VSD closure when PA pressures have fallen.

b. Postoperative Assessment.—Echocardiography is inadequate to provide delineation of CA anatomy when additional procedures are considered after initial complete repair, so additional imaging techniques must be utilized. Circumstances when these techniques are needed after repair of TOF include:

- Evaluation of the CA relationship to the sternum and the RV outflow tract in patients who will undergo additional cardiac surgical intervention.
- Evaluation of the CA relationship to the RV outflow tract in patients who will undergo either transcatheter or surgical intervention on the RV outflow tract. The relationship is particularly useful to identify CA anomalies and to predict those at higher potential risk for CA compression with placement of the transcatheter valve, often placed with pre-stenting of the RV outflow tract.
- Evaluation for CA lesions in patients with TOF who will undergo another cardiac procedure who may need CA intervention, typically men over the age of 35 years, premenopausal women 35 years or older with risk factors for atherosclerosis, postmenopausal women, and any adult patient with symptoms of potential myocardial ischemia.⁸⁷

3. Additional Imaging Techniques. CMR is the most common advanced imaging technique for post-operative assessment of TOF.¹⁵⁶ CMR is excellent at defining the relationship of the proximal CA to the outflow tracts. However, artifact from metallic stents and devices degrades CMR image quality, which can limit CA imaging, and there is a relatively high incidence of stent branch PA intervention after TOF repair. In addition, older patients are more likely to have a defibrillator or pacemaker, some of which may cause artifact or are contraindicated for MRI.²¹ Finally, pulmonary valve replacements (either surgical or percutaneous) often produce localized signal artifact with CMR.

CCT provides high-resolution CA imaging in patients of all ages with TOF. A pre-operative CCT study in 100 patients less than one year of age with TOF demonstrated 100% sensitivity and specificity compared to surgical findings for CA course at a dose of less than 1 millisievert.²¹ Patients were spontaneously breathing and without sedation for this study. CCT can show the course of the CA relative to the RV outflow tract after surgical repair and help assess for potential CA compression prior to interventional pulmonary valve replacement (Figure 30). ECG-gated CCT can also be used to quantify ventricular volumes and estimate EF with an accuracy comparable to MRI as long as a scanner with appropriate temporal resolution is used and contrast is modified to opacify both the right and left sides of the heart.

In the current era, non-invasive imaging of the CAs has largely replaced invasive angiography for the preoperative evaluation of patients with TOF. However, angiography of the CAs in patients with repaired TOF is commonly used during transcatheter pulmonary valve placement for relief of recurrent RV outflow tract obstruction in previously placed conduits of appropriate size (Figure 31A and B). In one series of patients undergoing transcatheter pulmonary valve placement, 6 of 124 patients had CA compression.¹⁵⁷ The largest series of transcatheter valves included 343 patients and demonstrated a 5% incidence of CA compression with test balloon angioplasty (Figure 31B). Of the 34 patients with TOF and anomalous CA course included in this series, 21% had CA compression.¹⁵⁸

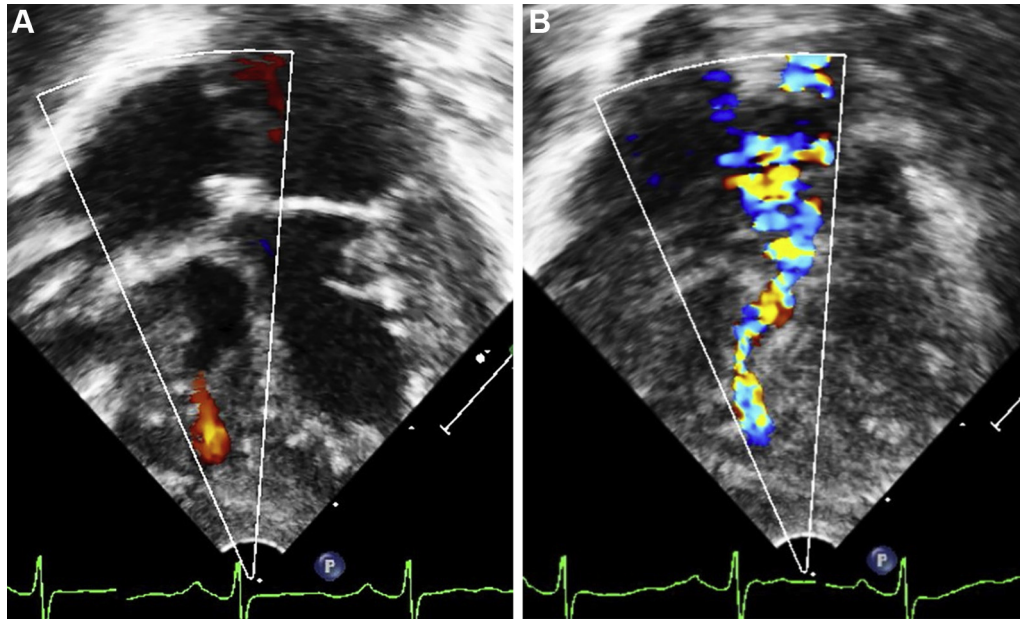


Figure 34 Low-scale color Doppler mapping of the right ventricle from an apical view in an infant with PA-IVS and systolic RV hypertension showing a small jet of systolic flow from the RV apex into the myocardium, representing a small RV-to-coronary connection (**A**), and a dilated coronary segment along the anterior interventricular groove with anterior tilting of the imaging plane, representing flow from the RV into that coronary segment (**B**).



Figure 35 Right ventricular angiogram showing multiple right ventricular-to-coronary connections in an infant with PA-IVS.

- Alternative imaging techniques (CCT, CMR, angiography) assessing coronary artery relationships to the RVOT are necessary prior to pulmonary valve replacement.

Recommended Imaging Strategy for Congenital Coronary Anomalies Associated with Tetralogy of Fallot

- TTE should be the primary screening tool for delineation of coronary anatomy in the preoperative assessment of TOF.
- After primary repair, delineation of coronary anatomy by CCT or CMR should be performed prior to pulmonary valve replacement.
- In patients undergoing transcatheter pulmonary valve replacement, coronary angiography may be sufficient to assess coronary anatomy during the procedure.

Key Points for Congenital Coronary Anomalies Associated with Tetralogy of Fallot

- Variations in CA origin and course are common in TOF and can impact initial surgical planning and risk of CA complications during later interventions.
- Echocardiography identifies CA branches from the RCA crossing the RVOT prior to initial surgical repair.

D. Truncus Arteriosus

1. Background. Truncus arteriosus is an uncommon type of CHD, in which a single arterial trunk arises from the heart, giving rise to the CAs, pulmonary arteries, and systemic arteries, in that order. Infants with truncus arteriosus undergo surgical repair that baffles the LV to the truncal root, creating a “neo-aortic” valve and outflow, with placement of an RV-to-PA conduit that must be serially replaced over time. The single semilunar truncal valve may have two, three, four, or more leaflets and usually overrides the ventricular septum through an outlet VSD. The proximal CA anatomy is most likely to be normal when there is a trileaflet truncal valve. However, CA anomalies are reported in up to 20% of

patients with truncus arteriosus. In a review of 39 autopsy specimens of subjects with truncus arteriosus, there was great variability in CA anatomy, with a tendency for the RCA to arise from the anterior right quadrant and for the LCA to arise from the anterior left quadrant (Figure 32).¹⁵⁹ Such a tendency was observed in 50% of bicuspid, 59% of tricuspid, and 66% of quadricuspid valves. In 18% of cases, a single CA ostium is present, usually arising from a posterior sinus.^{159,160} Recognized variants of CA anatomy in this condition include an LCx arising from the RCA (3.6%), and an LAD arising from the RCA (2.4%).¹⁶⁰ Patients with truncus arteriosus have marked variation in the location and shape of the CA ostia, which are commonly located above the sinotubular junction. The distal courses of the CAs are usually normal. The location around the truncal root is unpredictable, and is a risk factor for poor outcomes during surgical repair when the LCA arises near the pulmonary artery origin or when the RCA courses anterior to the truncal root.¹⁶¹ In a study of 30 autopsy specimens, 8 had an RV-to-PA conduit, all of which had injury to the anteriorly crossing RCA.¹⁶² Additionally, CA ostial stenosis due to a slit-like orifice or a proximal intramural course may lead to ischemia, particularly with low aortic diastolic pressure (which can be seen with significant truncal valve regurgitation).¹⁶³ There are rare case reports of a CA arising from a PA.

Anomalous CA origins, where one or both CAs did not arise from the expected sinus, have been associated with a higher mortality following truncus arteriosus repair. In a series of 106 subjects with truncus arteriosus who underwent surgical repair between 1976 and 1998, 13 had an anomalous CA, and 7 deaths were related to compression or distortion of that CA.¹⁶⁴ In the largest series of truncus arteriosus outcomes, abnormal CA anatomy is shown as a risk factor for early mortality.¹⁶⁵

2. Goals of Echocardiographic Imaging. TTE is an excellent modality to delineate the CA origin(s) in infants with truncus arteriosus. Definition of the sinus from which the CA originates, the height of the CA origin from the annulus or from the ascending aorta, the proximity of the CA to the pulmonary arteries, and the proximal CA course should be defined. Rare reports of anomalous CA from the PA, CA ostial stenosis, or intramural proximal CA course have been described.

TTE views for CA imaging in truncus arteriosus involve primarily the parasternal short- and long-axis views. In the parasternal short-axis view, the CAs may be visualized as they leave the truncal root, and the relationship of the CA origin to the truncal cusp can be defined. The parasternal long-axis and subcostal views can help define the location of the CA origin within the truncal valve sinus or the ascending aorta. Particular attention should be paid to the relationship of the CA to the PA, often requiring tilting the transducer superiorly and inferiorly to image these structures in the same plane. Color Doppler can provide visualization of anterograde color flow into the CA ostia. In exceedingly rare cases, if a CA arises from the PA, flow may be biphasic or retrograde into the CA ostia, depending on pulmonary vascular resistance.

3. Additional Imaging Techniques. In select cases, CCT is helpful in the preoperative assessment of anatomy (including CA origin and course) in infants with truncus arteriosus (Figure 33).¹⁶⁶ Similar to the imaging evaluation of patients with repaired TOF, knowledge of the CA relationships to the outflow tracts and sternum are important in patients with truncus arteriosus who may require transcatheter pulmonary valve replacement.

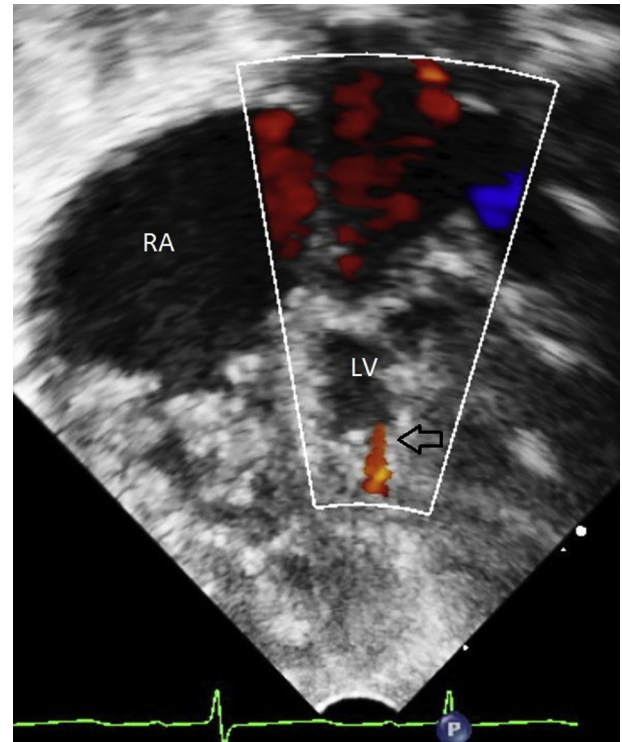


Figure 36 Low-scale color Doppler mapping of the left ventricle from an apical four-chamber view in an infant with the HLHS variant involving mitral stenosis and aortic atresia, showing flow from the hypoplastic left ventricle (LV) chamber into the myocardium (open arrow), representing a tiny left ventricular to coronary connection. RA, Right atrium.

Key Points for Congenital Coronary Anomalies Associated with Truncus Arteriosus

- Variations in CA origin and course are common in truncus arteriosus, including single CA, and can impact risk of CA complications during surgical interventions.
- Echocardiography may identify CA origins and the location/proximity of the CA ostia to the pulmonary arteries prior to initial surgical repair.
- Alternative imaging techniques (CCT, CMR, angiography) are necessary to assess CA course prior to subsequent pulmonary valve replacements.

Recommended Imaging Strategy for Congenital Coronary Anomalies Associated with Truncus Arteriosus

- TTE should be the primary screening tool for delineation of coronary anatomy in the preoperative assessment of truncus arteriosus.
- After primary repair, delineation of coronary anatomy by CCT or CMR should be performed prior to pulmonary valve replacement.
- In patients undergoing transcatheter pulmonary valve replacement, coronary angiography may be sufficient to assess coronary anatomy during the procedure.

E. Coronary Anomalies Associated with Single Ventricle Lesions

Significant congenital CA anomalies in the setting of functionally univentricular hearts are seen primarily in two settings: pulmonary atresia with intact ventricular septum (PA-IVS) and hypoplastic left heart syndrome (HLHS).

1. Pulmonary Atresia With Intact Ventricular Septum. a.

Background.—PA-IVS is a congenital lesion in which there is no blood flow between the RV and the pulmonary arteries in the absence of a VSD; there are varying degrees of tricuspid valve and RV hypoplasia. Abnormal connections between the RV and the CAs are a common feature related to high pressure in the RV cavity. The nomenclature for these RV-CA connections has been variable and has included coronary-cameral fistulae, myocardial sinusoids, and ventriculo-coronary communications. Intrinsic abnormalities of the CAs have been seen in almost half of the cases of PA-IVS,^{167,168} with most showing myointimal hyperplasia resulting in abnormal vascular architecture and stenosis or complete atresia of the arterial lumen.¹⁶⁹

Normal CA flow for the RV occurs during both systole and diastole, but the increased transmural pressure gradient of the hypertensive RV in PA-IVS results in only diastolic flow in both the right and LCA systems. In the presence of RV hypertension and CA stenosis or atresia, aortic diastolic pressure becomes insufficient for perfusion of the affected myocardium. Thus, the hypertensive RV becomes the primary source of CA blood flow for the myocardial segments distal to the area of CA obstruction or interruption.¹⁷⁰ RV-dependent CA circulation is seen in 5-34% of cases.¹⁷¹⁻¹⁷⁴ Recognition of this pathophysiologic state is important prior to establishing continuity between the RV and PA (also known as RV decompression) by surgical or transcatheter intervention, as this will reduce RV systolic pressure, compromising CA flow to the RV-dependent myocardial segments and resulting in ischemia and ultimately infarction.¹⁷⁵ The primary risk factor for RV-dependent CA circulation is tricuspid valve annular size, with risk increasing at annular Z-score thresholds of -2.5 ,^{171,176} below which the risk increases significantly. This is also the approximate tricuspid valve Z-score below which the likelihood of a biventricular circulation is low.¹⁷⁷

b. Goals of Echocardiographic Imaging.—The sensitivity of echocardiography for CA stenosis or atresia is low, and a normal-sized tricuspid valve (and RV) does not necessarily preclude the presence of RV-dependent CA circulation.¹⁷⁸ Dilation in the proximal CA may indicate fistulous connections to the RV. Recognition of tricuspid valve hypoplasia using Z-scores for tricuspid annular diameter from the apical four-chamber and parasternal long-axis views should raise awareness of potential sinusoidal connections.

Color Doppler using low Nyquist limits can identify flow between the RV and the CAs (Figure 34); bidirectional flow in the proximal CAs (anterograde in diastole, retrograde in systole) is an indirect indicator of RV-CA connections. RV-CA connections can appear as areas of flow along the RV endocardial surface in subcostal, apical, and parasternal views. Occasionally, turbulent color flow at higher Nyquist limits can identify areas of CA stenosis. Lack of identifiable flow into a proximal CA suggests ostial atresia or stenosis. Finally, dilation of other CA segments besides the left main, proximal LAD, and proximal RCA suggests abnormal connections to the RV.

c. Additional Imaging Techniques.—Other imaging modalities are almost always necessary to define CA anatomy in PA-IVS. TEE has

provided little if any additional information as it relates to intrinsic CA abnormalities. CCT is useful in assessing CA anatomy but can be limited in very small patients with fast heart rates. CMR is useful in the evaluation of the myocardial perfusion defects, since intrinsic CA abnormalities in PA-IVS are not necessarily limited to the RV, with some studies showing areas of ischemia, fibrosis, and infarction in the LV as well.¹⁷⁹⁻¹⁸¹ Additionally, particularly if there is evidence of worsening myocardial dysfunction, CMR is a useful surveillance tool to look for evidence of myocardial ischemia during long-term follow-up.¹⁸²

The primary advantage of catheterization with angiography is the ability to evaluate the CA anatomy and perform transcatheter intervention (if amenable) in a single examination. The ability to evaluate the CA flow via RV injection followed by aortic angiography and/or selective CA injection provides the most comprehensive evaluation of the CA anatomy. It is important for the operator to recognize interruptions in the CA distribution, as this primarily affects the initial palliation. This can be accomplished by using similar views for both the RV angiogram and aortic or selective CA angiogram to evaluate for absent segments, stenosis, and/or communications (Figure 35). If abnormalities are noted, angled angiography can be used as an adjunct to better delineate the specific area of concern. In addition to angiographic data, hemodynamic data can also be obtained that might be useful in determining the most appropriate surgical or transcatheter intervention.

The angiographic definition of RV-dependent CA circulation is made when atresia or severe stenosis of one or more ostial or CA interruptions is identified.^{170,177} RV-CA connections can exist without stenosis and should be delineated angiographically as these patients can still successfully undergo decompression.¹⁷⁰

Key Points for Congenital Coronary Anomalies Associated with Pulmonary Atresia with Intact Ventricular Septum

- Delineation of RV-dependent CA circulation is critical prior to RV decompression.
- Identification of abnormal RV-CA connections can be made with echocardiography, but confirmation of the anatomy is required prior to intervention and best accomplished by angiography.
- Tricuspid valve Z-score < -2.5 is a risk factor for poor prognosis with biventricular repair and for the presence of abnormal RV-CA connections.
- CMR is a useful tool to evaluate for myocardial abnormalities related to abnormal coronary perfusion both in the short and long term.

Recommended Imaging Strategy for Congenital Coronary Anomalies Associated with Pulmonary Atresia with Intact Ventricular Septum

- TTE may identify anatomic/physiologic features concerning for coronary anomalies, but it is usually inadequate as the sole tool to assess coronary anatomy in PA/IVS.
- Coronary angiography should be performed prior to any interventions that would result in decompression of the RV.

2. Hypoplastic Left Heart Syndrome. a. Background.–

Hypoplastic left heart syndrome (HLHS), defined as significant underdevelopment of the LV and its associated structures, has several subtypes that include atresia or hypoplasia of the aortic and mitral valves. Connections between the LV and CA vascular bed (LV-CA connections) have been seen in patients with HLHS by angiography and during autopsy¹⁸³⁻¹⁸⁶. These anomalies have been observed almost exclusively in the setting of mitral stenosis (MS) and aortic atresia (AA), suggesting that the absence of flow into the hypoplastic LV with mitral atresia precludes the formation of LV-CA connections. Pathologic review of postmortem specimens evaluating for the presence of CA abnormalities and evidence of abnormal RV histology suggestive of ischemia have not revealed any differences between those patients with and without CA abnormalities, including the subtype where they are usually found (hypoplastic left heart syndrome with mitral stenosis and aortic atresia),¹⁸⁷ and outcome data for that subtype have not shown a consistent pattern of risk.¹⁸⁸⁻¹⁹¹

b. Goals of Echocardiographic Imaging.–Imaging of patients with HLHS, particularly in terms of LV-CA connections in the setting of mitral stenosis and aortic atresia, is similar to the imaging protocol for PA-IVS with CA abnormalities. Low Nyquist limits with color mapping over the LV will often identify abnormal flow in the LV myocardium (Figure 36), which is highly suspicious for LV-CA connections. CA imaging can be challenging, particularly in the setting of the severe ascending aortic hypoplasia that is usually characteristic of this lesion. Following the Norwood procedure (where the native aorta is anastomosed to the ascending neo-aorta), imaging and Doppler interrogation of that connection is important in documenting patency, as it is the sole source of CA blood flow.

c. Additional Imaging Techniques.–TEE before and after stage I palliation can be useful in assessing RV function. CCT and CMR usually have limited use in these patients in the preoperative period in part because the LV is never decompressed with the Norwood palliation. Catheterization with angiography may be helpful if there is concern for abnormal LV-CA connections preoperatively, with evaluation primarily involving LV angiography to identify the abnormal communication. Direct injection of the CAs in patients with aortic atresia is typically avoided due to the risk for CA compromise during catheter engagement of the hypoplastic ascending aorta; this results from complete or near complete occlusion by the catheter, which then prevents retrograde CA filling. Confirmation of CA compromise can help guide clinical management in terms of standard palliation versus hybrid palliation and/or transplantation. In addition, angiography is sometimes useful in the immediate postoperative period for evaluating etiologies of ischemia, including stenosis or distortion of the anastomosis between the ascending aorta and the PA or thrombosis of the hypoplastic native aortic root.

Key Points for Congenital Coronary Anomalies Associated with Hypoplastic Left Heart Syndrome

- CA abnormalities are more common in the HLHS subtype of MS/AA.
- Echocardiography is typically adequate for the assessment of abnormal CA communications in patients with HLHS.
- Patients with abnormal CA communications are palliated in a similar manner to other subtypes of HLHS with outcomes that are largely similar.
- Direct imaging with angiography is typically reserved for postoperative patients in whom there is evidence of ischemia.

Recommended Imaging Strategy for Congenital Coronary Anomalies Associated with Hypoplastic Left Heart Syndrome

- TTE should be the primary screening tool for delineation of coronary anatomy in the preoperative assessment of HLHS.
- Coronary angiography may be performed in the rare circumstance where abnormal LV-CA connections are suspected.

NOTICE AND DISCLAIMER: This report is made available by ASE as a courtesy reference source for members. This report contains recommendations only and should not be used as the sole basis to make medical practice decisions or for disciplinary action against any employee. The statements and recommendations contained in this report are primarily based on the opinions of experts, rather than on scientifically-verified data. ASE makes no express or implied warranties regarding the completeness or accuracy of the information in this report, including the warranty of merchantability or fitness for a particular purpose. In no event shall ASE be liable to you, your patients, or any other third parties for any decision made or action taken by you or such other parties in reliance on this information. Nor does your use of this information constitute the offering of medical advice by ASE or create any physician-patient relationship between ASE and your patients or anyone else.

Reviewers: This document was reviewed by members of the ASE Guidelines and Standards Committee, ASE Board of Directors, ASE Executive Committee, and designated representatives from the Japanese Society of Echocardiography, and Society for Cardiovascular Angiography and Interventions. Reviewers included Azin Alizadehasl, MD, FASE, John P. Breinholt III, MD, Michael Cheezum, MD, FSCCT, Scott D. Choyce, RDCS, RVT, RDMS, FASE, Gregory Ensing, MD, FASE, Craig Fleishman, MD, FASE, Benjamin Freed, MD, FASE, Mark K. Friedberg, MD, FASE, Edward Gill, MD, FASE, Suzanne Golz, MS, RDCS, FASE, Renuka Jain, MD, FASE, Pei-Ni Jone, MD, FASE, James N. Kirkpatrick, MD, FASE, Wyman W. Lai, MD, MPH, FASE, Stephen H. Little, MD, FASE, Anuj Mediratta, MD, FASE, Andrew Pellett, PhD, RDCS, FASE, Dermot Phelan, MD, PhD, FASE, David H. Wiener, MD, FASE, and Satoshi Yasukochi, MD.

REFERENCES

1. Cheezum MK, Liberthson RR, Shah NR, Villines TC, O'Gara PT, Landzberg MJ, et al. Anomalous aortic origin of a coronary artery from the inappropriate sinus of Valsalva. *J Am Coll Cardiol* 2017;69:1592-608.
2. Fuse S, Kobayashi T, Arakaki Y, Ogawa S, Katoh H, Sakamoto N, et al. Standard method for ultrasound imaging of coronary artery in children. *Pediatr Int* 2010;52:876-82.
3. Jureidini SB, Marino CJ, Singh GK, Balfour IC, Chen SC. Assessment of the coronary arteries in children: an integral part of each transthoracic echocardiographic study. *J Am Soc Echocardiogr* 2003;16:899-900.
4. Brown LM, Duffy CE, Mitchell C, Young L. A practical guide to pediatric coronary artery imaging with echocardiography. *J Am Soc Echocardiogr* 2015;28:379-91.
5. Lai WW, Geva T, Shirali GS, Frommelt PC, Humes RA, Brook MM, et al. Guidelines and standards for performance of a pediatric echocardiogram: a report from the Task Force of the Pediatric Council of the

- American Society of Echocardiography. *J Am Soc Echocardiogr* 2006;19:1413-30.
6. Fratz S, Chung T, Greil GF, Samyn MM, Taylor AM, Valsangiacomo Buechel ER, et al. Guidelines and protocols for cardiovascular magnetic resonance in children and adults with congenital heart disease: SCMR expert consensus group on congenital heart disease. *J Cardiovasc Magn Reson* 2013;15:51.
 7. Harris MA, Whitehead KK, Shin DC, Keller MS, Weinberg PM, Fogel MA. Identifying abnormal ostial morphology in anomalous aortic origin of a coronary artery. *Ann Thorac Surg* 2015;100:174-9.
 8. Brothers JA, Whitehead KK, Keller MS, Fogel MA, Paridon SM, Weinberg PM, et al. Cardiac MRI and CT: differentiation of normal ostium and intraseptal course from slitlike ostium and interarterial course in anomalous left coronary artery in children. *Am J Roentgenol* 2015;204:W104-9.
 9. Brothers JA, Kim TS, Fogel MA, Whitehead KK, Morrison TM, Paridon SM, et al. Cardiac magnetic resonance imaging characterizes stenosis, perfusion, and fibrosis preoperatively and postoperatively in children with anomalous coronary arteries. *J Thorac Cardiovasc Surg* 2016;152:205-10.
 10. Beerbaum P, Sarikouch S, Laser KT, Greil G, Burchert W, Korperich H. Coronary anomalies assessed by whole-heart isotropic 3D magnetic resonance imaging for cardiac morphology in congenital heart disease. *J Magn Reson Imaging* 2009;29:320-7.
 11. Tang L, Merkle N, Schar M, Korosoglou G, Solaiyappan M, Hombach V, et al. Volume-targeted and whole-heart coronary magnetic resonance angiography using an intravascular contrast agent. *J Magn Reson Imaging* 2009;30:1191-6.
 12. Jin H, Zeng MS, Ge MY, Yun H, Yang S. 3D coronary MR angiography at 1.5 T: Volume-targeted versus whole-heart acquisition. *J Magn Reson Imaging* 2013;38:594-602.
 13. Ishida M, Sakuma H. Coronary MR angiography revealed: how to optimize image quality. *Magn Reson Imaging Clin N Am* 2015;23:117-25.
 14. Tangcharoen T, Bell A, Hegde S, Hussain T, Beerbaum P, Schaeffter T, et al. Detection of coronary artery anomalies in infants and young children with congenital heart disease by using MR imaging. *Radiology* 2011;259:240-7.
 15. Hussain T, Mathur S, Peel SA, Valverde I, Bilka K, Henningson M, et al. Coronary artery size and origin imaging in children: a comparative study of MRI and trans-thoracic echocardiography. *BMC Med Imaging* 2015;15:48.
 16. Strigl S, Beroukhim R, Valente AM, Annese D, Harrington JS, Geva T, et al. Feasibility of dobutamine stress cardiovascular magnetic resonance imaging in children. *J Magn Reson Imaging* 2009;29:313-9.
 17. Ntsinjana HN, Tann O, Hughes M, Derrick G, Secinaro A, Schievano S, et al. Utility of adenosine stress perfusion CMR to assess paediatric coronary artery disease. *Eur Heart J Cardiovasc Imaging* 2017;18:898-905.
 18. Noel CV, Krishnamurthy R, Moffett B, Krishnamurthy R. Myocardial stress perfusion magnetic resonance: initial experience in a pediatric and young adult population using regadenoson. *Pediatr Radiol* 2017;47:280-9.
 19. Liu A, Wijesurendra RS, Francis JM, Robson MD, Neubauer S, Piechnik SK, et al. Adenosine stress and rest T1 mapping can differentiate between ischemic, infarcted, remote, and normal myocardium without the need for gadolinium contrast agents. *JACC Cardiovasc Imaging* 2016;9:27-36.
 20. Goo HW. Coronary artery imaging in children. *Korean J Radiol* 2015;16:239-50.
 21. Vastel-Amzallag C, Le Bret E, Paul JF, Lambert V, Rohnean A, El Fassy E, et al. Diagnostic accuracy of dual-source multislice computed tomographic analysis for the preoperative detection of coronary artery anomalies in 100 patients with tetralogy of Fallot. *J Thorac Cardiovasc Surg* 2011;142:120-6.
 22. Han BK, Lindberg J, Overman D, Schwartz RS, Grant K, Lesser JR. Safety and accuracy of dual-source coronary computed tomography angiography in the pediatric population. *J Cardiovasc Comput Tomogr* 2012;6:252-9.
 23. Cheng Z, Wang X, Duan Y, Wu L, Wu D, Chao B, et al. Low-dose prospective ECG-triggering dual-source CT angiography in infants and children with complex congenital heart disease: first experience. *Eur Radiol* 2010;20:2503-11.
 24. Mahabadi AA, Achenbach S, Burgstahler C, Dill T, Fischbach R, Knez A, et al. Safety, efficacy, and indications of beta-adrenergic receptor blockade to reduce heart rate prior to coronary CT angiography. *Radiology* 2010;257:614-23.
 25. Weustink AC, Neeffjes LA, Kyzropoulos S, van Straten M, Neoh Eu R, Meijboom WB, et al. Impact of heart rate frequency and variability on radiation exposure, image quality, and diagnostic performance in dual-source spiral CT coronary angiography. *Radiology* 2009;253:672-80.
 26. Roberts WT, Wright AR, Timmis JB, Timmis AD. Safety and efficacy of a rate control protocol for cardiac CT. *Br J Radiol* 2009;82:267-71.
 27. Meinel FG, Henzler T, Schoepf UJ, Park PW, Huda W, Spearman JV, et al. ECG-synchronized CT angiography in 324 consecutive pediatric patients: spectrum of indications and trends in radiation dose. *Pediatr Cardiol* 2015;36:569-78.
 28. Siegel MJ, Ramirez-Giraldo JC, Hildebolt C, Bradley D, Schmidt B. Automated low-kilovoltage selection in pediatric computed tomography angiography: phantom study evaluating effects on radiation dose and image quality. *Invest Radiol* 2013;48:584-9.
 29. Einstein AJ, Wolff SD, Manheimer ED, Thompson J, Terry S, Uretsky S, et al. Comparison of image quality and radiation dose of coronary computed tomographic angiography between conventional helical scanning and a strategy incorporating sequential scanning. *Am J Cardiol* 2009;104:1343-50.
 30. Kondo C. Myocardial perfusion imaging in pediatric cardiology. *Ann Nucl Med* 2004;18:551-61.
 31. Duvall WL, Croft LB, Ginsberg ES, Einstein AJ, Guma KA, George T, et al. Reduced isotope dose and imaging time with a high-efficiency CZT SPECT camera. *J Nucl Cardiol* 2011;18:847-57.
 32. Gerretsen SC, Kooi ME, Schalla S, Delhaas T, Snoep G, Van Engelsehoven JM, et al. Magnetic resonance imaging of the coronary arteries. *Cardiovasc J Afr* 2007;18:248-59.
 33. Ntsinjana HN, Hughes ML, Taylor AM. The role of cardiovascular magnetic resonance in pediatric congenital heart disease. *J Cardiovasc Magn Reson* 2011;13:51.
 34. Lamers LJ, Moran M, Torgeson JN, Hokanson JS. Radiation reduction capabilities of a next-generation pediatric imaging platform. *Pediatr Cardiol* 2016;37:24-9.
 35. Taylor AJ, Rogan KM, Virmani R. Sudden cardiac death associated with isolated congenital coronary artery anomalies. *J Am Coll Cardiol* 1992;20:640-7.
 36. Frommelt PC. Congenital coronary artery abnormalities predisposing to sudden cardiac death. *Pacing Clin Electrophysiol* 2009;32(Suppl 2):S63-6.
 37. Penalver JM, Mosca RS, Weitz D, Phoon CK. Anomalous aortic origin of coronary arteries from the opposite sinus: a critical appraisal of risk. *BMC Cardiovasc Disord* 2012;12:83.
 38. Maron BJ, Haas TS, Ahluwalia A, Rutten-Ramos SC. Incidence of cardiovascular sudden deaths in Minnesota high school athletes. *Heart Rhythm* 2013;10:374-7.
 39. Virmani R, Burke AP, Farb A. Sudden cardiac death. *Cardiovasc Pathol* 2001;10:211-8.
 40. Lorber R, Srivastava S, Wilder TJ, McIntyre S, DeCampi WM, Williams WG, et al. Anomalous aortic origin of coronary arteries in the young: echocardiographic evaluation with surgical correlation. *JACC Cardiovasc Imaging* 2015;8:1239-49.
 41. Angelini P. Anomalous origin of the left coronary artery from the opposite sinus of Valsalva: typical and atypical features. *Tex Heart Inst J* 2009;36:313-5.
 42. Frommelt PC, Frommelt MA, Tweddell JS, Jaquiss RD. Prospective echocardiographic diagnosis and surgical repair of anomalous origin of a coronary artery from the opposite sinus with an interarterial course. *J Am Coll Cardiol* 2003;42:148-54.

43. Mery CM, Lawrence SM, Krishnamurthy R, Sexson-Tejtel SK, Carberry KE, McKenzie ED, et al. Anomalous aortic origin of a coronary artery: toward a standardized approach. *Semin Thorac Cardiovasc Surg* 2014;26:110-22.
44. Sachdeva S, Frommelt MA, Mitchell ME, Tweddell JS, Frommelt PC. Surgical unroofing of intramural anomalous aortic origin of a coronary artery in pediatric patients: single-center perspective. *J Thorac Cardiovasc Surg* 2018;155:1760-8.
45. Frommelt PC, Berger S, Pelech AN, Bergstrom S, Williamson JG. Prospective identification of anomalous origin of left coronary artery from the right sinus of Valsalva using transthoracic echocardiography: importance of color Doppler flow mapping. *Pediatr Cardiol* 2001;22:327-32.
46. Cohen MS, Herlong RJ, Silverman NH. Echocardiographic imaging of anomalous origin of the coronary arteries. *Cardiol Young* 2010;20(Suppl 3):26-34.
47. Lee S, Uppu SC, Lytrivi ID, Sanz J, Weigand J, Geiger MK, et al. Utility of multimodality imaging in the morphologic characterization of anomalous aortic origin of a coronary artery. *World J Pediatr Congenit Heart Surg* 2016;7:308-17.
48. Angelini P, Velasco JA, Ott D, Khoshnevis GR. Anomalous coronary artery arising from the opposite sinus: descriptive features and pathophysiologic mechanisms, as documented by intravascular ultrasonography. *J Invasive Cardiol* 2003;15:507-14.
49. Miller JA, Anavekar NS, El Yaman MM, Burkhart HM, Miller AJ, Julsrud PR. Computed tomographic angiography identification of intramural segments in anomalous coronary arteries with interarterial course. *Int J Cardiovasc Imaging* 2012;28:1525-32.
50. Lee HJ, Hong YJ, Kim HY, Lee J, Hur J, Choi BW, et al. Anomalous origin of the right coronary artery from the left coronary sinus with an interarterial course: subtypes and clinical importance. *Radiology* 2012;262:101-8.
51. Keith JD. The anomalous origin of the left coronary artery from the pulmonary artery. *Br Heart J* 1959;21:149-61.
52. Williams IA, Gersony WM, Hellenbrand WE. Anomalous right coronary artery arising from the pulmonary artery: a report of 7 cases and a review of the literature. *Am Heart J* 2006;152:1004 e9-e17.
53. Svensson A, Themudo R, Cederlund K. Anomalous origin of right coronary artery from the pulmonary artery. *Eur Heart J* 2017;38:3069.
54. Hekmat V, Rao SM, Chhabra M, Chiavarelli M, Anderson JE, Nudel DB. Anomalous origin of the right coronary artery from the main pulmonary artery: diagnosis and management. *Clin Cardiol* 1998;21:773-6.
55. Wesselhoeft H, Fawcett JS, Johnson AL. Anomalous origin of the left coronary artery from the pulmonary trunk. Its clinical spectrum, pathology, and pathophysiology, based on a review of 140 cases with seven further cases. *Circulation* 1968;38:403-25.
56. Roberts WC. Major anomalies of coronary arterial origin seen in adulthood. *Am Heart J* 1986;111:941-63.
57. Berre LL, Baruteau AE, Fraise A, Boulmier D, Jimenez M, Gallet B, et al. Anomalous origin of the left coronary artery from the pulmonary artery presenting in adulthood: a French nationwide retrospective study. *Semin Thorac Cardiovasc Surg* 2017.
58. Krexi L, Sheppard MN. Anomalous origin of the left coronary artery from the pulmonary artery (ALCAPA), a forgotten congenital cause of sudden death in the adult. *Cardiovasc Pathol* 2013;22:294-7.
59. Backer CL, Stout MJ, Zales VR, Muster AJ, Weigel TJ, Idriss FS, et al. Anomalous origin of the left coronary artery. A twenty-year review of surgical management. *J Thorac Cardiovasc Surg* 1992;103:1049-57. discussion 57-8.
60. Vouhe PR, Tamisier D, Sidi D, Vernant F, Mauriat P, Pouard P, et al. Anomalous left coronary artery from the pulmonary artery: results of isolated aortic reimplantation. *Ann Thorac Surg* 1992;54:621-6. discussion 7.
61. Lambert V, Touchot A, Losay J, Piot JD, Henglein D, Serraf A, et al. Midterm results after surgical repair of the anomalous origin of the coronary artery. *Circulation* 1996;94(Suppl 9):I138-43.
62. Cochrane AD, Coleman DM, Davis AM, Brizard CP, Wolfe R, Karl TR. Excellent long-term functional outcome after an operation for anomalous left coronary artery from the pulmonary artery. *J Thorac Cardiovasc Surg* 1999;117:332-42.
63. Jin Z, Berger F, Uhlemann F, Schroder C, Hetzer R, Alexi-Meskishvili V, et al. Improvement in left ventricular dysfunction after aortic reimplantation in 11 consecutive paediatric patients with anomalous origin of the left coronary artery from the pulmonary artery. Early results of a serial echocardiographic follow-up. *Eur Heart J* 1994;15:1044-9.
64. Takeuchi S, Imamura H, Katsumoto K, Hayashi I, Katohgi T, Yozu R, et al. New surgical method for repair of anomalous left coronary artery from pulmonary artery. *J Thorac Cardiovasc Surg* 1979;78:7-11.
65. Bunton R, Jonas RA, Lang P, Rein AJ, Castaneda AR. Anomalous origin of left coronary artery from pulmonary artery. Ligation versus establishment of a two coronary artery system. *J Thorac Cardiovasc Surg* 1987;93:103-8.
66. Isomatsu Y, Imai Y, Shin'oka T, Aoki M, Iwata Y. Surgical intervention for anomalous origin of the left coronary artery from the pulmonary artery: the Tokyo experience. *J Thorac Cardiovasc Surg* 2001;121:792-7.
67. Sanders SP, Parness IA, Colan SD. Recognition of abnormal connections of coronary arteries with the use of Doppler color flow mapping. *J Am Coll Cardiol* 1989;13:922-6.
68. Koike K, Musewe NN, Smallhorn JF, Freedom RM. Distinguishing between anomalous origin of the left coronary artery from the pulmonary trunk and dilated cardiomyopathy: role of echocardiographic measurement of the right coronary artery diameter. *Br Heart J* 1989;61:192-7.
69. Frommelt MA, Miller E, Williamson J, Bergstrom S. Detection of septal coronary collaterals by color flow Doppler mapping is a marker for anomalous origin of a coronary artery from the pulmonary artery. *J Am Soc Echocardiogr* 2002;15:259-63.
70. Patel SG, Frommelt MA, Frommelt PC, Kutty S, Cramer JW. Echocardiographic diagnosis, surgical treatment, and outcomes of anomalous left coronary artery from the pulmonary artery. *J Am Soc Echocardiogr* 2017;30:896-903.
71. Kurup RP, Daniel R, Kumar RK. Anomalous origin of the left coronary artery from the pulmonary artery in infancy with preserved left ventricular function: potential pitfalls and clues to diagnosis. *Ann Pediatr Cardiol* 2008;1:65-7.
72. Schmitt B, Bauer S, Kutty S, Nordmeyer S, Nasser B, Berger F, et al. Myocardial perfusion, scarring, and function in anomalous left coronary artery from the pulmonary artery syndrome: a long-term analysis using magnetic resonance imaging. *Ann Thorac Surg* 2014;98:1425-36.
73. Mertens L, Weidemann F, Sutherland GR. Left ventricular function before and after repair of an anomalous left coronary artery arising from the pulmonary trunk. *Cardiol Young* 2001;11:79-83.
74. Ginde S, Earing MG, Bartz PJ, Cava JR, Tweddell JS. Late complications after Takeuchi repair of anomalous left coronary artery from the pulmonary artery: case series and review of literature. *Pediatr Cardiol* 2012;33:1115-23.
75. Pena E, Nguyen ET, Merchant N, Dennie C. ALCAPA syndrome: not just a pediatric disease. *Radiographics* 2009;29:553-65.
76. Castaldi B, Vida V, Reffo E, Padalino M, Daniels Q, Stellin G, et al. Speckle tracking in ALCAPA patients after surgical repair as predictor of residual coronary disease. *Pediatr Cardiol* 2017;38:794-800.
77. Secinaro A, Ntsinjana H, Tann O, Schuler PK, Muthurangu V, Hughes M, et al. Cardiovascular magnetic resonance findings in repaired anomalous left coronary artery to pulmonary artery connection (ALCAPA). *J Cardiovasc Magn Reson* 2011;13:27.
78. Latson LA. Coronary artery fistulas: how to manage them. *Catheter Cardiovasc Interv* 2007;70:110-6.
79. Frommelt MA, Frommelt PC. Echocardiography in pediatric and adult congenital heart disease. Philadelphia: Lippincott Williams & Wilkins; 2012. p. 512.
80. Sharma UM, Aslam AF, Tak T. Diagnosis of coronary artery fistulas: clinical aspects and brief review of the literature. *Int J Angiol* 2013;22:189-92.

81. Uysal F, Bostan OM, Semizel E, Signak IS, Asut E, Cil E. Congenital anomalies of coronary arteries in children: the evaluation of 22 patients. *Pediatr Cardiol* 2014;35:778-84.
82. Cheung DL, Au W-K, Cheung HH, Chiu CS, Lee WT. Coronary artery fistulas: long-term results of surgical correction. *Ann Thorac Surg* 2001;71:190-5.
83. Valente AM, Lock JE, Gauvreau K, Rodriguez-Huertas E, Joyce C, Armsby L, et al. Predictors of long-term adverse outcomes in patients with congenital coronary artery fistulae. *Circ Cardiovasc Interv* 2010;3:134-9.
84. Saboo SS, Juan YH, Khandelwal A, George E, Steigner ML, Landzberg M, et al. MDCCT of congenital coronary artery fistulas. *Am J Roengenol* 2014;203:W244-52.
85. Holzer JR, Ciotti G, Pozzi M, Kitchiner D. Review of an institutional experience of coronary arterial fistulas in childhood set in context of review of the literature. *Cardiol Young* 2004;14:380-5.
86. Said SA. Characteristics of congenital coronary artery fistulas complicated with infective endocarditis: analysis of 25 reported cases. *Congenit Heart Dis* 2016;11:756-65.
87. Warnes CA, Williams RG, Bashore TM, Child JS, Connolly HM, Dearani JA, et al. ACC/AHA 2008 guidelines for the management of adults with congenital heart disease: a report of the American College of Cardiology/American Heart Association task force on practice guidelines. *Circulation* 2008;118:e714-833.
88. Yoshikawa J, Katao H, Yanagihara K, Takagi Y, Okumachi F, Yoshida K, et al. Noninvasive visualization of the dilated main coronary arteries in coronary artery fistulas by cross-sectional echocardiography. *Circulation* 1982;65:600-3.
89. Shakudo M, Yoshida K, Yamaura Y. Noninvasive diagnosis of coronary artery fistula by Doppler color flow mapping. *J Am Coll Cardiol* 1989;13:1572-7.
90. Detorakis EE, Foukarakis E, Karavolias G, Dermitzakis A. Cardiovascular magnetic resonance and computed tomography in the evaluation of aneurysmal coronary-cameral fistula. *J Radiol Case Rep* 2015;9:10-21.
91. Barbosa MM, Katina T, Oliveira HG, Neuenschwander FE, Oliveira EC. Doppler echocardiographic features of coronary artery fistula: report of 8 cases. *J Am Soc Echocardiogr* 1999;12:149-54.
92. Lin FC, Chang HJ, Chern MS, Wen MS, Yeh SJ, Wu D. Multiplane transesophageal echocardiography in the diagnosis of congenital coronary artery fistula. *Am Heart J* 1995;130:1236-44.
93. Gillebert C, Van Hoof R, Van de Werf F, Piessens J, De Geest H. Coronary artery fistulas in an adult population. *Eur Heart J* 1986;7:437-43.
94. Mottin B, Baruteau A, Boudjemline Y, Piechaud FJ, Godart F, Lussan JR, et al. Transcatheter closure of coronary artery fistulas in infants and children: a French multicenter study. *Catheter Cardiovasc Interv* 2016;87:411-8.
95. Armsby LR, Keane JF, Sherwood MC, Forbess JM, Pery SB, Lock JE. Management of coronary artery fistulae. Patient selection and results of transcatheter closure. *J Am Coll Cardiol* 2002;39:1026-32.
96. Qureshi SA, Tynan M. Catheter closure of coronary artery fistulas. *J Interv Cardiol* 2001;14:299-307.
97. Yim D, Yong MS, d'Udekem Y, Brizard CP, Konstantinov IE. Early surgical repair of the coronary artery fistulae in children: 30 years of experience. *Ann Thorac Surg* 2015;100:188-94.
98. Kamiya H, Yasuda T, Nagamine H, Sakakibara N, Nishida S, Kawasuji M, et al. Surgical treatment of congenital coronary artery fistulas: 27 years' experience and a review of the literature. *J Card Surg* 2002;17:173-7.
99. Gowda ST, Forbes TJ, Singh H, Kovach JA, Prieto L, Latson LA, et al. Remodeling and thrombosis following closure of coronary artery fistula with review of management: large distal coronary artery fistula—close or not to close? *Catheter Cardiovasc Interv* 2013;82:132-42.
100. Gowda ST, Latson LA, Kuttu S, Prieto LR. Intermediate to long-term outcome following congenital coronary artery fistulae closure with focus on thrombus formation. *Am J Cardiol* 2011;107:302-8.
101. Vinograd CA, Ostermayer S, Lytrivi ID, Ko HH, Parness I, Geiger M, et al. Prevalence and outcomes of coronary artery ectasia associated with isolated congenital coronary artery fistula. *Am J Cardiol* 2014;114:111-6.
102. Bogers AJ, Quaegebeur JM, Huysmans HA. Early and late results of surgical treatment of congenital coronary artery fistula. *Thorax* 1987;42:369-73.
103. Hiraishi S, Horiguchi Y, Fujino N, Takeda N, Nakae S, Kasahara S. Effect of suture closures of coronary artery fistula on aneurysmal coronary artery and myocardial ischemia. *Am J Cardiol* 1998;81:1263-7.
104. Chiu SN, Wu MH, Lin MT, Wu ET, Wang JK, Lue HC. Acquired coronary artery fistula after open heart surgery for congenital heart disease. *Int J Cardiol* 2005;103:187-92.
105. Pellikka PA, Nagueh SF, Elhendy AA, Kuehl CA, Sawada SG. American Society of Echocardiography recommendations for performance, interpretation, and application of stress echocardiography. *J Am Soc Echocardiogr* 2007;20:1021-41.
106. Schmitt R, Froehner S, Brunn J, Wagner M, Brunner H, Cherevaty O, et al. Congenital anomalies of the coronary arteries: imaging with contrast-enhanced, multidetector computed tomography. *Eur Radiol* 2005;15:1110-21.
107. Zenooz NA, Habibi R, Mammen L, Finn JP, Gilkeson RC. Coronary artery fistulas: CT findings. *Radiographics* 2009;29:781-9.
108. Stamm C, Li J, Ho SY, Redington AN, Anderson RH. The aortic root in supravalvular aortic stenosis: the potential surgical relevance of morphologic findings. *J Thorac Cardiovasc Surg* 1997;114:16-24.
109. Vaideeswar P, Desphande R, Sivaraman A, Jain N. Pathology of the diffuse variant of supravalvular aortic stenosis. *Cardiovasc Pathol* 2001;9:33-7.
110. van Son JAM, Jacques WD, Danielson GK, Gordon. Pathology of coronary arteries, myocardium, and great arteries in supravalvular aortic stenosis. *J Thorac Cardiovasc Surg* 1994;108:21-8.
111. Faury G, Pezet M, Knutsen RH, Boyle WA, Heximer SP, McLean SE, et al. Developmental adaptation of the mouse cardiovascular system to elastin haploinsufficiency. *J Clin Invest* 2003;112:1419-28.
112. Collins RT 2nd, Kaplan P, Somes GW, Rome JJ. Long-term outcomes of patients with cardiovascular abnormalities and Williams syndrome. *Am J Cardiol* 2010;105:874-8.
113. Collins RT 2nd. Cardiovascular disease in Williams syndrome. *Circulation* 2013;127:2125-34.
114. Stamm C, Friehs I, Ho SY, Moran AM, Jonas RA, del Nido PJ. Congenital supravalvular aortic stenosis: a simple lesion? *Eur J Cardiothorac Surg* 2001;19:195-202.
115. Martin MM, Lemmer JH, Shaffer E, Dick M, Bove EL. Obstruction to left coronary artery blood flow secondary to obliteration of the coronary ostium in supravalvular aortic stenosis. *Ann Thorac Surg* 1988;45:16-20.
116. van Son JAM, Danielson GK, Puga FJ, Schaff HV, Rastogi A, Edwards WD, et al. Supravalvular aortic stenosis: long-term results of surgical treatment. *J Thorac Cardiovasc Surg* 1994;107:103-15.
117. van Pelt NC, Wilson NJ, Lear G. Severe coronary artery disease in the absence of supravalvular stenosis in a patient with Williams syndrome. *Pediatr Cardiol* 2005;26:665-7.
118. Gray JC 3rd, Krazinski AW, Schoepf UJ, Meinel FG, Pietris NP, Suranyi P, et al. Cardiovascular manifestations of Williams syndrome: imaging findings. *J Cardiovasc Comput Tomogr* 2013;7:400-7.
119. Kim YM, Yoo SJ, Choi JY, Kim SH, Bae EJ, Lee YT. Natural course of supravalvular aortic stenosis and peripheral pulmonary arterial stenosis in Williams' syndrome. *Cardiol Young* 1999;9:37-41.
120. Thiene G, Ho SY. Aortic root pathology and sudden death in youth: review of anatomical varieties. *Appl Pathol* 1986;4:237-45.
121. Bird LM, Billman GF, Lacro RV, Spicer RL, Jariwala LK, Hoyme HE, et al. Sudden death in Williams syndrome: report of ten cases. *J Pediatr* 1996;129:926-31.
122. Yilmaz AT, Arslan M, Ozal E, Byngol H, Tatar H, Ozturk OY. Coronary artery aneurysm associated with adult supravalvular aortic stenosis. *Ann Thorac Surg* 1996;62:1205.
123. Ergul Y, Nisli K, Kayserili H, Karaman B, Basaran S, Dursun M, et al. Evaluation of coronary artery abnormalities in Williams syndrome patients using myocardial perfusion scintigraphy and CT angiography. *Cardiol J* 2012;19:301-8.

124. Burch TM, McGowan FX Jr, Kussman BD, Powell AJ, DiNardo JA. Congenital supravalvular aortic stenosis and sudden death associated with anesthesia: what's the mystery? *Anesth Analg* 2008;107:1848-54.
125. Vincent WR, Buckberg GD, Hoffman JIE. Left ventricular subendocardial ischemia in severe valvar and supravalvular aortic stenosis. A common mechanism. *Circulation* 1974;49:326-33.
126. Wessel A, Gravenhorst V, Buchhorn R, Gosch A, Partsch CJ, Pankau R. Risk of sudden death in the Williams-Beuren syndrome. *Am J Med Genet A* 2004;127A:234-7.
127. Kececioğlu D, Kotthoff S, Vogt J. Williams-Beuren syndrome: a 30-year follow-up of natural and postoperative course. *Eur Heart J* 1993;14:1458-64.
128. Horowitz PE, Akhtar S, Wulff JA, Al Fadley F, Al Halees Z. Coronary artery disease and anesthesia-related death in children with Williams syndrome. *J Cardiothorac Vasc Anesth* 2002;16:739-41.
129. Paul JF, Rohnean A, Sigal-Cinqualbre A. Multidetector CT for congenital heart patients: what a paediatric radiologist should know. *Pediatr Radiol* 2010;40:869-75.
130. Das KM, Momenah TS, Larsson SG, Jadoon S, Aldosary AS, Lee EY. Williams-Beuren syndrome: computed tomography imaging review. *Pediatr Cardiol* 2014;35:1309-20.
131. Su JT, Chung T, Muthupillai R, Pignatelli RH, Kung GC, Diaz LK, et al. Usefulness of real-time navigator magnetic resonance imaging for evaluating coronary artery origins in pediatric patients. *Am J Cardiol* 2005;95:679-82.
132. Latham GJ, Ross FJ, Eisses MJ, Richards MJ, Geiduschek JM, Joffe DC. Perioperative morbidity in children with elastin arteriopathy. *Paediatr Anaesth* 2016;26:926-35.
133. Cohen MS, Eidem BW, Cetta F, Fogel MA, Frommelt PC, Ganame J, et al. Multimodality imaging guidelines of patients with transposition of the great arteries: a report from the American Society of Echocardiography developed in collaboration with the Society for Cardiovascular Magnetic Resonance and the Society of Cardiovascular Computed Tomography. *J Am Soc Echocardiogr* 2016;29:571-621.
134. Jatene AD, Fontes VF, Paulista PP, de Souza LC, Neger F, Galantier M, et al. Successful anatomic correction of transposition of the great vessels. A preliminary report. *Arq Bras Cardiol* 1975;28:461-4.
135. Pasquali SK, Hasselblad V, Li JS, Kong DF, Sanders SP. Coronary artery pattern and outcome of arterial switch operation for transposition of the great arteries: a meta-analysis. *Circulation* 2002;106:2575-80.
136. Wang C, Chen S, Zhang H, Liu J, Xu Z, Zheng J, et al. Anatomical classifications of the coronary arteries in complete transposition of the great arteries and double outlet right ventricle with subpulmonary ventricular septal defect. *Thorac Cardiovasc Surg* 2017;65:26-30.
137. Metton O, Calvaruso D, Gaudin R, Mussa S, Raisky O, Bonnet D, et al. Intramural coronary arteries and outcome of neonatal arterial switch operation. *Eur J Cardiothorac Surg* 2010;37:1246-53.
138. Rastelli GC, McGoon DC, Wallace RB. Anatomic correction of transposition of the great arteries with ventricular septal defect and subpulmonary stenosis. *J Thorac Cardiovasc Surg* 1969;58:545-52.
139. Nikaidoh H. Aortic translocation and biventricular outflow tract reconstruction. A new surgical repair for transposition of the great arteries associated with ventricular septal defect and pulmonary stenosis. *J Thorac Cardiovasc Surg* 1984;88:365-72.
140. Honjo O, Kotani Y, Bharucha T, Mertens L, Caldarone CA, Redington AN, et al. Anatomical factors determining surgical decision-making in patients with transposition of the great arteries with left ventricular outflow tract obstruction. *Eur J Cardiothorac Surg* 2013;44:1085-94. discussion 94.
141. Wong D, Golding F, Hess L, Caldarone CA, Van Arsdell G, Manlhiot C, et al. Intraoperative coronary artery pulse Doppler patterns in patients with complete transposition of the great arteries undergoing the arterial switch operation. *Am Heart J* 2008;156:466-72.
142. Nield LE, Dragulescu A, MacColl C, Manlhiot C, Brun H, McCrindle BW, et al. Coronary artery Doppler patterns are associated with clinical outcomes post-arterial switch operation for transposition of the great arteries. *Eur Heart J Cardiovasc Imaging* 2018;19:461-8.
143. Legendre A, Losay J, Touchot-Kone A, Serraf A, Belli E, Piot JD, et al. Coronary events after arterial switch operation for transposition of the great arteries. *Circulation* 2003;108(Suppl 1):II186-90.
144. Han BK, Lesser JR. CT imaging in congenital heart disease: an approach to imaging and interpreting complex lesions after surgical intervention for tetralogy of Fallot, transposition of the great arteries, and single ventricle heart disease. *J Cardiovasc Comput Tomogr* 2013;7:338-53.
145. Ou P, Mousseaux E, Azarine A, Dupont P, Agnoletti G, Vouhe P, et al. Detection of coronary complications after the arterial switch operation for transposition of the great arteries: first experience with multislice computed tomography in children. *J Thorac Cardiovasc Surg* 2006;131:639-43.
146. Ou P, Celermajer DS, Marini D, Agnoletti G, Vouhe P, Brunelle F, et al. Safety and accuracy of 64-slice computed tomography coronary angiography in children after the arterial switch operation for transposition of the great arteries. *JACC Cardiovasc Imaging* 2008;1:331-9.
147. Manso B, Castellote A, Dos L, Casaldaliga J. Myocardial perfusion magnetic resonance imaging for detecting coronary function anomalies in asymptomatic paediatric patients with a previous arterial switch operation for the transposition of great arteries. *Cardiol Young* 2010;20:410-7.
148. Li J, Soukias ND, Carvalho JS, Ho SY. Coronary arterial anatomy in tetralogy of Fallot: morphological and clinical correlations. *Heart* 1998;80:174-83.
149. Need LR, Powell AJ, del Nido P, Geva T. Coronary echocardiography in tetralogy of Fallot: diagnostic accuracy, resource utilization and surgical implications over 13 years. *J Am Coll Cardiol* 2000;36:1371-7.
150. Gupta D, Saxena A, Kothari SS, Juneja R, Rajani M, Sharma S, et al. Detection of coronary artery anomalies in tetralogy of Fallot using a specific angiographic protocol. *Am J Cardiol* 2001;87:241-4. A9.
151. Kaneko Y, Okabe H, Nagata N, Kobayashi J, Murakami A, Takamoto S. Pulmonary atresia, ventricular septal defect, and coronary-pulmonary artery fistula. *Ann Thorac Surg* 2001;71:355-6.
152. Patil NP, Mishra S, Agarwal S, Satsangi DK. Left main coronary artery atresia with tetralogy of Fallot: a novel association. *J Thorac Cardiovasc Surg* 2012;144:e87-9.
153. Kervancioglu M, Tokel K, Varan B, Yildirim SV. Frequency, origins and courses of anomalous coronary arteries in 607 Turkish children with tetralogy of Fallot. *Cardiol J* 2011;18:546-51.
154. Humes RA, Driscoll DJ, Danielson GK, Puga FJ. Tetralogy of Fallot with anomalous origin of left anterior descending coronary artery. Surgical options. *J Thorac Cardiovasc Surg* 1987;94:784-7.
155. Stout KK, Daniels CJ, Aboulhosn JA, Bozkurt B, Broberg CS, Colman JM, et al. 2018 AHA/ACC guideline for the management of adults with congenital heart disease: executive summary: a report of the American College of Cardiology/American Heart Association task force on clinical practice guidelines. *Circulation* 2019;139:e637-97.
156. Kilner PJ, Geva T, Kaemmerer H, Trindade PT, Schwitler J, Webb GD. Recommendations for cardiovascular magnetic resonance in adults with congenital heart disease from the respective working groups of the European Society of Cardiology. *Eur Heart J* 2010;31:794-805.
157. McElhinney DB, Hellenbrand WE, Zahn EM, Jones TK, Cheatham JP, Lock JE, et al. Short- and medium-term outcomes after transcatheter pulmonary valve placement in the expanded multicenter US melody valve trial. *Circulation* 2010;122:507-16.
158. Morray BH, McElhinney DB, Cheatham JP, Zahn EM, Berman DP, Sullivan PM, et al. Risk of coronary artery compression among patients referred for transcatheter pulmonary valve implantation: a multicenter experience. *Circ Cardiovasc Interv* 2013;6:535-42.
159. de la Cruz MV, Cayre R, Angelini P, Noriega-Ramos N, Sadowinski S. Coronary arteries in truncus arteriosus. *Am J Cardiol* 1990;66:1482-6.
160. Suzuki A, Ho SY, Anderson RH, Deanfield JE. Coronary arterial and sinus anatomy in hearts with a common arterial trunk. *Ann Thorac Surg* 1989;48:792-7.

161. Oddens JR, Bogers AJ, Witsenburg M, Bartelings MM, Bos E. Anatomy of the proximal coronary arteries as a risk factor in primary repair of common arterial trunk. *J Cardiovasc Surg (Torino)* 1994;35:295-9.
162. Lenox CC, Debich DE, Zuberbuhler JR. The role of coronary artery abnormalities in the prognosis of truncus arteriosus. *J Thorac Cardiovasc Surg* 1992;104:1728-42.
163. Chaudhari M, Hamilton L, Hasan A. Correction of coronary arterial anomalies at surgical repair of common arterial trunk with ischaemic left ventricular dysfunction. *Cardiol Young* 2006;16:179-81.
164. Schreiber C, Eicken A, Balling G, Wottke M, Schumacher G, Un Paek S, et al. Single centre experience on primary correction of common arterial trunk: overall survival and freedom from reoperation after more than 15 years. *Eur J Cardiothorac Surg* 2000;18:68-73.
165. Naimo PS, Fricke TA, Yong MS, d'Udekem Y, Kelly A, Radford DJ, et al. Outcomes of truncus arteriosus repair in children: 35 years of experience from a single institution. *Semin Thorac Cardiovasc Surg* 2016;28:500-11.
166. Hong SH, Kim YM, Lee CK, Lee CH, Kim SH, Lee SY. 3D MDCT angiography for the preoperative assessment of truncus arteriosus. *Clin Imaging* 2015;39:938-44.
167. Daubeney PE, Sharland GK, Cook AC, Keeton BR, Anderson RH, Webber SA. Pulmonary atresia with intact ventricular septum: impact of fetal echocardiography on incidence at birth and postnatal outcome. UK and Eire collaborative study of pulmonary atresia with intact ventricular septum. *Circulation* 1998;98:562-6.
168. Daubeney PE, Delany DJ, Anderson RH, Sandor GG, Slavik Z, Keeton BR, et al. Pulmonary atresia with intact ventricular septum: range of morphology in a population-based study. *J Am Coll Cardiol* 2002;39:1670-9.
169. Calder AL, Co EE, Sage MD. Coronary arterial abnormalities in pulmonary atresia with intact ventricular septum. *Am J Cardiol* 1987;59:436-42.
170. Giglia TM, Mandell VS, Connor AR, Mayer JE Jr., Lock JE. Diagnosis and management of right ventricle-dependent coronary circulation in pulmonary atresia with intact ventricular septum. *Circulation* 1992;86:1516-28.
171. Hanley FL, Sade RM, Blackstone EH, Kirklin JW, Freedom RM, Nanda NC. Outcomes in neonatal pulmonary atresia with intact ventricular septum. A multiinstitutional study. *J Thorac Cardiovasc Surg* 1993;105:406-27.
172. Jahangiri M, Zurakowski D, Bichell D, Mayer JE, del Nido PJ, Jonas RA. Improved results with selective management in pulmonary atresia with intact ventricular septum. *J Thorac Cardiovasc Surg* 1999;118:1046-55.
173. Ashburn DA, Blackstone EH, Wells WJ, Jonas RA, Pigula FA, Manning PB, et al. Determinants of mortality and type of repair in neonates with pulmonary atresia and intact ventricular septum. *J Thorac Cardiovasc Surg* 2004;127:1000-7. discussion 7-8.
174. Cheung EW, Richmond ME, Turner ME, Bacha EA, Torres AJ. Pulmonary atresia/intact ventricular septum: influence of coronary anatomy on single-ventricle outcome. *Ann Thorac Surg* 2014;98:1371-7.
175. Cools B, Boshoff D, Heying R, Rega F, Meyns B, Geuwillig M. Transventricular balloon dilation and stenting of the RVOT in small infants with tetralogy of Fallot with pulmonary atresia. *Catheter Cardiovasc Interv* 2013;82:260-5.
176. Satou GM, Perry SB, Gauvreau K, Geva T. Echocardiographic predictors of coronary artery pathology in pulmonary atresia with intact ventricular septum. *Am J Cardiol* 2000;85:1319-24.
177. Humpl T, Soderberg B, McCrindle BW, Nykanen DG, Freedom RM, Williams WG, et al. Percutaneous balloon valvotomy in pulmonary atresia with intact ventricular septum: impact on patient care. *Circulation* 2003;108:826-32.
178. Mair DD, Julsrud PR, Puga FJ, Danielson GK. The Fontan procedure for pulmonary atresia with intact ventricular septum: operative and late results. *J Am Coll Cardiol* 1997;29:1359-64.
179. Gentles TL, Colan SD, Giglia TM, Mandell VS, Mayer JE Jr., Sanders SP. Right ventricular decompression and left ventricular function in pulmonary atresia with intact ventricular septum. The influence of less extensive coronary anomalies. *Circulation* 1993;88(5 Pt 2):II183-8.
180. Akiba T, Becker AE. Disease of the left ventricle in pulmonary atresia with intact ventricular septum. The limiting factor for long-lasting successful surgical intervention? *J Thorac Cardiovasc Surg* 1994;108:1-8.
181. Ekman-Joelsson BM, Berggren H, Boll AB, Sixt R, Sunnegardh J. Abnormalities in myocardial perfusion after surgical correction of pulmonary atresia with intact ventricular septum. *Cardiol Young* 2008;18:89-95.
182. Rathod RH, Prakash A, Powell AJ, Geva T. Myocardial fibrosis identified by cardiac magnetic resonance late gadolinium enhancement is associated with adverse ventricular mechanics and ventricular tachycardia after Fontan operation. *J Am Coll Cardiol* 2010;55:1721-8.
183. O'Connor WN, Cash JB, Cottrill CM, Johnson GL, Noonan JA. Ventriculo-coronary connections in hypoplastic left hearts: an autopsy microscopic study. *Circulation* 1982;66:1078-86.
184. Sauer U, Gittenberger-de Groot AC, Geishauer M, Babic R, Buhlmeier K. Coronary arteries in the hypoplastic left heart syndrome. Histopathologic and histometrical studies and implications for surgery. *Circulation* 1989;80(3 Pt 1):I168-76.
185. Roberson DA, Cui W, Cuneo BF, Van Bergen AH, Javois AJ, Bharati S. Extensive left ventricular to coronary artery connections in hypoplastic left heart syndrome. *Echocardiography* 2008;25:529-33.
186. Nathan M, Williamson AK, Mayer JE, Bacha EA, Juraszek AL. Mortality in hypoplastic left heart syndrome: review of 216 autopsy cases of aortic atresia with attention to coronary artery disease. *J Thorac Cardiovasc Surg* 2012;144:1301-6.
187. Baffa JM, Chen SL, Guttenberg ME, Norwood WI, Weinberg PM. Coronary artery abnormalities and right ventricular histology in hypoplastic left heart syndrome. *J Am Coll Cardiol* 1992;20:350-8.
188. Siehr SL, Maeda K, Connolly AA, Tacy TA, Reddy VM, Hanley FL, et al. Mitral stenosis and aortic atresia—a risk factor for mortality after the modified Norwood operation in hypoplastic left heart syndrome. *Ann Thorac Surg* 2016;101:162-7.
189. Vida VL, Bacha EA, Larrazabal A, Gauvreau K, Dorfman AL, Marx G, et al. Surgical outcome for patients with the mitral stenosis-aortic atresia variant of hypoplastic left heart syndrome. *J Thorac Cardiovasc Surg* 2008;135:339-46.
190. Sathanandam SK, Polimenakos AC, Roberson DA, elZein CF, Van Bergen A, Husayni TS, et al. Mitral stenosis and aortic atresia in hypoplastic left heart syndrome: survival analysis after stage I palliation. *Ann Thorac Surg* 2010;90:1599-607. discussion 607-8.
191. Ghanayem NS, Allen KR, Tabbutt S, Atz AM, Clabby ML, Cooper DS, et al. Interstage mortality after the Norwood procedure: results of the multicenter single ventricle reconstruction trial. *J Thorac Cardiovasc Surg* 2012;144:896-906.